THE IMPACT OF THE DRILL SPACING ON THE APPROACH TO MINERAL RESOURCE ESTIMATION

Wendy Marcia Keiller

327464

School of Mining Engineering, University of the Witwatersrand, Johannesburg, South Africa.

Supervisor: Prof C E Dohm

A research report submitted to the Faculty of Engineering and the Built Environment, University of the Witwatersrand, in fulfilment of the requirements for the Degree of Master of Science in Mining Engineering by coursework and project (M.Sc. 50/50).

2021

DECLARATION

I, Wendy Marcia Keiller (Student number: 327464), am registered for the Degree of Master of Science in Mining Engineering in the year 2020. I declare that this research report is my own, unaided work, except for where I have referenced and acknowledged the work of others. I am aware that the University of the Witwatersrand may take disciplinary action against me if I have failed to acknowledge the work of others in my research.

29th day of September 2021

ABSTRACT

Mineral Resource estimation is a vital step in the mining value chain as its outcomes form the foundation of all further mine design, planning and decision making. It is important to use an appropriate Mineral Resource estimation methodology suited to the project phase, and amount of data available, in order to generate a meaningful and reliable estimate. The purpose of this research is to investigate and assess the impact of data spacing on the Mineral Resource estimation methodology.

This research is presented as a case study applied to the Ventersdorp Contact Reef of the Witwatersrand Basin. The methodology is presented for six different scenarios of increasing data density from an initial surface drilling program, with minimal, widely spaced data, to resource exploitation, with denser sampling data typical of a South African underground gold mine layout.

The methodology for defining homogenous domains is refined and adjusted as additional data becomes available. Geozones delineated during early project phases, based on widely spaced data, require adjustment as trends emerge from closely spaced sampling data.

For initial project phases, with limited data, global estimation techniques using statistical distribution theory is appropriate. Application of the Sichel t lognormal distribution and the 2-parameter lognormal distribution highlight the significance of identifying an appropriate distribution model for a global mean estimate.

As data density increases, the spatial distribution theory captured by the semi-variogram becomes more relevant and local estimation theory is applied. An overall increased nugget effect and decreased variogram range is observed as data density increases. For the ordinary kriging, the impact of the variogram model together with the data configuration and block to be estimated is presented in terms of kriging performance indicators, including block variance, kriging variance, the Lagrange multiplier, slope of regression and kriging efficiency.

This research demonstrates the necessity of aligning the estimation methodology to the stage of the resource development as a function of the amount of and spatial distribution of the available data. Data spacing has a substantial effect of on geological domaining, resource estimation methodology, resource classification, and subsequently reserve estimation and mine planning.

ACKNOWLEDGEMENTS

I wish to express my gratitude to Prof C E Dohm for answering my first phone call, her outstanding post-graduate courses, my research topic, patient teaching, many conversations and invaluable mentorship.

My research would not have been possible without the inspirational leadership and multitudinous support (financial, professional, and personal) from VBKOM (Pty) Ltd, Paul Obermeyer and all my VBKOM colleagues.

I wish to show my appreciation to Lynsey Houston for the endless support and meticulous proof-reading, and to Michelle Pienaar and Russell Johnson for the advice and encouragement.

To my husband, James Brunke, my inspirational family and extended family, friends, and Pippin and Took, for their band-aid superpowers that were so critical over the last few years.

TABLE OF CONTENTS

LIST OF FIGURES

LIST OF TABLES

TABLE OF ABBREVIATIONS

2D	Two-dimensional
3D	Three-dimensional
Au	Gold
cm.g/t	Gold value or gold accumulation
COMRO	Chamber of Mines Research Organisation
CRG	Central Rand Group
CW	Channel Width
EDA	Exploratory Data Analysis
g/t	Gold grade
KE	Kriging Efficiency
LN(2)	2-parameter lognormal
KV	Kriging Variance
QKNA	Quantitative Kriging Neighbourhood Analysis
RIF	Reef in footwall
RIH	Reef in hanging wall
RPEEE	Reasonable Prospects for Eventual Economic Extraction
SAMREC Code	The South African Code for the Reporting of Exploration Results, Mineral Resources and Mineral Reserves
SLOR	Slope of Regression
SMU	Selective Mining Unit
VCR	Ventersdorp Contact Reef

SOUTH AFRICAN MINING TERMINOLOGY

Development	Underground network of excavated tunnels designed for effective mining requirements
Channel Width	The overall reef width, including the conglomerate and internal quartzite bands (Storrar, 1977)
Panel/Stope	An excavation mined on-reef, near perpendicular to the raise line. A typical panel length is 30 m with a width of approximately 1.2 m.
Raise line	Inclined tunnel mined up-dip and on-reef
Reef	Gold bearing conglomerate layer
Reef drive	Horizontal tunnel mined on-reef
Reef in footwall	The basal contact of the reef is not exposed during stoping operations
Reef in hanging wall	The top contact of the reef is not exposed during stoping operations
Stope width	The measured width of the excavation made during stoping operations (Storrar, 1977)

1 INTRODUCTION

Mineral deposits need to be estimated at different stages of resource development to quantify their associated tonnages and grades in order to generate interest for future investment and ideally, for economic extraction. The Mineral Resource development process will always begin with a sparse dataset for a new exploration target. The number of boreholes to be drilled is limited by the exploration budget available and a phased approach to increasing the number of boreholes allows for continuous assessment and evaluation of the project viability while limiting the financial risk.

During the early stages of a resource development project, reducing Mineral Resource estimate uncertainty is strongly linked to decreasing the data spacing by undertaking infill drilling programs as documented in numerous Public Reports and announcements by listed companies. During exploitation and advanced project stages additional drilling is also linked to increasing the geoscientific confidence in the Mineral Resource, however, other methods of reducing uncertainty, such as estimation methodology changes, become possible due to increased data collection. De Waele, *et al.* (2018) presented case studies highlighting that confidence in the Mineral Resource was increased in most geological environments by improving the geological model. Gilchrist (2019) documented the evolution of a Copper deposit from a 2D inverse distance squared model to a 3D geostatistical model over a 10-year period of resource project development and concluded that improving both the understanding of the geological model and the reliability of the estimation methodology will lead to an improved (reduced uncertainty in the) resource model that may ultimately optimise mining operations and metallurgical beneficiation.

It is intuitive that increased drilling and sampling information will lead to an improved estimate, and that data spacing has a direct impact on the confidence of the Mineral Resource estimate, as reflected in the resource classification. This statement is supported by Silva *et al.* (2019) who demonstrated that resource uncertainty is proportional to data spacing by quantifying uncertainty using simulation. Various authors refer to estimation errors that may arise due to insufficient data density. Clark (1979) stated that fewer numbers of data pairs decrease the estimate reliability, which was reiterated in 2004 by Dominy *et al.*, who stated that in most cases, the only way to continue with a project was to increase the amount and quality of data, as the data density controls the ability to resolve issues around mineralisation continuity.

1.1 Purpose of the Study

A widely spaced drilling grid is used for initial exploration drilling programs. If this initial drilling is successful, this grid is filled in as the project progresses to the next phase of exploration drilling. The purpose is to investigate and assess the impact of additional data on the choice of an appropriate estimation methodology, from global estimation based on statistical distributional theory, to local estimation based on the spatial distribution theory captured by the semi-variogram, and consequently, on how the resource estimation methodology results differ between the various scenarios considered in this research study.

Vann *et al.* (2014) emphasise that the most important approach to resource estimation is common sense. Unfortunately, time constraints in the workplace often dictate how much time can be spent exploring the resource estimation methodology, and as a result, the resource geologist often follows a set methodology.

Sinclair and Blackwell (2004) noted that resource estimation should be viewed as an evolving project from discovery to mine closure. Routine practice, without paying attention to how data sparsity may impact the reliability of the estimation results, should be avoided. Generalised and comprehensive resource estimation methodology is well documented in literature (Isaaks and Srivastava,1989, Clark and Harper, 2000, Rossi and Deutsch, 2014). This research aims to reflect on how the approach to estimation may change depending on the resource project development stage and associated data spacing.

Mineral Resource estimation can be more difficult without the use of the Bayesian approach to infer known statistical parameters to an unknown area. In a new exploration project, the spatial structure of a deposit may be poorly represented by a sparse dataset. The drilling grid spacing, and therefore amount of relevant data available, must be considered when deciding on the methodology for the estimation process.

1.2 Research Background and Context

This research is presented as a case study applied to the narrow tabular Ventersdorp Contact Reef (VCR) of the Witwatersrand Basin. Six scenarios of decreasing data spacing by increasing the data density were generated to represent the gradual accumulation of drilling and sampling information as a resource project progresses through successive drilling phases, from Exploration Target identification to Mineral Resource exploitation.

1.3 Research Objectives

The objective of this research study is to investigate and assess the effects of widely spaced, sparse datasets to abundant, closely spaced datasets on the estimation methodology and the ability to generate an experimental semi-variogram, and hence the semi-variogram model.

The aim is to investigate and assess how the data spacing at each phase of resource development impacts resources estimation assessment from a global estimate to local estimation. The impact of decreasing drilling spacing i.e., increasing sampling density is interpreted by comparing the semi-variogram model and estimation results for sequential scenarios of increasing spatial sampling density.

1.4 Research Questions

The goal is aimed at answering the following questions:

- *How does the drill spacing influence the estimation methodology as it decreases?*
- *How does the drill spacing impact the variography as it decreases, and the sampling density increases?*

1.5 Research Motivation

The motivation for this research stems from the reality that whilst the systematic and stepwise approach to Mineral Resource estimation methodology is well documented in literature, the approach is mostly generalised and is not discussed in sufficient detail to suit different project phases with vastly different data spacing. It is important to formulate an appropriate methodology for Mineral Resource estimation suited to the project phase in order to generate a meaningful and reliable estimate.

The systematic resource estimation process documented in the literature does not provide sufficient detail on the data spacing at each phase of resource development, nor on its impact on estimation results. A need has been identified for investigating and providing more detail on the estimation approach, relative to the data spacing, at each phase of project development. Therefore, an investigation by case study of the VCR was embarked on to determine how the additional information impacts the approach to each step of the estimation process.

1.6 Research Methodology

The intuitive idea that additional information should lead to improved estimation has been supported by evidence from the literature presented in Chapter 2. Six different scenarios are compared to investigate and assess the impact of additional drilling on the approach to Mineral Resource development. These scenarios represent the sequential phases of a Mineral Resource development project as new data is acquired. Scenario One represents the initial drilling phase and Scenario Six represents the final resource exploitation phase.

This research study follows the natural progression of Mineral Resource development on gold mines in the Witwatersrand Basin and the relevant information for each scenario is presented for each step of the estimation process. The Mineral Resource estimation process followed for this research is outlined below:

1) **Geological domaining**

   Geological domaining is undeniably a fundamental step in the resource estimation process and will improve the quality of the resource model as supported by literature in Chapter 2 and Chapter 3. Channel width describes the thickness of the reef and is used as a geological characteristic to aid definition of geological domains in this research. The term “geozone” is applied instead of “geological domain” to clarify the use of reef thickness in the absence of additional geological information (such as footwall lithology, mineralogy, or alteration), which was not included in the data provided.

Relative cumulative frequency distribution plots, independent of channel width class interval, were initially utilised to determine broad channel width intervals for use in colour-coded plots which aided delineation of geozone boundaries. As more information became available the methodology was refined, and indicator kriging applied to a channel width threshold was used to determine geozone (or domain) boundaries based on the probability of reef to be either thick or thin, testing different channel widths as the indicator variable.

2) Exploratory data analysis

Sinclair (1998) emphasized the importance of Exploratory Data Analysis (EDA) procedures used to evaluate data in a structured approached by initially applying basic methods and progressing to more complicated methods as relevant. EDA should improve the quality of the estimate and assist with correct geological domain definition, (Sinclair, 1998).

For this research, the following EDA procedures were applied:

- Data validation to improve the data quality by identifying, removing, or correcting data errors,
- Statistical summaries (e.g., means and variances) to define the statistical characteristics of the data,
- Graphical summaries (e.g., frequency plots) to indicate the shape of the data distribution,
- Outlier investigation using the lognormal probability plot.

3) Global estimation

Global estimation techniques using statistical distribution models were utilised for scenarios with insufficient data for geostatistical techniques. A global mean with upper and lower confidence limits was calculated using the Sichel t and a 2-parameter lognormal (LN(2)) distribution model.

4) **Quantifying spatial variability**

Variography analyses were conducted for each scenario to investigate the influence of additional data on the semi-variogram and to determine if geostatistical analysis was appropriate. This analysis included an investigation of anisotropy in each geological domain using variogram contour maps and experimental variogram analysis. The variogram contour map is a useful visual tool to help the practitioner identify preferred continuity directions and understand the spatial structure within the data.

5) **Local estimation**

Local block estimation utilising the ordinary kriging technique was conducted using Datamine Studio 3 software for the scenarios that produced meaningful variograms. Kriging variance, slope of regression, kriging efficiency and the Lagrange multiplier were compared for the different scenarios to determine the effects of additional data on the estimation error. Meaningful colour-coding legend intervals for these kriging performance indicators were determined using inflection points on their individual cumulative relative frequency plots.

Estimation block sizes used in this research are either typical of block sizes used for conventional deep level mining operations or represent mining within a specific period. A 60 m x 60 m block represents a period mined over one year (based on an average panel length of 30 m and an advance of 10 m per month. Refer to APPENDIX A). A 30 m x 30 m block represents a period mined over a quarter of the year and 10 m x 10 m blocks are commonly used in areas of closely spaced data.

Isaaks and Srivastava (1989) noted that fewer discretising points will increase computational speed, but decrease accuracy, and prove by case study that a minimum of 4 x 4 discretisation points provided sufficient accuracy for a 2D estimate. A typical QKNA discretisation exercise (APPENDIX B) was completed showing that a block discretisation of 6 x 6 is appropriate for all estimates.

The kriging search neighbourhood is informed by the range of the semi-variogram model for each domain. The search area was increased by a factor of 2 for the second search and a third search area was expanded to fill the total area considered with block estimates. A minimum number of five samples and a maximum number of 25 samples were used for all estimates in line with industry best practice. At least five samples are required to calculate a meaningful variance estimate. Domain boundaries, where relevant and as developed using appropriate methodology for Scenarios Four, Five and Six, have been applied as hard boundaries in this research.

Block size and search neighbourhood optimisation ultimately reduces the conditional bias in the resultant kriged estimates as far as possible. For this research, consistent kriging parameters were defined, and estimates will most likely show some improvement by inclusion of a quantitative kriging neighbourhood analysis as outlined by Vann *et al*. (2003).

A post-processing estimation technique for large blocks at a size of 210 m x 210 m is presented. The local estimation model validation was conducted by visual validation and swath plots, and the comparison of the data statistics to the estimate statistics were deemed to be reasonable.

6) Value-tonnage estimate calculation

Selectivity plots, such as grade-tonnage curves and metal-tonnage curves (Q/T plot), highlight the impact of the support effect on estimates of different supports. For this research, value-tonnage curves are presented to correspond with gold-value (cm.g/t) estimates. Support refers to the volume of the sample or block centred on the point of observation for a sample or estimation for a block.

7) Mineral Resource Classification

A simplistic Mineral Resource classification methodology has been proposed and utilised in this research based on geostatistical criteria and under the assumption of reasonable prospects for eventual economic extraction (RPEEE) as economic studies are outside the scope of this research. The search radius applied in kriging (a function of the variogram range), kriging variance, kriging efficiency and the slope of regression are considered criteria for grade estimation confidence. A Competent Person would use several considered geoscientific criteria and ultimately apply expert opinion for classifying individual blocks.

1.7 Research Study Layout

This research study report is structured as follows:

- Chapter One provides an introduction to the research topic, the research objectives, research questions, and the motivation for this research. A detailed outline of the research methodology is described.
- Chapter Two presents important literature relevant to the Mineral Resource estimation process followed for each Scenario including the information, support, regression effect and conditional bias.
- Chapter Three summarises the geological characteristics of the VCR including an overview of the regional geology from literature.
- Chapter Four addresses data validation and discusses the datasets generated for each of the six scenarios used in the case study.
- Chapter Five presents the results of the case study. The Mineral Resource estimation process followed for each of the six scenarios is presented. Scenario Six includes a variance size of area analysis.
- Chapter Six presents a summary of the scenario findings and results.
- Chapter Seven presents a summary of the main findings and conclusions of the research.

1.8 Assumptions

The quality assurance and quality control reports for this dataset were not available and were not reviewed. It was assumed that a code-compliant quality control protocol was followed in the acquisition (sampling and assaying) of the original data on which the simulated dataset used in this research was generated.

A density of 2.71 g/cm^3 has been applied to all tonnage calculations in this research. This density is used as an example for the VCR in Minnitt (2014).

The assumption of RPEEE has been applied to allow for declaration of geoscientific Mineral Resource confidence in this research. This assumption is deemed reasonable within the framework of the research dataset which was simulated from underground sampling data collected during mining production over several decades.

The SAMREC Code (2016) states that the potential viability must be appropriately considered including geological, mining engineering, processing, and economic assumptions which may influence the potential for economic extraction. However, the details of RPEEE are not discussed as an economic viability study was outside the scope of this research.

1.9 Chapter Summary

Chapter One introduces the research study with some background information and context. The purpose of this research study is to investigate and assess the impact of additional data on the choice of an appropriate estimation methodology. Chapter one defines the research questions based on a need for adjusting the estimation approach to suit the data spacing at each project phase. The layout of the report is presented as well as assumptions made.

2 LITERATURE REVIEW

The following literature review discusses aspects and methods relevant to the Mineral Resource estimation process followed for this research.

2.1 Geological Domaining

Geological domaining is a fundamental step in the resource estimation process. Krige (1997) stated that the spatial structure of data will reflect the style of mineralisation and that a solid understanding of the geological model is key to obtaining a meaningful semi-variogram model for any Mineral Resource estimate. Geological domaining is the process of identifying and delineating zones of homogeneous, or stationary, geological characteristics to reduce the risk of estimation error. Statistical and geostatistical analyses should confirm the geological domaining. Local estimation techniques assume that the zone of interest is geologically and statistically homogenous.

Incorporating the geological controls on mineralisation produces improved estimates compared to domaining based on grade-shells as demonstrated by Emery and Ortiz (2005) in a case study on a porphyry copper deposit. Duke and Hanna (2014) describe grade-shell domaining as only one part of interpreting geological domains, and ultimately these zones should incorporate all available geological information. Rather than grade-shell domaining, the geological domaining in this research was based on the slope and terrace model, described in literature reviewed in Chapter 3.2.

Domain boundary analysis is important to determine if spatial grade correlation is present across a boundary, as the estimate may be improved by utilising soft boundaries, (Emery and Ortiz, 2006). Soft boundaries between domains are required if there is a transitional change from one domain to another. Hard boundaries prevent data from one domain being used in the estimation of another domain. Hard boundaries are required if domains show distinctly different statistical populations.

2.2 Exploratory Data Analysis

The dataset used for this research incorporated artificial error designed to reflect common errors that could easily occur on a mining operation, such as duplicated sampling points. Data validation and error elimination provide an assurance of quality in the final Mineral Resource estimate. Exploratory data analysis assists in geological domaining by defining distinct zones that require independent estimation and early recognition of spatial trends is an important part of exploratory data analysis, (Sinclair, 1998).

2.3 Global Estimation

Estimation methods involve global or local techniques to quantify tonnage and grade for each scenario presented in this research. Sinclair and Blackwell (2004) described a global estimate as an average grade and tonnage calculated over a large area of the deposit. A global estimate represents the long-term planning estimate of the in-situ resource considering limited economic factors and is calculated during early project phases for the entire resource or large blocks, (Sinclair and Blackwell, 2004).

This research considers gold accumulation presented throughout the report as gold value (cm.g/t). Krige (1981) stated that the two basic variables of 2D orebodies are gold value (cm.g/t) and channel width (cm). Meaningful averages may be derived from these correlated variables without the need for the weighting correction required for gold grade (g/t) which is a critical consideration for the application of both statistical and geostatistical models (Krige, 1981). The correlation between channel width and gold mineralisation is supported in VCR literature (McWha, 1994) as presented in Chapter 3.3, and is confirmed by the conditional expectation plots for this research data

During early project phases a global estimation approach is appropriate as there is insufficient data to apply geostatistical techniques. The arithmetic mean of a positively skewed distribution may be a deceptive estimate of the mean value due to the overstated influence of high-grade outliers, (Dohm, 1995). Dohm (1995) discussed that the mean estimate of a positively skewed dataset may be improved by using the log-transformed data values which follow a more symmetrical distribution. The log-transformed data is used to estimate the parameters of the lognormal distribution and are then substituted into the ore distribution model to calculate a mean estimate, (Dohm, 1995).

Analysing statistical summaries and the fitting of a probability frequency distribution model to the histogram allows for the determination of a statistical distribution model which best describes the underlying mineralisation distribution. Accurate identification of a representative statistical model allows for consideration thereof in the estimation process, (Dohm, 1995).

The Sichel t estimator is applicable to 2-parameter lognormal distributions with less than 40 data points and has been applied to Scenario One in this research. Sinclair and Blackwell (2004) noted that the Sichel t estimator is useful for estimating the mean of small lognormal datasets due to the over-estimation of the mean by other estimators.

The Sichel t estimator for the mean (Sichel, 1966) is represented by the equation:

$$\mu^* = t = e^{\xi}\gamma_n(V) \qquad \textit{Equation 1}$$

Where ξ is the mean of the log transformed gold values x = *ln(value cm.g/t)* and $\gamma_n(V)$ is Sichel's variance factor, dependent on the biased sample variance V of the log transformed values, and sample size n, as determined from the Sichel t statistical tables (Sichel, 1966).

The sample variance, V, in the Sichel t estimator is a biased log variance and is represented by the equation:

$$V = \frac{1}{n}\left(\sum\left(x_i - \bar{\xi}\right)^2\right) \qquad \textit{Equation 2}$$

The 2-parameter lognormal distribution, or LN(2), is used to estimate lognormally distributed data with more than 40 datapoints. The 2-parameter estimator for the mean is represented by the following equation:

$$\mu^* = \tau = e^{\xi+\frac{1}{2}\sigma_L^2} \qquad \textit{Equation 3}$$

Where ξ is the mean of the log transformed values and the following equation is the variance of the log transformed sample values (Sichel, 1966):

$$\sigma_L^2 = \frac{1}{n-1}\Sigma(x_i - \bar{\xi})^2 \qquad \textit{Equation 4}$$

The 3-parameter lognormal distribution involves in addition to the calculation of the log mean and log variance parameters the estimation of a third parameter, β, (known as the additive constant) to be added to the sample values prior to the log transformation, (Krige, 1960, and Rendu ,1981). Some disadvantages of this distribution include difficult back-transformation from lognormal to normal space. Asymmetrical distributions with an artificial positive shift in grade values with a decreased variance is observed when applied to distributions that are not lognormal, (Dohm, 1995).

2.4 Spatial Variability

The variogram is used to measure the spatial variability of grades within a deposit and is therefore critical to any geostatistical study (Deutsch and Journel, 1998). This research compared the variogram for different scenarios to understand the effect of data density on the variogram. The scenarios with sparse data may make variogram interpretation more difficult due to the lack of data available for the variogram calculation, (Rossi and Deutsch, 2014). The variogram can be explained as the expected squared difference between two data points separated by a distance vector **h**. The variogram is therefore a measure of geological variability for a specific distance and direction, (Rossi and Deutsch, 2014).

Rossi and Deutsch (2014) defined the variogram using the following equation:

$$2\gamma(h) = Var[Z(i) - Z(i+h)] = E\{[Z(i) - Z(i+h)]^2\} \qquad \textit{Equation 5}$$

Where Z is the variable of interest and $Z(u)$ is the variable of interest at location u.

In the video "What the Heck is a Variogram?" Isaaks (2013) gives insight into how two sample datasets can appear statistically identical, however, when looking at the data in relation to the geographical location, a difference is observed. This practical video compares sediment sampling from two different stream's profiles. The correlogram shows how the correlation coefficient decreases with an increasing distance (or separation vector) for the data from Stream A. The data from Stream B, however, do not show this same relationship. Isaaks (2013) shows that the correlogram estimates the correlation between two sample points and a certain distance and/or direction. This simple comparison of two stream's profiles shows how important geostatistics can be in assessing the continuity of a mineral deposit.

Isaaks (2013) explains the calculation of the semi-variogram as the average squared difference of the distance from each sample point to the x = y graphical line, at a separation distance and direction (separation vector $\vec{h}$ or lag), divided by twice the number of data pairs. The semi-variogram definition is given as:

$$\gamma(\vec{h}) = \frac{1}{2N(\vec{h})}\sum\left(Z_i - Z_{i+\vec{h}}\right)^2 \qquad \textit{Equation 6}$$

Where Z is the variable of interest, Z_i is the variable of interest at location i and $N(h)$ the number of data pairs at separation distance h.

The variogram does not depend on a specific location as the entire dataset is scanned for sample pairs that match the defined tolerance parameters, such as the lag distance and tolerance angle.

2.4.1 Semi-Variogram Features

The continuity and spatial structure of the mineralisation is described by the variogram model for each scenario. The semi-variogram model parameters capture the random component (nugget), the range of continuity and the sill, or population variance, of the data (refer to Figure 2-1). In this research the variogram models are analysed and interpreted as they change with increasing data density for each scenario considered.

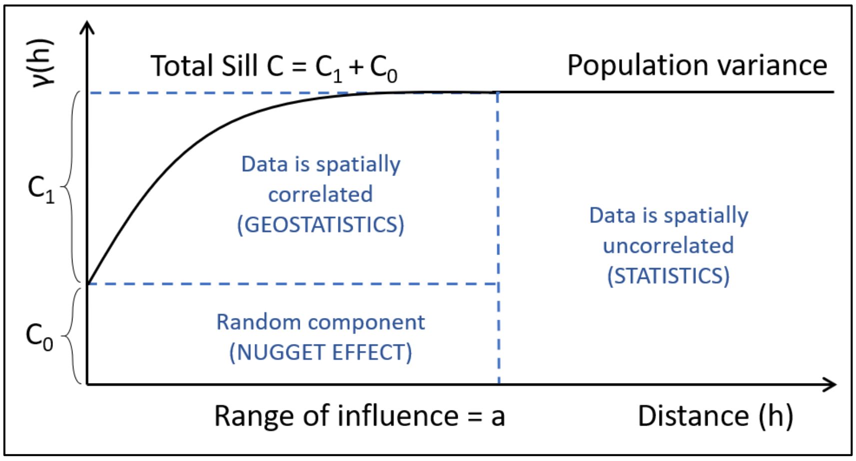

Figure 2-1: Simple variogram. Adapted from Dohm (2018).

2.4.2 The Nugget Effect

The nugget effect has a significant impact on kriging results and may be the most important feature to consider when modelling the semi-variogram for each scenario. An over-estimated nugget effect leads to overly smoothed estimates, with all blocks displaying a similar mean. This makes selective mining impossible and will lead to the incorrect assignment of payable ore. Similarly, under-estimation of the nugget effect will result in overly selective mining, also resulting in the incorrect assignment of payable ore (Morgan, 2011).

The nugget effect ("C_0" in Figure 2-1) is an indication of the inherent variability of grades within an orebody. The nugget effect can be explained as the variance observed in repeat samples; in samples taken directly adjacent to one another; or as samples spaced at a distance less than the smallest distance between samples. Rossi and Deutsch (2014) noted that the nugget effect incorporates this very short-scale structure near the origin, as well as errors associated with sampling.

2.4.3 The Sill

The sill ("C" in Figure 2-1) is the level at which the semi-variogram plateaus, indicating the semi-variogram value where samples no longer have spatial correlation. The sill can be described as the best estimate of the population variance of the deposit. Importantly, the level of the sill for different scenarios may change as additional data is added to a dataset. Kriging weights are mostly unaffected by the longest sill structure in a nested model, so painstaking precision is not necessary to adequately model this level, (Guibal, 2001).

2.4.4 The Range of Influence

The range of influence ("a" in Figure 2-1) is the distance at which samples become spatially uncorrelated and geostatistical methods can no longer be applied to the data. This distance occurs when the semi-variogram model stabilises or plateaus as it approaches the sill. Kriging weights and estimation search distances are critically affected by short range variogram structure, (Guibal, 2001) and therefore, the short-range structure for all scenarios will be modelled with careful consideration.

2.4.5 Anisotropy

If present, a preferred direction of continuity in the ore values is a feature of the spatial structure of the deposit. Continuity directions are best understood when the geological model is well defined as the mineralisation style is fully understood.

A variogram map, or variogram contour plot, is a useful tool to help visualise preferential continuity directions in the data. The variogram must be studied in conjunction with the geological model at various directions to determine the preferred direction of continuity, (Guibal, 2001).

2.5 Local Estimation

As a project advances and additional drilling information is accumulated, local block estimates based on the spatial distribution captured by the semi-variogram may improve the resource estimate. Local estimates are commonly used for short- and medium-term planning as the ore and waste classification is effectively defined using smaller blocks, (Sinclair and Blackwell, 2004). In this research, local estimation techniques were applied to scenarios that represent more advanced project phases.

Kriging is a spatial estimation technique used to allocate optimum weighting to sample values to calculate the best unbiased linear estimate with minimum estimation variance between the estimated grade and the sampled grade. This process is dependent on the semi-variogram model that describes the inherent spatial variability of the samples within a geozone.

Ordinary kriging relies on the assumption of stationarity. Isaaks & Srivastava (1998) state that the underlying distribution of the random variable of interest is the same within a stationary domain and there is no trend in the data. Well-defined geozones of homogenous (stationary) statistical and geostatistical characteristics are required to produce reliable kriged estimates without under- or over-estimation.

Ordinary kriging is still the most commonly applied technique in Mineral Resource estimation. Ordinary kriging is used for interpolation of data and is a good indicator of possible trends as the mean is continuously re-estimated within each search neighbourhood, (Rossi and Deutsch, 2014). The Lagrange multiplier is introduced to constrain the sum of the sample weighting to one, thus ensuring the ordinary kriged estimate is unbiased.

Simple kriging may be used in scenarios where the local mean value is assumed known and stationary (Rossi and Deutsch, 2014). Simple kriging utilises an unconstrained set of equations and assigns an appropriate weight to the known local mean value, (Sinclair and Blackwell, 2004). The authors also noted the extensive application of simple kriging to gold deposits in South Africa due to large amounts of data from which the local mean grade can be determined.

Indicator kriging involves the use of simple or ordinary kriging to estimate an indicator variable (Sinclair and Blackwell, 2004). An indicator variable is a variable that has been transformed to either a 0 or 1. The resultant indicator kriging estimates represent the probability of the variable being above or below an indicator cut-off value. This technique can be used to estimate relative proportions of continuous data above a threshold, such as channel width, as presented in this research, or other characteristics such as ore versus waste when the indicator is applied to grades.

Various kriging performance indicators are analysed to assess the quality of an estimate. The kriging variance, slope of the regression, weight to the mean, kriging efficiency, Lagrange multiplier, and the sample weights are some measures to consider when assessing the conditional bias and confidence in the estimation methodology followed (Deutsch *et al*., 2014).

Kriging variance is the minimum estimation variance between the estimated value and the sample value, and a low kriging variance indicates a smaller error. The kriging variance is only dependent on the spatial correlation (as described by the semi-variogram) of the sampling configuration between the data as well as the block to be estimated (area A for 2D or volume for 3D). In terms of the semi-variogram, the kriging variance is defined as:

$$KV = \Sigma w_i \bar{\gamma}(z_i, A) - \bar{\gamma}(A, A) + \lambda \qquad \textit{Equation 7}$$

Where w_i is the weight of the variable of interest at location i, $\bar{\gamma}$ is the average semi-variogram model value describing the spatial relationship between z_i, the variable of interest at location i, and the block, A. λ is the Lagrange multiplier (Clark and Harper, 2000).

2.6 The Information, Support, and Regression Effects

The information effect, support effect, and regression effect explain how sampling may affect estimation results (Dohm, 2018). The information effect is observed when limited data is used to generate the resource model. Rossi and Deutsch (2014) state that the information effect must be understood and explain that a long-term resource model is not suitable for ore/waste-block decision making. However, the short-term resource model, with closely spaced data, will enable better ore/waste-block decision making due to the increased amount of available data once mining has commenced.

The support effect refers to the change in variance as the support increases from samples to blocks and is also captured by the volume-variance relationship, (Dohm, 1995). The support effect is observed when the variance of samples and blocks usually at different support are considered in the estimation process.

Rossi and Deutsch (2014) graphically represent the volume-variance effect on the estimated tonnage above a certain cut-off in Figure 2-2. Even though the mean grade estimate of different distributions will remain the same, the variance will decrease as volume (block size) increases, because of the averaging of sample values within blocks. A point (sample) distribution will always have a larger variance than a block distribution for the same attribute (Rossi and Deutsch, 2014).

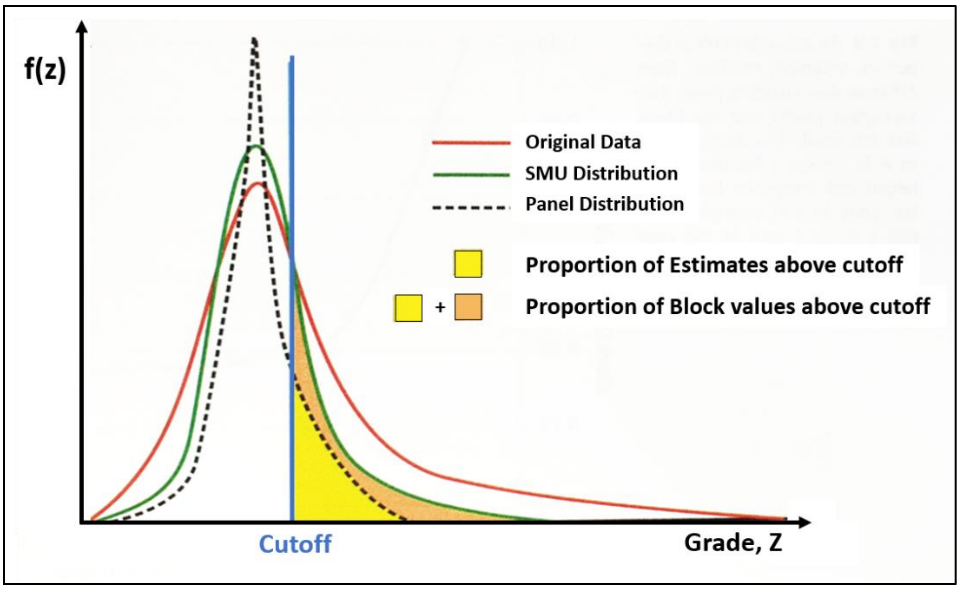

Figure 2-2: Volume-variance relationship between original data, SMU distribution and panel distribution (adapted from Rossi and Deutsch, 2014, p123)

The proportion of block estimates above a specific cut-off will change for blocks of different sizes as presented in Figure 2-2. Practically, this means that the actual tonnes mined at the SMU block size will be more than the tonnes planned based on the panel estimate block size, for the same cut-off grade. Both the information effect and the support effect influence the regression effect; the overestimation of high values and the underestimation of low values, (Dohm, 2018).

2.7 Conditional Bias

Krige recognised a statistical regression approach to eliminate conditional bias in resource estimates (Vann *et al*., 2003). This statistical approach led to the development of spatial geostatistics and the kriging technique. An overview of this literature is summarised in Krige (1981). Kriging is the best linear unbiased estimator. However, in reality, kriging will only be unbiased if the distribution is normal and the mean is known (, 1977)

David (1977) described a property of kriging which states that when blocks are estimated to have a particular grade (Z^*_v) the blocks will, <u>on average</u>, have that grade (as cited in Vann, 2003). Vann (2003) explains this further by stating that during kriging some estimated blocks (Z^*_v), will be higher than the mean grade and some estimated blocks (Z^*_v), will be lower than the mean grade. However, when the high-grade blocks are on average too high, and the low-grade blocks are on average too low, we observe conditional bias.

In 1996, Krige stated that estimates must be conditionally unbiased, however Isaaks (2004) stated that "*a conditionally unbiased and accurate predictor is an oxymoron*". He concluded that although conditional bias will most likely always exist, it can be minimised. The correlation between the estimated block grades (Z^*_v), and true grades (Z_v) will never be equal to one, due to the lack of information when calculating block estimates Vann (2003).

Krige (1996) describes the effect of the data accessed on conditional bias and stresses the importance of model validation using statistical techniques. Isaaks (2004) notes that methods applied to manage the information and the support effect may be useful. Isaaks (2004) stated that conditional bias must be recognised and understood.

Figure 2-3 presents the regression between estimated block grades (Z^*_v), and true grades (Z_v) and highlights how conditional bias can lead to the misclassification of ore and waste blocks at a specific cut-off value. The ellipse represents the scatter plot of the block grades (Z^*_v) versus the true grades (Z_v). Misclassification occurs due to the regression of the true values given the estimated value.

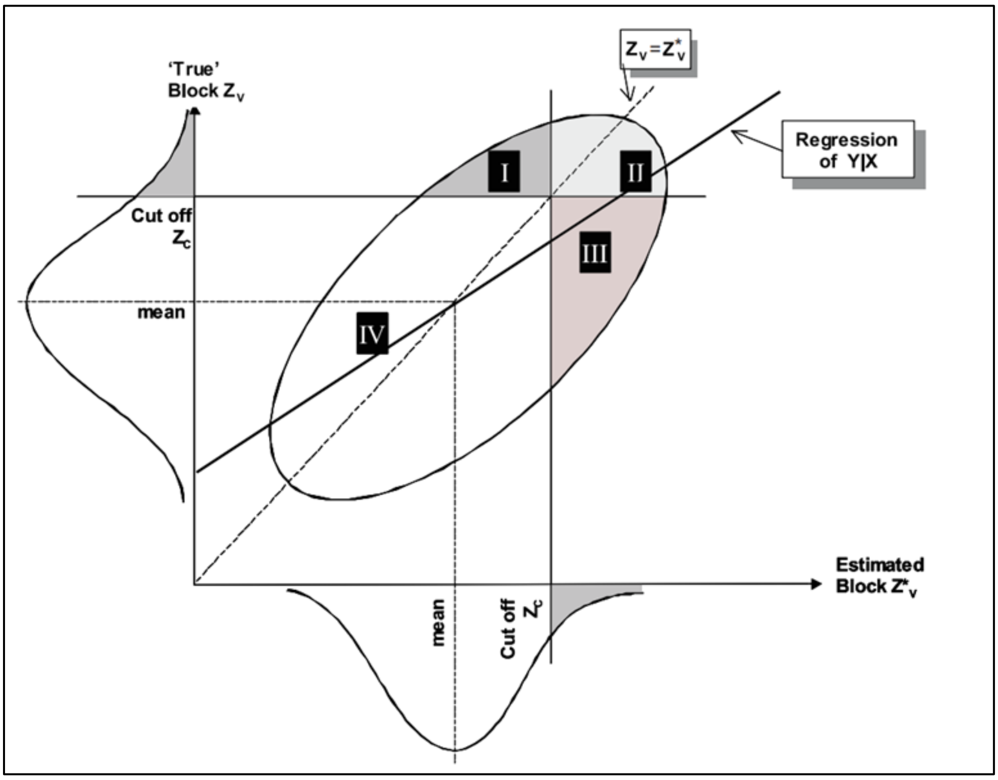

Figure 2-3: Information effect diagram showing linear regression (from Vann et al., 2003)

At cut-off value Zc:

- Quadrant II is correctly classified as ore,
- Quadrant IV is correctly classified as waste,
- Quadrant I is incorrectly classified. The blocks are estimated to be below the cut-off but are actually payable at cut-off Zc,
- Quadrant III is incorrectly classified. The blocks are estimated to be above the cut-off but are actually unpayable at cut-off Zc.

Deutsch (2007) describes the solid black line in Figure 2-3 as the regression of the true values (Z_v) given (conditioned) by the estimated values (Z^*_v), which is an indication of conditional bias in the estimate results and is represented by the equation:

$$E\{Z_v|Z_v^* = z\} \cong a + bz \neq z \qquad \textit{Equation 8}$$

In words, this equation can be expressed as the expected true value of the block given the estimated value for the block, which is equal to a specific value, *z* (for example 1%Cu), which is approximately equal to the intercept, *a*, added to the slope, *b*, multiplied by the specific value, *z*, and is not equal to the specific value, *z* (for example 1%Cu). This is due to the skewness presented in the sampling distribution as presented on the y-axis in Figure 2-3.

Measures for conditional bias are the slope of regression and the kriging efficiency. Mapping the kriging variance indicates the relative estimate quality but maps of the slope of regression are more useful (Vann et al., 2003).

The slope of regression (SLOR), ideally equal to one for a conditionally unbiased estimate, defines the relationship between the estimated block value and the true block value. A high slope of regression indicates that the results tend towards one, and a low slope of regression indicates a poor relationship between the estimate value and the true value. Clark, 2015, presents the slope of regression as:

$$SLOR = \frac{\sigma_B^2 - \sigma_k^2 + \lambda}{\sigma_B^2 - \sigma_k^2 + 2\lambda} \qquad \textit{Equation 9}$$

Where σ_B^2 is the block variance, σ_k^2 is the kriging variance, and λ is the Lagrange multiplier (Clark, 2015).

Kriging efficiency (KE) is a measure of the efficiency of the block estimate methodology (Krige, 1997). A high kriging efficiency, ideally equal to one, means that the variance of the block estimates is approximately equal to the variance of the true block values (Deutsch *et al*., 2014) and is observed together with a low kriging variance. A low kriging efficiency indicates poor kriging methodology. The kriging efficiency is defined by Krige 1997:

$$KE = \frac{\sigma_B^2 - \sigma_k^2}{\sigma_B^2} \qquad \textit{Equation 10}$$

Where σ_B^2 is the block variance and σ_k^2 is the kriging variance.

Block variance is a constant value calculated using the total variance for a fixed variogram (the sill) and for a fixed 2D block size and is represented by the equation:

$$\sigma_B^2 = \sigma^2 - \bar{\gamma}(A, A) \qquad \textit{Equation 11}$$

Where σ_B^2 is the total variance and $\bar{\gamma}$ is the semi-variogram model value describing the spatial variability relationship of the fixed 2D block size, A (Clark and Harper, 2000).

A practical analysis done by Krige (1997) investigated the effect of spatial structure on conditional biases in ordinary kriging. Krige identified that poor kriging efficiencies corresponded to a poor slope of regression, poor spatial structure, and low numbers of data. This research compared different scenarios of increasing data density and the effect on the kriging efficiency.

2.8 Mineral Resource Classification

The South African Code for the Reporting of Exploration Results, Mineral Resources and Mineral Reserves (the SAMREC Code) outlines the minimum standards, recommendations and guidelines for technical and Public Reporting of Exploration Results, Mineral Resources and Mineral Reserves in South Africa (SAMREC Code, 2016).

The SAMREC Code (2016) states that Mineral Resource estimation is inherently subject to some level of uncertainty and inaccuracy and that the uncertainty in the estimates should be discussed in documentation and reflected in the appropriate choice of Mineral Resource categories.

Resource classification changes from Exploration Target to Mineral Resource, categorised into Inferred, Indicated, or Measured, with increasing geoscientific knowledge and confidence. The SAMREC Code defines an Exploration Target as a "*statement or estimate of the exploration potential of a mineral deposit in a defined geological setting where the statement or estimate, quoted as a range of tonnes and a range of grade, relates to mineralisation for which there has been insufficient exploration to estimate Mineral Resources*". Furthermore, an Exploration Target may not form part of any Mineral Resource tabulation or be used in a Technical Study or economic assessment.

The SAMREC Code defines a Mineral Resource as "*a concentration or occurrence of solid material of economic interest in or on the Earth's crust in such form, grade or quality and quantity that there are reasonable prospects for eventual economic extraction. The location, quantity, grade, continuity and other geological characteristics of a Mineral Resource are known, estimated or interpreted from specific geological evidence and knowledge, including sampling*."

The SAMREC Code is not prescriptive, and the Competent Person will allocate the Mineral Resource into Inferred, Indicated and Measured based on several criteria. Geometric criteria, such as drillhole spacing, are easily understood, and thresholds should be based on industry best practice, the type of deposit, calibration with uncertainty quantified by geostatistics, and expert judgement (Deutsch, et al., 2007). Probabilistic resource categorisation using conditional simulation, provides uncertainty quantification and may be used as classification support in conjunction to geometric criteria ((Deutsch, et al., 2007). Ultimately, the Competent Person is responsible for classification criteria that discloses the uncertainty associated with the Mineral Resource and appropriately conveys financial risk (Rossi and Deutsch, 2014).

2.9 Chapter Summary

This chapter summarises important literature relevant to this research study. A brief discussion on the importance of geological domaining highlights the impact thereof on the variogram model and resultant geostatistical results. Exploratory data analysis is briefly described. A statistical approach to global estimation is summarised, including the Sichel t estimator and 2-parameter lognormal distribution.

The semi-variogram is explained with reference to important semi-variogram features, such as the sill, the range, and the nugget effect. A geostatistical approach to local estimation is summarised, including a brief description of ordinary kriging, simple kriging, and indicator kriging.

The literature review discusses the three effects of how sampling may affect the estimation results, namely: the information effect, the support effect and the regression effect. An overview of conditional bias, and two measures thereof, the slope of regression and kriging efficiency, are also provided.

3 GEOLOGICAL BACKGROUND

This chapter provides a summary of the reviewed geological literature describing the formation of the Witwatersrand Basin as well as geological characteristics of the Ventersdorp Contact Reef (VCR).

3.1 Regional Geology

The VCR is developed in at least five of the major Witwatersrand Basin goldfields including the Welkom, Klerksdorp, Carletonville, West Rand and Central Rand goldfields (Figure 3-1). In 1998, Robb and Robb, tabled a conservative estimate at the time of 3081 tonnes of gold produced from the VCR in the Klerksdorp, Carletonville and West Rand goldfields.

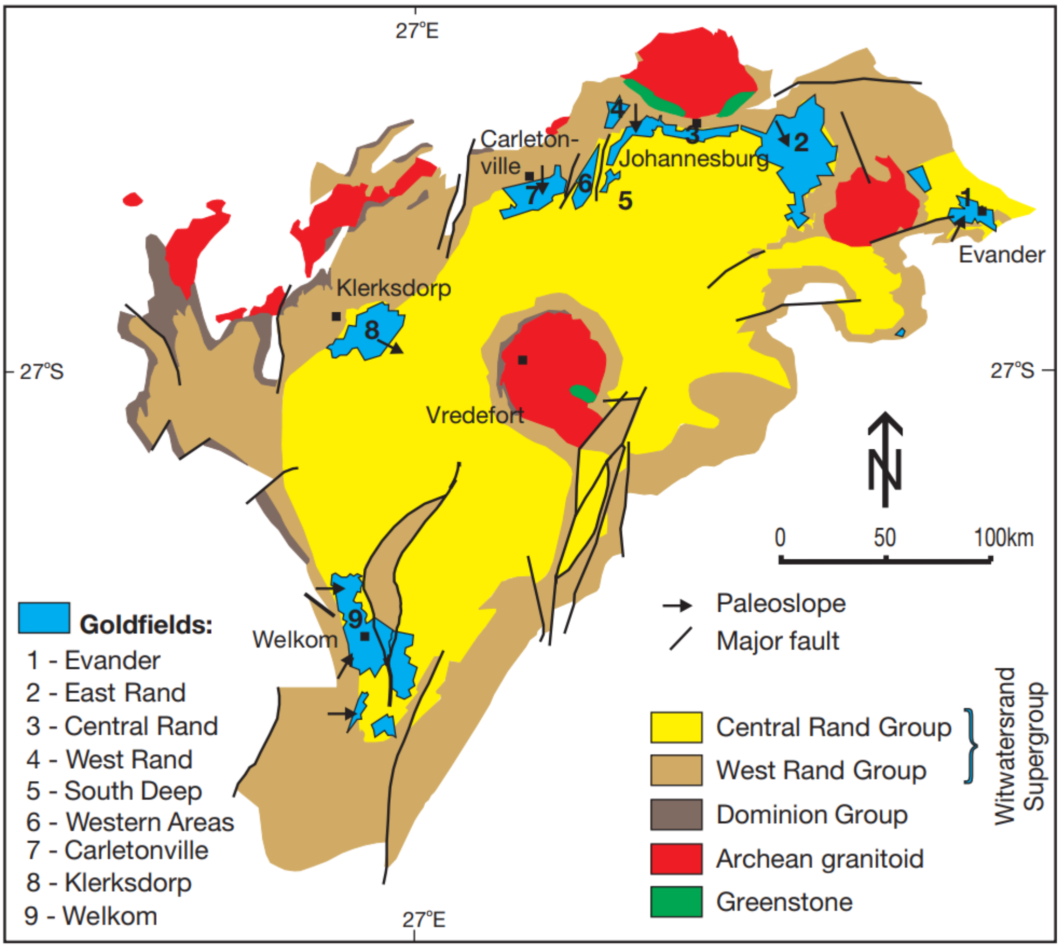

Figure 3-1: Map depicting the location of goldfields within the Witwatersrand Basin (Frimmel et al., 2005, after Frimmel and Minter, 2002)

The Witwatersrand Basin formed because of plate tectonic activity in an Archaean greenstone-granite gold-bearing terrane, (McCarthy, 2006). A phase of crustal extension prior to the development of the Witwatersrand Basin resulted in the extrusion of the Dominion Group lavas and sediments at approximately 3074 ± 6 Ma, (Armstrong *et al*., 1991; Jolley *et al*., 2004) forming the basement of the overlying Witwatersrand Supergroup (Armstrong *et al*., 1991).

This crustal extension was followed by subduction from 3.08 Ga to 2.64 Ga, leading to the formation of the intracontinental Witwatersrand Basin (Frimmel *et al*., 2005). Robb *et al*. (1991) suggested that the sediments deposited into the Witwatersrand Basin represent a tidally dominated epicontinental sequence deposited into a fluvio-deltaic-dominated foreland basin. The Witwatersrand Supergroup is divided into the lower West Rand Group and upper Central Rand Group.

The West Rand Group is characterised by a meta-sedimentary sequence of sandstone and shale attaining a maximum thickness of 5150 m in the west and thinning to 830 m in the east, (Robb and Robb, 1998). The West Rand Group is divided into the Hospital Hill, Government and Jeppestown Subgroups based on the ratio of sandstone to shale as well as observed separational unconformities (Robb and Robb, 1998).

The Central Rand Group (CRG) is characterised by a meta-sedimentary sequence dominated by sandstone, conglomerate and minor shale attaining a maximum thickness of 2880 m and thinning to 650 m towards the southeast, (Robb and Robb, 1998). The CRG (Figure 3-2) is divided into the lower Johannesburg Subgroup and the upper Turffontein Subgroup. The most important gold-bearing conglomerates occur within the CRG and are recorded to have yielded approximately 40% of the world's total gold production (Gartz and Frimmel, 1999).

Some interesting research by McCarthy and Ogilvie (2020) revisits the glacial theory for the depositional environment of the Witwatersrand conglomerates. However, this theory has not been further explored in this research

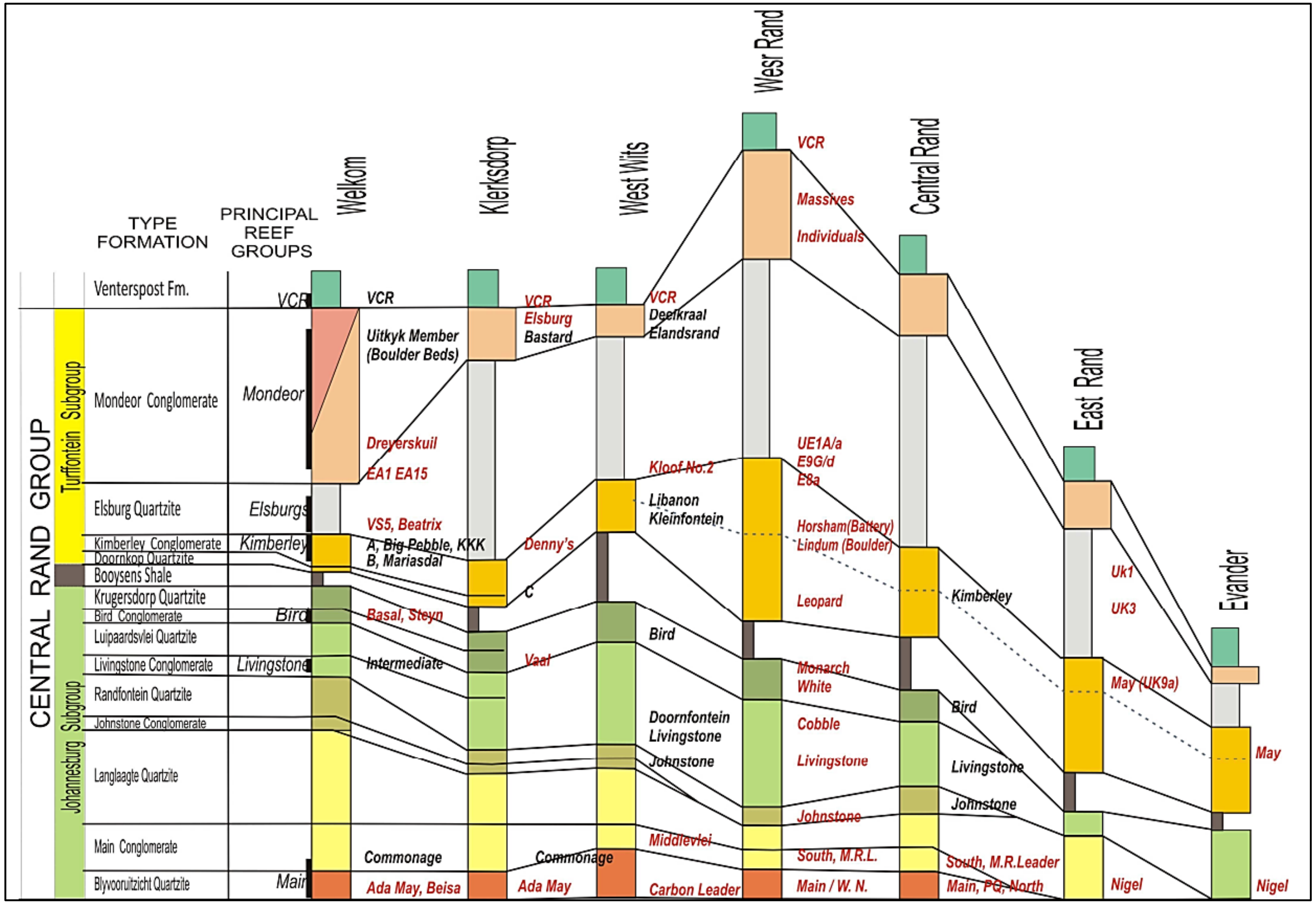

Figure 3-2: Stratigraphy of the VCR and Central Rand Group with important reefs indicated in red (Tucker et al., 2016, after SACS, 1980; McCarthy, 2006 and Pretorius, 1974)

3.2 The Ventersdorp Contact Reef Geology

Although widely regarded as one of the famous Witwatersrand Supergroup gold reefs, the VCR was deposited onto the completely lithified units of the CRG, (McCarthy, 2006). The VCR is the basal conglomerate of the Venterspost Formation at the base of the Ventersdorp Supergroup as presented stratigraphically in Figure 3-2 (Tucker et al., 2016). Evidence of a hiatus before VCR deposition is indicated by the pronounced angular unconformity of 4° to 15° between the VCR and the underlying CRG, (Hall *et al.*, 1997). The VCR was dated at 2729 ± 19 Ma using U-Pb zircon SHRIMP analyses by Kositcin *et al*. (2003).

Viljoen and Reimold (1994) noted that compressional tectonic forces active in the north-western margin of the Witwatersrand Basin were responsible for the sediment source and the depositional environment of the basin. At 2714 ± 8 Ma an extensional event resulted in the extrusion of the Klipriviersberg Group flood basalts of the Ventersdorp Supergroup and the VCR deposition was abruptly terminated (Armstrong *et al*., 1991).

These active tectonic controls during the VCR deposition led to the formation of different VCR types in different areas of the Witwatersrand Basin. McCarthy (1994) described a Western Deep Levels VCR Type as an extensive conglomerate sheet with widespread mineralisation over variable palaeotopography on a low angle of unconformity (erosional or slope and terrace model), and a South Deep VCR Type, which is characterised by a narrow zone of mineralisation which degenerates basin-ward into numerous bands of conglomerate and internal sand partings (stratigraphic model).

Extensive research by McWha (1994), Henning et al. (1994) and Germs and Schweitzer (1994) as well as collaboration of the Regional VCR Working Group (1991 - 1994), resulted in the development of the slope and terrace model, now commonplace on Western Deep Levels operations. The fluvial depositional environment, varying footwall lithology and angle of unconformity resulted in the formation of a series of slopes (risers) and flatter terraced areas of VCR at different elevations (refer to Figure 3-3 for a simplified interpretation of the slope and terrace model). The palaeotopography is the reason for the highly irregular reef thickness, with thicker channel width deposits occurring on the terraced areas separated by thinner channel width slope areas.

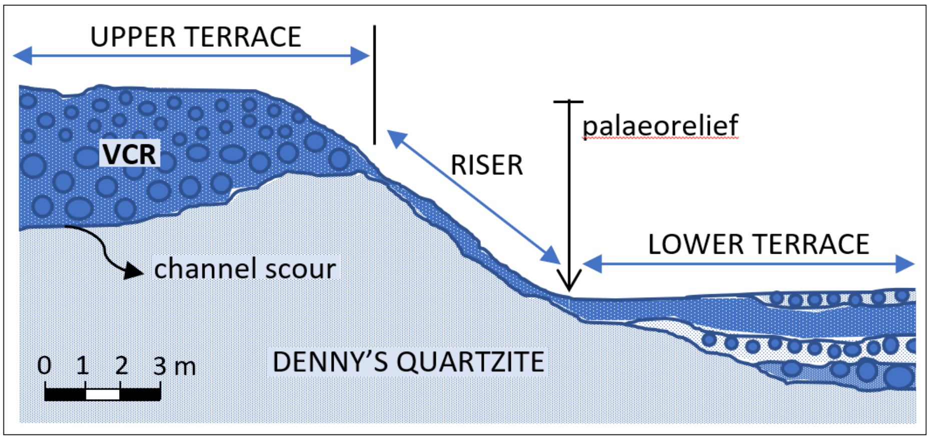

Figure 3-3: Mapped VCR section illustrating the slope (riser) and terrace model. Adapted from Henning et al. (1994).

A focus of the Regional VCR Working Group was the regional channel width plan. This plan enabled correlation of channel width to footwall rock type and aided in the delineation of numerous directional palaeochannels (Regional VCR Working Group, 1994).

The VCR is notably different to younger CRG reefs. Some of the distinguishing characteristics of the VCR may include the presence of a green or dark coloured matrix, highly irregular reef thickness, the occasional presence of inter-reef lavas, and the inclusion of very large clasts, (Hall *et al.*, 1997). A major difference is the widespread alteration of the VCR caused by the overlying Klipriviersberg Group flood basalts (Gartz and Frimmel, 1999). Frimmel *et al*. (2005) regarded the mafic composition of the overlying flood basalts as the reason for the different mineralogy observed in the VCR as compared to other CRG reefs. The mineralogy is composed of quartz, chlorite, muscovite, sericite, pyrite, pyrrhotite, bornite, sphalerite, chalcopyrite, and galena (Henning *et al*., 1994; Zhao *et al*., 1994).

3.3 The Ventersdorp Contact Reef Mineralisation

Gold mineralisation is partly due to the erosion of the underlying CRG reefs (McCarthy, 1994) and is thought to have undergone localised re-mobilisation by metamorphic fluids derived from the basin (Zhao *et al*., 2006 as cited in Tucker *et al*., 2016).

Higher gold grades are generally associated with terraced VCR deposition and lower gold grades with the thinner sloped VCR deposition. Dohm (1995), showed that at Elandsrand, the VCR gold value and channel width show a positive linear correlation for channel widths up to approximately 20 cm, thereafter the gold value shows high variability that is more pronounced for channel widths between 20 cm to 40 cm.

McWha (1994) noted that understanding the distribution of the terraces and slopes at Western Deep Levels South Mine was required for resource estimation due to the higher total gold content in the terrace reef. He further noted that although slope reef (typically less than 30 cm) can have a higher gold grade, the total gold content is lower than terrace reef due to the decreased thickness of the slope reef.

Smits (1994) noted that gold mineralisation in the VCR is more erratic than observed in the CRG reefs due to the coarseness of the predominantly authigenic gold which precipitated after remobilisation. Coarse gold will contribute to the nugget effect and increased variability. Jolley et al. (2004) studied the thrust-fracture array associated with Early Klipriviersberg deformation as a control on hydrothermal gold mineralisation and noted that the structural deformation, and therefore fluid flow, is partly controlled by the underlying footwall lithology, nature of the VCR as well as the thrust size and geometry.

The elevated grade variability in the VCR was highlighted by Krige (1993). In a study dataset of 2924 samples, the untransformed relative variance decreased by 96%, from 12.29 to just 0.545, by the removal of one high-grade outlier with a value of 70915 cm.g/t. Krige (1993), showed that the variance for the VCR (Mixed Facies) is higher than most other CRG reefs and the range observed for the slope of regression is larger compared to other CRG reefs.

The erratic palaeotopography and erratic mineralisation make estimation of the VCR gold grade difficult (McWha, 1994). The Bayesian approach using known *a priori* information plays an important role in resource estimation with limited data due to the high variability in grade and spatial characteristics of the VCR (Krige, 1993).

3.4 Geological Background Summary

In summary, the VCR is the basal conglomerate of the Venterspost Formation at the base of the Ventersdorp Supergroup unconformably overlying the Central Rand Group of the Witwatersrand Supergroup. During reef deposition active tectonic forces resulted in the deposition of different VCR types in different locations within the Witwatersrand Basin. The VCR channel width displays considerable thickness variation due to the underlying lithology type, palaeotopography, the angle of unconformity, and other factors. Extensive research led to the development of the Slope of Terrace model which assisted with geozone delineation as there is a correlation between gold mineralisation and reef thickness on some mining operations. The VCR gold grade mineralisation shows high variability and therefore a high nugget effect due to local gold remobilisation.

4 DATA VALIDATION

The dataset used in this research was created from the “Deep Mine– Mining for the Future Research Project (1998 – 2001)” of the then Chamber of Mines Research Organisation (COMRO). Various mining houses participated in the project and provided original Ventersdorp Contact Reef (VCR) sampling data for the COMRO Deep Mine project. The Mineral Resource branch of the project focussed on the creation of improved models of grade and spatial distribution of the gold values to be used in the Deep Mine Project investigations. The dataset used for this research is a subset of realistic sampling from one realisation of the conditional simulations of the original grade data. All sampling grids for the Scenarios are generated from this simulated dataset requiring the assumption of negligible sample support difference between surface drillholes and underground channel sampling.

The 2D dataset is typical for a South African deep level underground gold mine, consisting of raise lines and reef drives (sampled at roughly every 2 m), panels with an average length of 30 m (sampled at 5 m intervals after roughly every 10 m mining advance) and widely spaced surface drilling data. The data covers an area of approximately 2 km^2.

Quality control is vital throughout the Mineral Resource estimation process. For the purposes of this project, it was assumed that the data collection methodology (sampling and assaying) used as input for the Deep Mine project had undergone a compliant quality assurance and quality control process in accordance with the SAMREC Code and that no bias was introduced by these methods.

Dominy *et al*. (2004) affirms that data quality should be considered and audited at every stage of a project. Sinclair (1998) listed the first aim of exploratory data analysis as: “*to recognise and eliminate errors*”. The dataset in this study was checked for errors before the smaller data subsets were generated. The original dataset initially consisted of 11887 datapoints.

The original dataset was checked for exact duplicates, XY location duplicates, zero grade values, zero channel width values and unrealistic channel width values. Exact duplicates (907) were removed from the dataset, and it was noted that data overlapped in specific areas. Coordinate duplicates (44) were removed from the dataset which indicated that some repeat samples may have been included in the original dataset. An additional three datapoints (3) were removed due to unrealistic channel widths. These unrealistic channel widths ranged from 711 cm to 811 cm and were presumed to be transcription errors.

The resultant final validated dataset consisted of 10933 datapoints of sufficient quality for Mineral Resource estimation. The data were rotated by 22° to orientate the raise line sampling in a north-south direction.

4.1 Scenario Data

Five smaller data subsets were generated from the validated simulated dataset, resulting in a total of six datasets that will represent six different scenarios of increasing sample density (Figure 4-1). The data increase for each scenario in the case study has been governed by a representative and systematic sampling protocol that adheres to the practicalities of the deep-level underground resource development. As sampling has not targeted specific areas of economic interest; data declustering was not considered necessary for statistical and geostatistical analyses or model validation.

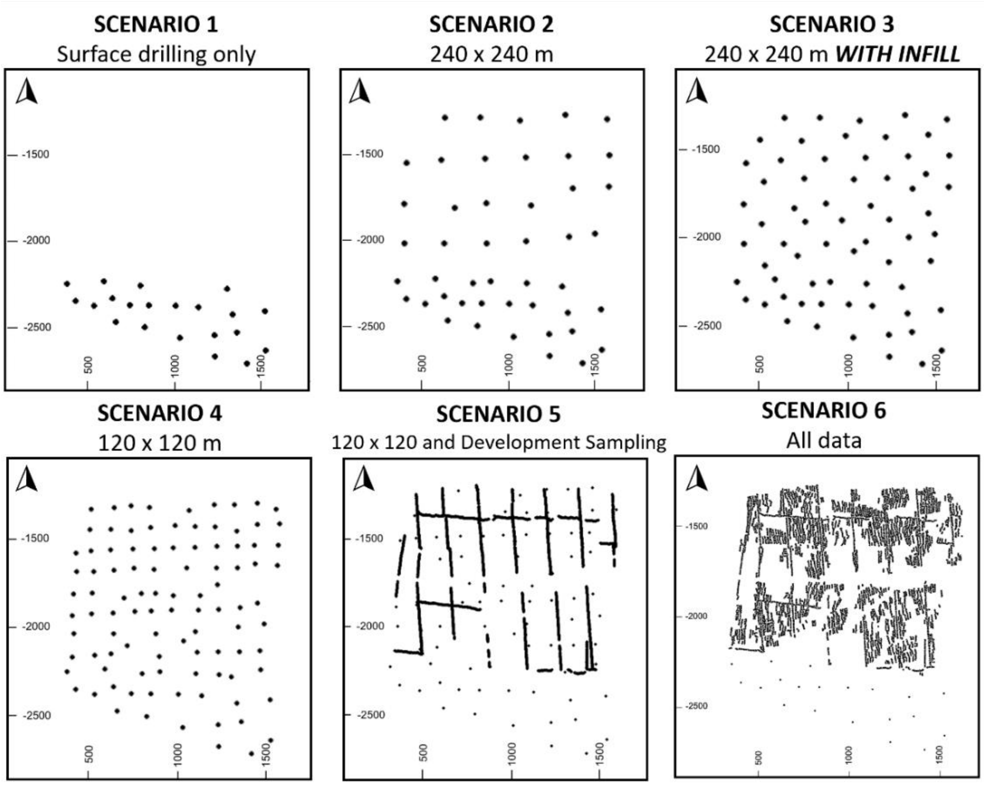

Figure 4-1: Sampling location plots of the six scenarios

Scenario One contains 21 datapoints. It represents the initial drilling phase of an exploration project and contains only surface drilling data over a limited area.

Scenario Two contains 46 datapoints. The data spacing is approximately equal to 240 m x 240 m which represents a second surface drilling phase over a larger area.

Scenario Three contains 66 datapoints. The data spacing includes infill drilling within the previous 240 m x 240 m drilling grid resulting in a data spacing of roughly 200 m x 200 m.

Scenario Four contains 99 datapoints. It represents an advanced drilling phase and the data spacing is approximately 120 m x 120 m.

Scenario Five contains 3591 datapoints. It is a representation of resource development and includes all the surface drilling at 120 m x 120 m, in addition to all underground development sampling from raise lines and reef drives at a spacing of approximately 2 m.

Scenario Six contains 10933 datapoints. It represents data typical of an underground gold mine consisting of raise lines and reef drive sampling (at a sample spacing of approximately 2 m), panel sampling (30 m x 10 m area) consisting of composite chip samples of the channel width at approximately 5 m in the reef dip direction and 10 m in the reef strike direction (APPENDIX A) , as well as widely spaced surface drilling data.

4.2 Data Validation Summary

The dataset used for this research represents a realistic sampled subset of one realisation of a series of conditional simulations produced by the Chamber of Mines Research Organisation. The data were validated, and recognised errors have been removed. Five smaller data subsets were generated from the validated realisation to represent the development of a resource project from initial drilling to infill drilling, to advanced drilling, and finally, resource exploitation (the validated realisation).

5 SCENARIO RESULTS

5.1 Scenario One

Scenario One represents the initial drilling phase of an exploration project aimed at proving mineralisation. Figure 5-1 indicates the 21 diamond drillholes over a limited target area based on geological information that may have included regional geology studies, geophysical studies, and geological mapping.

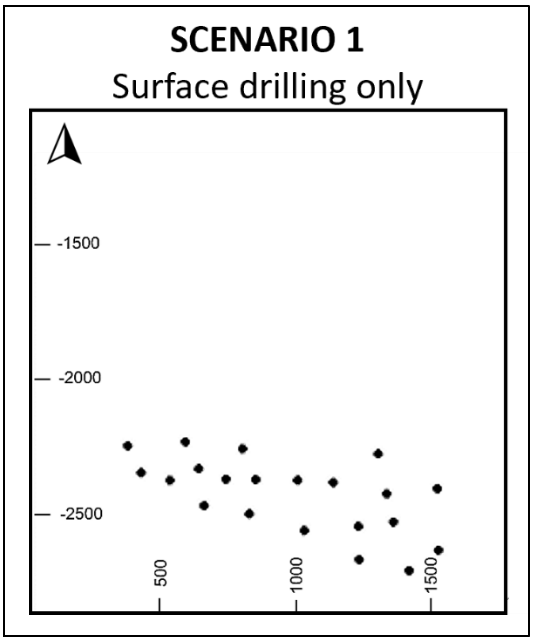

Figure 5-1: Scenario One data location

The limited number of datapoints did not allow for geozone definition in Scenario One and a global Sichel t estimate was calculated to report an Exploration Target with wide confidence limits.

5.1.1 Scenario One Geozones

Geological domaining is the process of identifying and delineating zones of homogeneous geological characteristics to reduce risk. The geological domaining methodology followed for this research focused on identifying geozones based on channel width (reef thickness) variation which is based on the slope and terrace model described in Chapter 3.2.

A colour-coded channel width plot was generated to determine if any reef thickness trends were present in order to justify geozone delineation. The colour-coded intervals were based on slope changes in the cumulative relative frequency distribution plot for channel width (Figure 5-2). The cumulative relative frequency distribution plots are generated from the individual 21 channel width intersections.

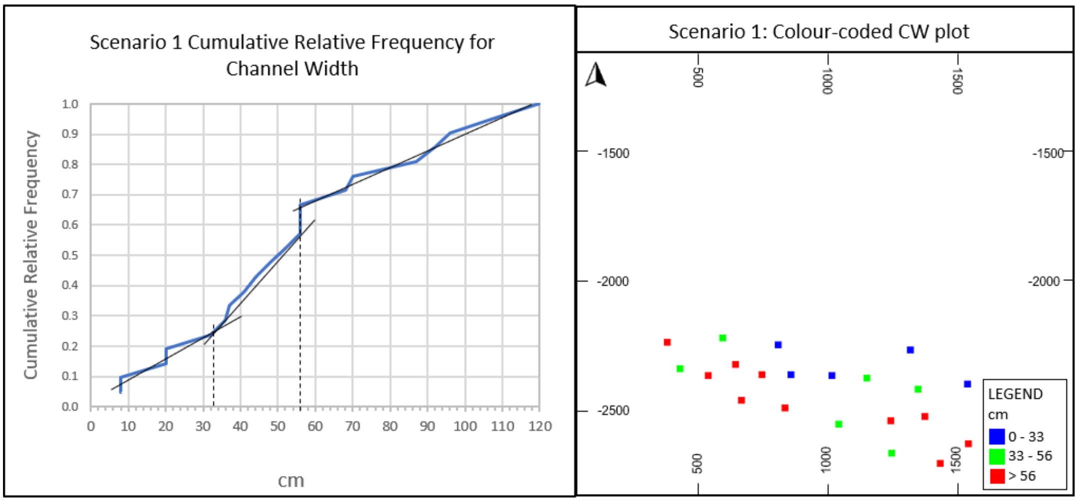

Figure 5-2: Scenario One cumulative relative frequency distribution and colour-coded CW plot

Three broad channel width intervals were identified by inflection points on the cumulative relative frequency distribution curve in Figure 5-2. No clear channel width trends were evident in the colour-coded plot of the surface drilling reef intersections.

A second colour-coded plot of the gold value (cm.g/t) was based on inflection points on the cumulative relative frequency distribution of the gold values (Figure 5-3). The data could be separated into three broad grade intervals.

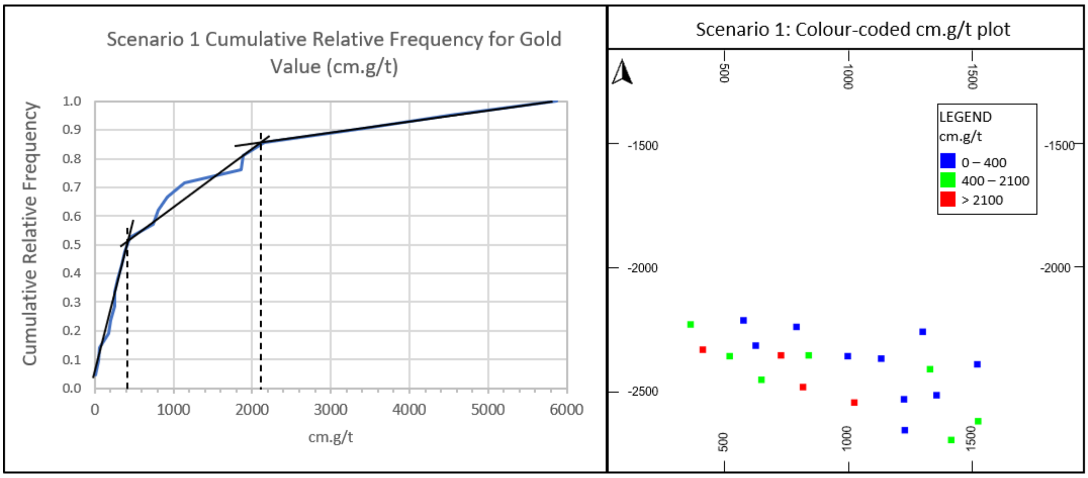

Figure 5-3: Scenario One cumulative frequency distribution of cm.g/t and colour coding intervals

Both channel width and gold value (cm.g/t) suggested that there was insufficient data to delineate meaningful geozones at the initial drilling stage of the resource development with only 21 data points.

5.1.2 Scenario One Exploratory Data Analysis

Statistical characteristics of samples may be used to estimate population parameters, and by analysing the data using different graphs, the data distribution can be understood (Davis, 2002). Table 5-1 presents the basic summary statistics for Scenario One. The log transformed data is presented for calculation of the Sichel t global estimate.

Table 5-1: Scenario One Summary Statistics

Scenario 1 Gold and Channel Width Statistics			
	cm.g/t	**ln(cmgt)**	**cm**
Min	12	2.484907	8.00
Max	5 865	8.676758	120.00
N	21	21	21
Range	5 853	6.191851	112.00
Mean	1 229	6.234003	55.00
Median	451	6.111467	52.00
Mode	-	-	56.00
Q_1	249	5.517452	34.00
Q_3	1 863	7.529943	78.50
IQR	1 614	2.012491	44.50
Variance	2 411 388	2.289745	950.57
Std Dev	1 553	1.513190	30.83
CoV	1.26	0.24	0.56

Scenario One box plots for the observed cm.g/t values and the log-transformed ln(cm.g/t) values are presented in Figure 5-4. The real space data cm.g/t box plot indicates a positively skewed distribution with the mean higher than the median and it could be assumed to be a lognormal distribution. However, the ln(cm.g/t) boxplot on the right does not reflect the symmetry expected of a normal distribution and therefore the distribution of the cm.g/t values is not a true lognormal distribution (Chamberlain, 1997) as the mean is not exactly equal to the median and is slightly negatively skewed.

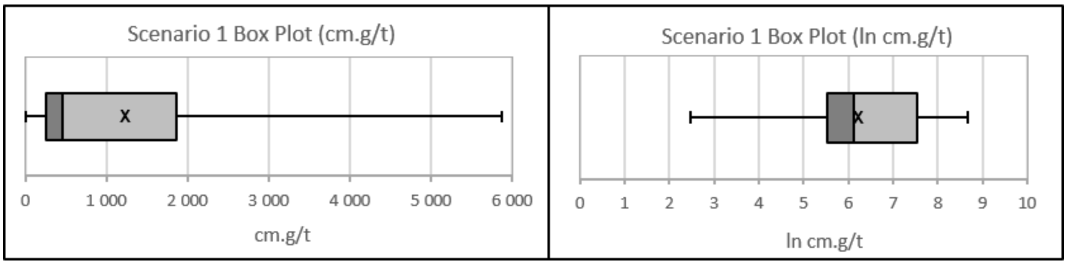

Figure 5-4: Scenario One the cm.g/t and ln(cm.g/t) box plots

Box plots represent the distribution of small datasets more adequately than histograms and associated frequency distribution polygons. With less than 50 samples, meaningful and representative histograms cannot be generated, variograms cannot be constructed, and geostatistical results become meaningless (Sichel, 1987). Davis (2002) stated that intervals that contain few observations will produce less robust histograms. There was too little data to produce meaningful relative frequency polygons at the initial drilling stage of the project.

5.1.3 Scenario One Global Value (cm.g/t) Estimate

A global mean value estimate was calculated for Scenario One. A local estimate could not be calculated as the data was too widely spaced and spatial continuity could not be captured in the variogram due to insufficient data.

The Sichel t estimator is applicable to lognormal distributions with less than 40 data points (Sichel, 1966), and is calculated using *Equation 1* as:

$$\mu^* = t = e^{\xi}\gamma_n(V)$$

$$\mu^* = e^{6.234003} \text{ x } 2.9811$$

$$\mu^* = 1523 \text{ cm.g/t}$$

The lower 90% confidence limit was 823 cm.g/t and the upper 90% confidence limit was 4716 cm.g/t. The confidence limit was calculated using the Sichel's factor Ψ 0.05 (*V*,n) upper and lower statistical tables. The high upper limit is expected for a positively skewed distribution with limited data and is noted as possible upside potential, however, the lower limit is the more important value as it identifies the minimum global mean estimate and can be used to highlight risk and influence financial decision making.

A global mean channel width estimate for Scenario One was calculated using the Student's t-distribution applicable to normal distributions with less than 30 data points.

The estimate for the mean channel width using the *t*-distribution is represented by the equation:

$$\mu^* = \bar{z} = \frac{1}{n}\sum_{i=1}^{n} z_i \qquad \textit{Equation 12}$$

$$\mu^* = 55.00 \text{ cm}$$

The confidence limits were calculated using the five percentage points of the *t*-distribution with $\mathbf{v}$ = n – 1 = 20 degrees of freedom. The lower 90% confidence limit was 35.39 cm, and the upper 90% confidence limit was 74.61 cm.

The global estimate for both the gold value (cm.g/t) and the channel width reflect relatively wide confidence intervals which indicate high uncertainty in the estimates of these means that are based on few observations. The lack of geoscientific knowledge in Scenario One resulted in low project confidence and associated high financial risk.

5.1.4 Scenario One Exploration Target

The estimate for Scenario One is reported as an Exploration Target as there is insufficient exploration to estimate Mineral Resources. The SAMREC Code (2016) states that "*there must be a likelihood that this exploration target occurs in an area of geological prospectivity for that commodity and mineralisation type*" for the reporting of exploration results. This is true for Scenario One as we know the hypothetical project in located within the Witwatersrand Basin. As mineralisation continuity could not yet be proven, the geological continuity should be confirmed by other exploration data.

Scenario One identified an Exploration Target of between approximately 0.4 million tonnes and 5 million tonnes with an average gold value (cm.g/t) of approximately 800 to 4700 cm.g/t. Values are rounded to reflect a lower level of confidence (refer to Table 5-2).

Table 5-2: Scenario One: Value-Tonnage Range

Scenario One Exploration Target					
	Area (m^2)	**CW (cm)**	**Tonnage (Mt)**	**Value (cm.g/t)**	**Grade (g/t)**
Minimum	480 000	35	0.46	823	23.26
Maximum	2 822 400	74	5.66	4 716	63.73

The upper and lower limits of the Sichel t global estimate were used to calculate minimum and maximum grades. The maximum area was calculated as the entire lease area over which the mineralisation continuity is assumed by geological information. The minimum area was calculated using a polygon delineating the drilling area only. A fixed in-situ density of 2.71 t/m^3 has been applied for tonnage calculations. At this stage of the resource development, the density testing may be relatively inaccurate due to the limited data and the tonnage calculation rounding should reflect low confidence. A value-tonnage curve is not calculated for Scenario One as a value-tonnage estimate is not appropriate at this stage of the resource development due to limited data.

5.1.5 Scenario One Summary

A limited area included only 21 boreholes for the initial drilling phase to prove mineralisation and generate investment for continuation of the resource project. At this stage of the resource development there are too few data to delineate geozones. The positively skewed distribution is best represented by a box plot. A global mean estimate is calculated for Scenario One using a Sichel-t estimator for lognormal distributions of less than 40 data points. An Exploration Target for Scenario One is represented by ranges of the minimum and maximum values as there is insufficient data to declare a Mineral Resource and the project is associated with high financial risk.

5.2 Scenario Two

Scenario Two represents the second drilling phase of an exploration project aimed at proving mineralisation over a larger area. The results of the first drilling phase are assumed to have satisfied economic criteria, resulting in additional investment for the project, and exploration continued. An additional 25 diamond drilling boreholes were drilled over the entire lease area resulting in a total of 46 datapoints. The average data spacing was 240 m x 240 m (refer to Figure 5-5).

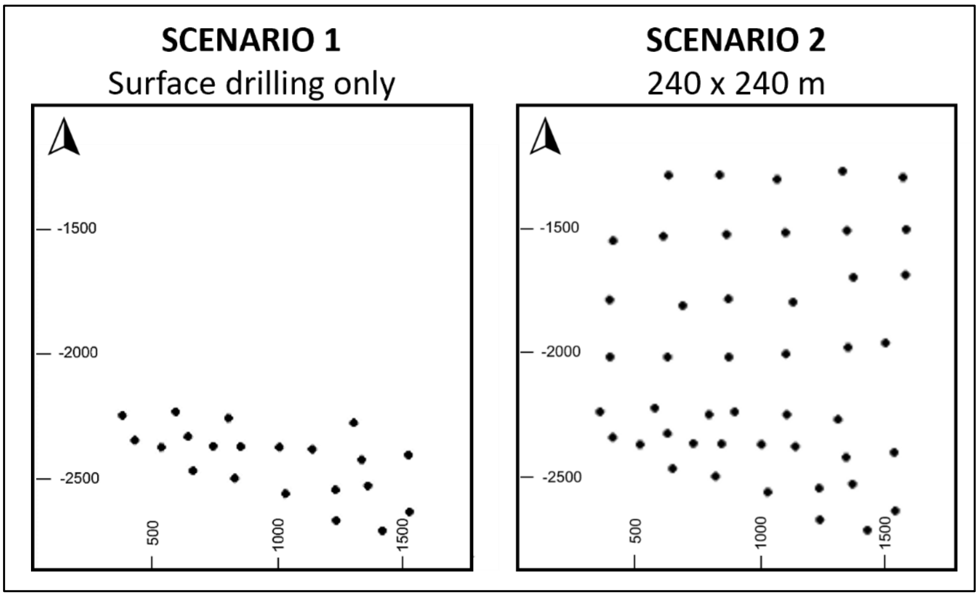

Figure 5-5: Scenarios One and Two data location

5.2.1 Scenario Two Geozones

A similar geozone domaining analysis as before was completed for Scenario Two by representing the data on a colour-coded channel width plot and colour-coded gold value (cm.g/t) plot. Although the channel width data was defined by six intervals for this scenario, a clear reef thickness trend was still not evident in the colour-coded channel width plot (Figure 5-6).

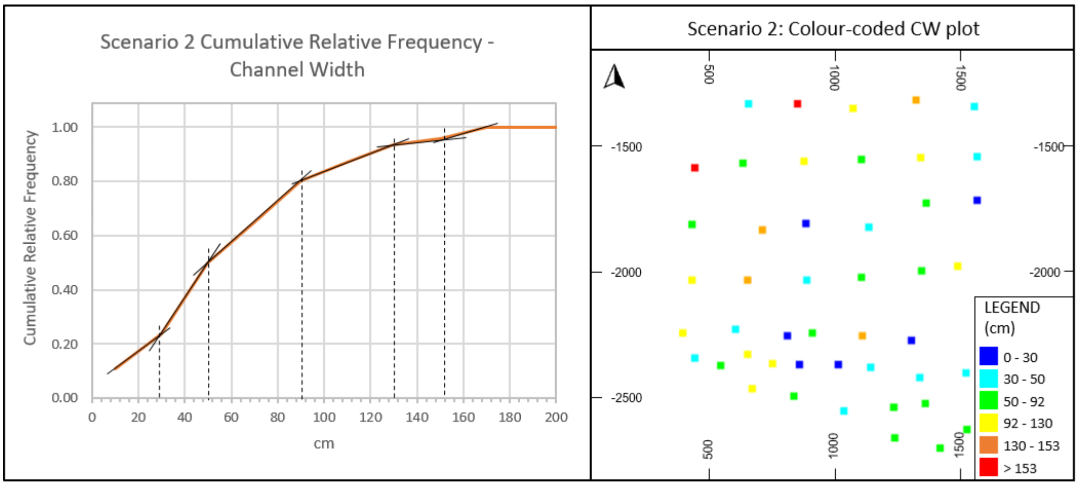

Figure 5-6: Scenario Two cumulative relative frequency distribution and colour-coded CW plot

Gold value (cm.g/t) was divided into three broad intervals (high-, medium-, and low-grade) for Scenario Two, identified using the cumulative relative frequency distribution plot (Figure 5-7), as opposed to the two intervals for Scenario One. However, a trend was still not evident in the colour-coded gold value (cm.g/t) plot.

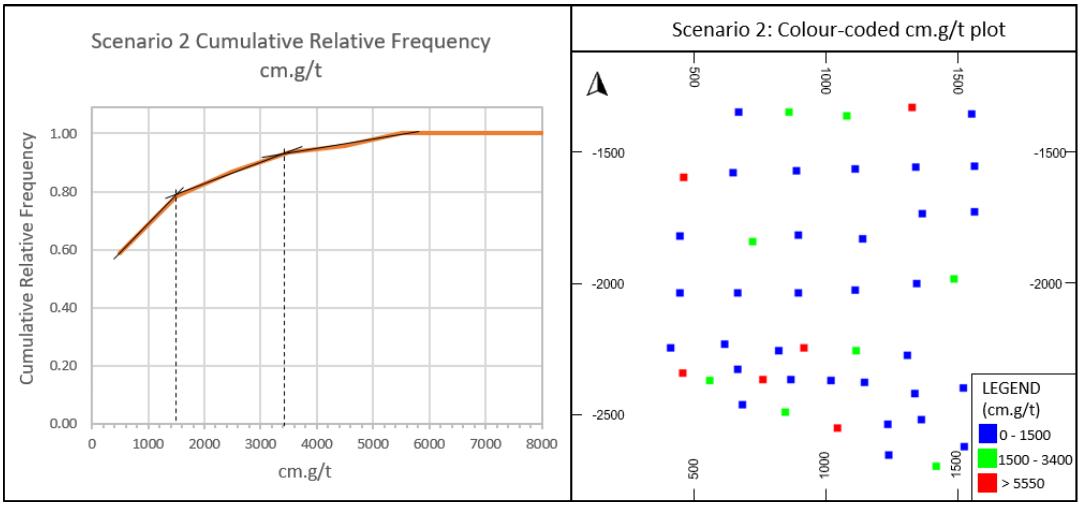

Figure 5-7: Scenario Two cumulative relative frequency distribution of cm.g/t and colour coding intervals

Scenario Two has too few data to indicate reef thickness or value trends and it is still not possible to form an opinion on geozone domains at this stage of the project.

5.2.2 Scenario Two Exploratory Data Analysis

Table 5-3 presents the statistical summary for Scenario Two. The log transformed data is also presented as this data was used to calculate the global 2-parameter lognormal global estimate.

Table 5-3: Scenario Two Summary Statistics

Scenario 2: Gold and Channel Width Statistics			
	cm.g/t	ln(cmgt)	cm
Min	12	2.484907	8.00
Max	5 865	8.676758	173.00
N	46	46	46
Range	5 853	6.191851	165.00
Mean	1 323	6.504279	71.33
Median	813	6.700704	59.50
Mode	66	4.189655	20.00
Q_1	337	6.700704	40.00
Q_3	1 878	7.537952	99.25
IQR	1 541	0.837248	59.25
Variance	2 001 840	1.852303	1 740.09
Std Dev	1 415	1.360993	41.71
CoV	1.07	0.21	0.58

Box plots for Scenario Two indicate that the data distribution is positively skewed (Figure 5-8). The lognormal box plot is presented as the transformed lognormal data was used in the statistical calculation of the global estimate. As for Scenario One, the box plot of the lognormal data for Scenario Two does not present a true lognormal distribution. However, this was assumed for the global estimation.

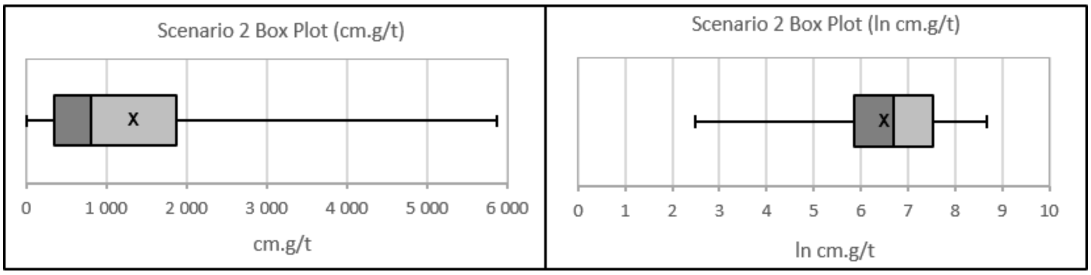

Figure 5-8: Scenario Two cm.g/t and ln(cm.g/t) box plots

5.2.3 Scenario Two Global Value (cm.g/t) Estimate

Despite the increase in the number of datapoints from Scenario One, the 46 boreholes for Scenario Two are still too widely spaced to capture spatial correlation and a statistical global estimate is appropriate.

The global estimate for Scenario Two was calculated using a 2-parameter lognormal distribution for datasets with more than 40 samples. The amount of data at the second drilling phase of the project is not sufficient to refine the shape of the underlying distribution and log-probability plots generated from small datasets are not meaningful (Sichel, 1987), making the determination of a third parameter difficult. From *Equation 3* and *Equation 4* the 2-parameter lognormal global estimate of the mean is calculated as

$$\mu^* = \tau = e^{\xi + \frac{1}{2}\sigma_L^2}$$

$$\mu^* = e^{6.504279+(0.5*1.893466)}$$

$$\mu^* = 1722 \text{ cm.g/t}$$

The lower 90% confidence limit is 1233 cm.g/t and the upper 90% confidence limit is 2404 cm.g/t. The confidence limits were calculated using the value obtained from the statistical table defining five percentage points of the normal distribution (1.645). The global estimate for the mean for Scenario Two has notably narrower confidence limits than observed for Scenario One, which were 823 cm.g/t and 4716 cm.g/t, respectively.

A global mean channel width estimate was calculated as the arithmetic average for a normal distribution with more than 30 data points.

$$\mu^* = 71.33 \text{ cm}$$

This value was slightly higher than the Scenario One value of 55.00 cm. The lower 90% confidence limit was 61.10 cm, and the upper 90% confidence limit is 81.56 cm. The confidence limits were calculated using the value obtained from the statistical table defining five percentage points of the normal distribution.

5.2.4 Scenario Two Exploration Target

The results for Scenario Two are reported as an Exploration Target as there is still insufficient exploration to estimate Mineral Resources. Evidence of assumed continuity of the mineralisation could be confirmed by other geological information (e.g., geophysical studies).

Scenario Two identifies an Exploration Target of between approximately 2.9 million tonnes and 6.2 million tonnes with an average grade approximately between 1200 cm.g/t to 2400 cm.g/t. Values are rounded to reflect a lower level of confidence (refer to Table 5-4). The range of the Exploration Target is narrower than for the Exploration results of Scenario One, which were estimated between 0.4 and 5 million tonnes.

Table 5-4: Scenario Two value-tonnage range estimation

Scenario Two Exploration Target					
	Area (m^2)	**CW (m)**	**Tonnage (Mt)**	**Value (cm.g/t)**	**Grade (g/t)**
Minimum	1 771 500	61	2.93	1 233	20.18
Maximum	2 822 400	82	6.24	2 403	29.46

The global estimates upper and lower confidence limits were used to calculate the minimum and maximum grades. The maximum area has been calculated as the entire lease area over which mineralisation continuity is assumed by geological information. The minimum area has been calculated using a polygon delineating the drilling area only. Tonnage calculations are based on a fixed in-situ density of 2.71 t/m^3 using only 46 samples for the density determination.

5.2.5 Scenario Two Summary

The methodology for Scenario Two confirmed that the wide data spacing could still not prove mineralisation continuity and spatial continuity could not be captured in the variogram due to insufficient data.

A statistical 2-parameter lognormal global estimate produced narrower confidence limits than the Sichel t estimate utilised in Scenario One. The estimate presents a higher degree of confidence in mineralisation of the reported Exploration Target over a larger area of the project.

5.3 Scenario Three

The positive drilling results and Exploration Target assessment from Scenario Two are assumed to have satisfied economic criteria, resulting in additional investment for the project, and exploration continued. Scenario Three represents the infill drilling program phase aimed at proving mineralisation continuity. An additional 20 diamond drilling boreholes were drilled as infill points on the 240 m x 240 m drillhole spacing of Scenario Two. The total number of holes drilled was 66 and the average drillhole spacing was approximately 200 m x 200 m (refer to Figure 5-9).

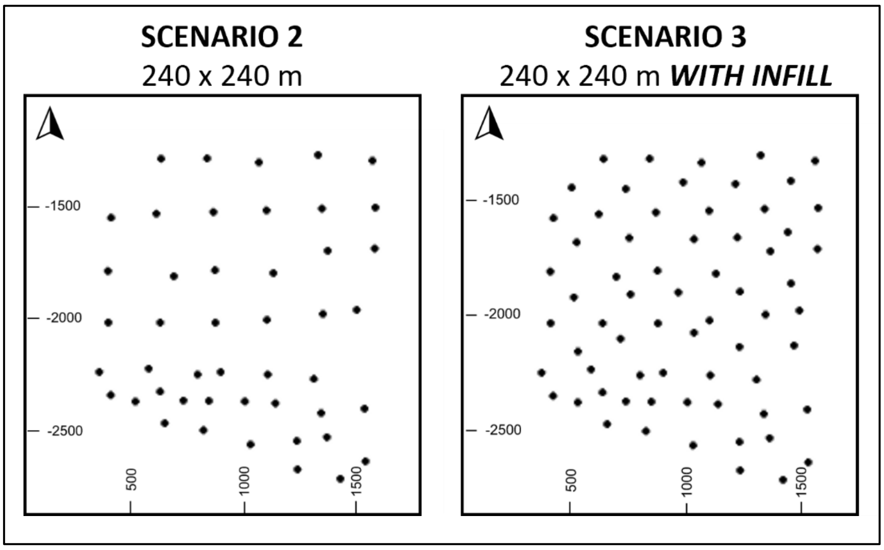

Figure 5-9: Scenarios Two and Three data location

5.3.1 Scenario Three Geozones

An indicator kriging exercise was utilised for geozone delineation using channel width as the indicator variable. Indicator kriging allows domains to be identified by assessing the resultant indicator kriging estimates that represent the probability of each block to belong to a grade domain (Emery and Ortiz, 2005). The indicator variables for 120 m x 120 m blocks were calculated by assigning values of zero to all channel width data less than 75 cm and assigning a value of one to all values greater or equal to 75 cm.

The cumulative relative frequency distribution plot based on individual observations (Figure 5-10) was used to identify the indicator cut-off values for distinguishing thick reef (75 cm) and thin reef (32 cm).

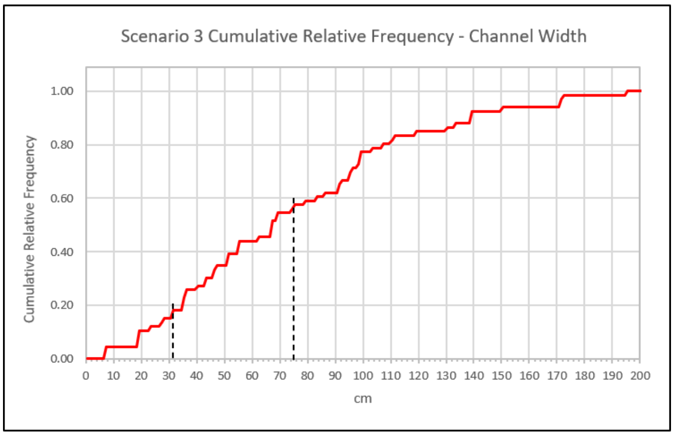

Figure 5-10: Scenario Three cumulative relative frequency distribution independent of class interval

The standardised (normalised) experimental indicator variograms are presented in Figure 5-11. The experimental indicator variogram for the Thick Domain with a cut-off at 75 cm (thick reef) produced a meaningful variogram that resulted in the indicator variogram model with a nugget of 0.4 and a range of 463 m as presented in Figure 5-11.

The experimental indicator variogram for the Thin Domain with a cut-off at 32 cm approximated a pure nugget effect (Figure 5-11) indicating that reef widths below 32 cm occur randomly within the data for Scenario Three and a thin reef domain could not be delineated.

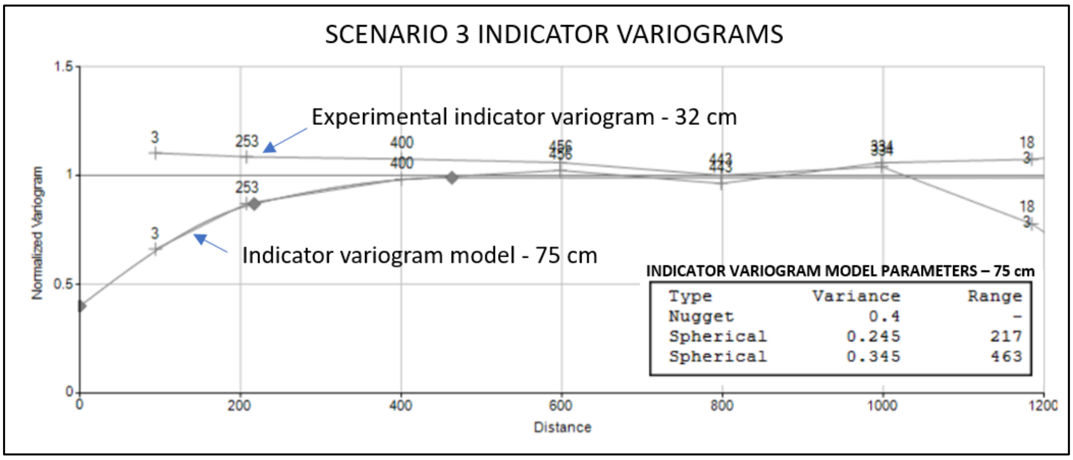

Figure 5-11: Scenario Three Experimental indicator variogram (32 cm) and indicator variogram model (75 cm)

The results of the thick reef (≥ 75 cm) indicator kriged estimate are presented in Figure 5-12. The red blocks represent areas where there is a high probability (0.65 or greater) that the channel width is greater than, or equal to, 75 cm. The indicator kriging technique assisted in defining a possible thick reef domain and Scenario Three was therefore separated into a Thick Domain (red) and a Thin Domain (green) as presented in Figure 5-12.

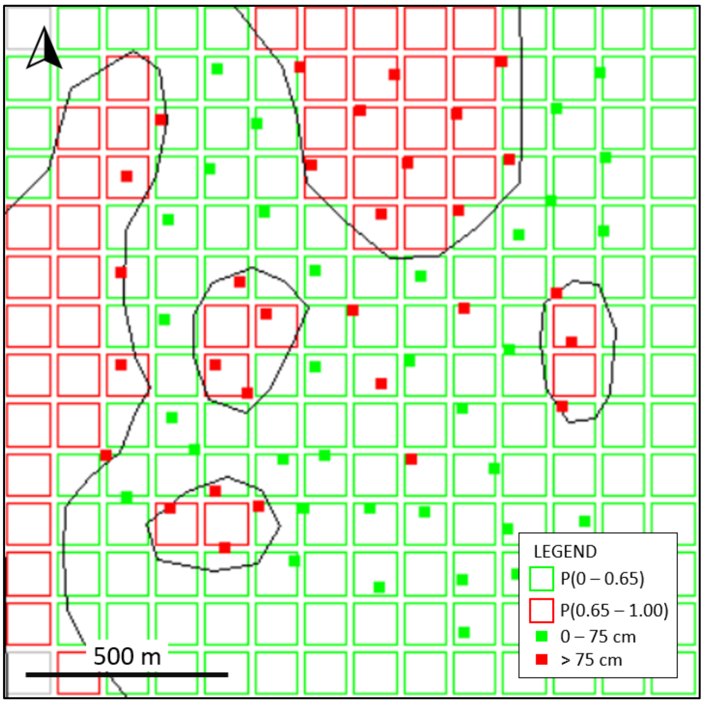

Figure 5-12: Scenario Three indicator kriging plot

The colour-coded channel width plot (Figure 5-13) confirmed the geozone boundaries identified by indicator kriging as the thicker reef width data were contained within the delineated areas. No data with a low channel width of between 0 and 52 cm (blue points) fell within the geozone boundaries.

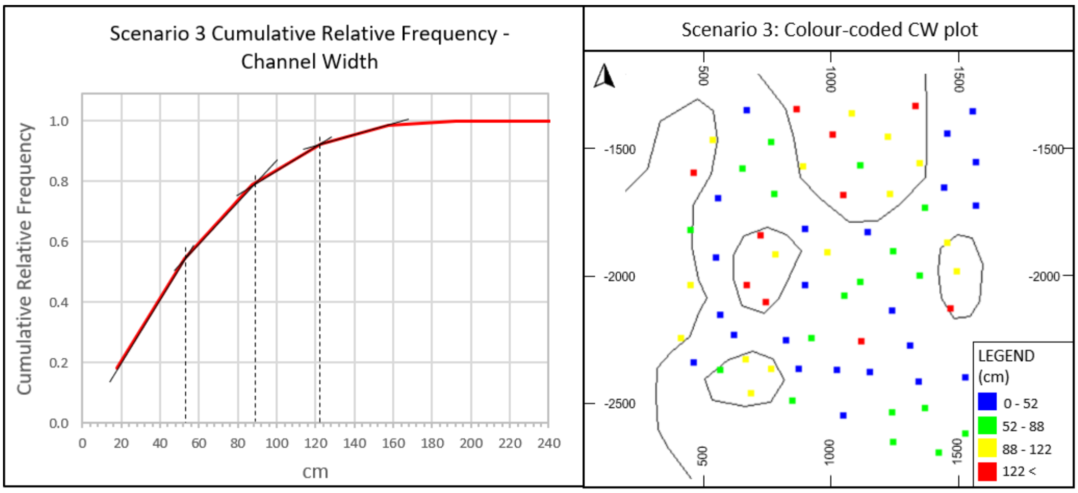

Figure 5-13: Scenario Three cumulative relative frequency distribution for channel width and colour-coded channel width plot

However, by comparing the colour-coded channel width plot in Figure 5-13 and the colour-coded cm.g/t plot in Figure 5-14, it was apparent that the geozones identified by channel width were not as obvious in the gold value (cm.g/t) colour-coded plot, and the channel width trend was not confirmed by the gold values (cm.g/t).

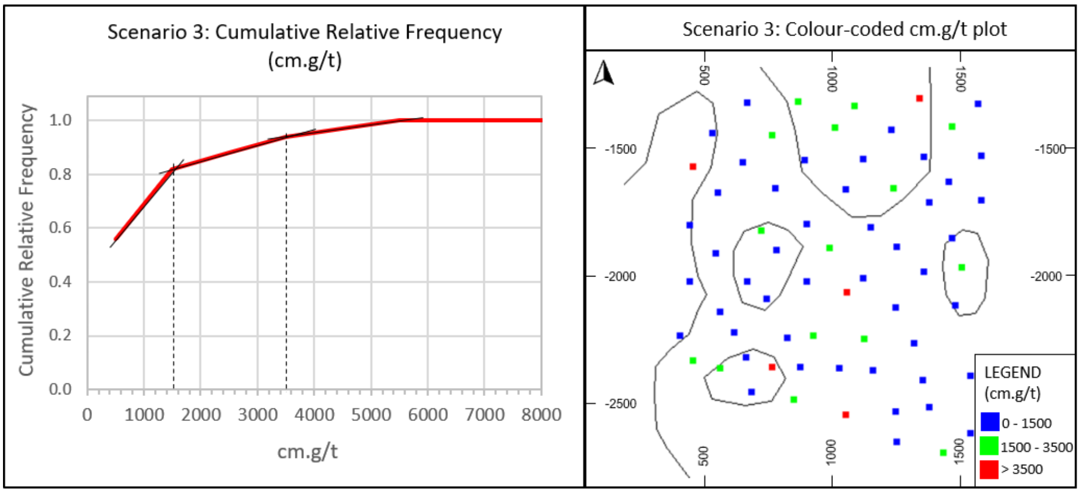

Figure 5-14: Scenario Three cumulative relative frequency distribution for cm.g/t and colour-coded cm.g/t plot

5.3.2 Scenario Three Exploratory Data Analysis

Statistical analyses were required to confirm the delineated geozones. The summary statistics for Scenario Three Thick and Thin domains are presented in Table 5-5. The mean values of the gold values (cm.g/t), log transformed values ln (cm.g/t) and channel width (cm) are highlighted.

Table 5-5: Scenario Three Summary Statistics

Scenario 3: Gold and Channel Width Statistics per domain											
THICK DOMAIN				THIN DOMAIN				TOTAL DOMAIN			
	cm.g/t	**ln(cmgt)**	**cm**		**cm.g/t**	**ln(cmgt)**	**cm**		**cm.g/t**	**ln(cmgt)**	**cm**
Min	23	3.135494	75.00	Min	4	1.386294	8.00	Min	4	1.386294	8.00
Max	5 865	8.676758	196.00	Max	4 923	8.501673	131.00	Max	5 865	8.676758	196.00
N	26	26	26	N	40	40	40	N	66	66	66
Range	5 842	5.541264	121.00	Range	4 919	7.115379	123.00	Range	5 861	7.290463	188.00
Mean	1 540	6.776555	118.77	Mean	1 118	6.176221	47.10	Mean	1 284	6.412716	75.33
Median	954	6.850550	106.00	Median	632	6.411623	45.50	Median	813	6.700704	68.00
Mode	807	6.693324	100.00	Mode	-	-	68.00	Mode	807	6.693324	68.00
Q_1	565	6.335112	96.25	Q_1	251	5.524384	29.75	Q_1	309	5.730820	38.00
Q_3	1 964	7.582037	140.00	Q_3	1 480	7.288267	64.25	Q_3	1 878	7.537952	100.00
IQR	1 399	1.246925	43.75	IQR	1 229	1.763883	34.50	IQR	1 569	1.807132	62.00
Variance	2 170 465	1.630440	1 015.56	Variance	1 537 837	2.643931	611.19	Variance	1 829 635	2.330723	1 996.83
Std Dev	1 473	1.276887	31.87	Std Dev	1 240	1.626017	24.72	Std Dev	1 353	1.526671	44.69
CoV	0.96	0.19	0.27	CoV	1.11	0.26	0.52	CoV	1.05	0.24	0.59

The mean gold (cm.g/t) values of the Thick and Thin Domains were 1540 cm.g/t and 1118 cm.g/t respectively. Box plots for both domains are presented for comparison in Figure 5-15. The data for both geozones indicate positively skewed distributions, as for Scenario One and Scenario Two.

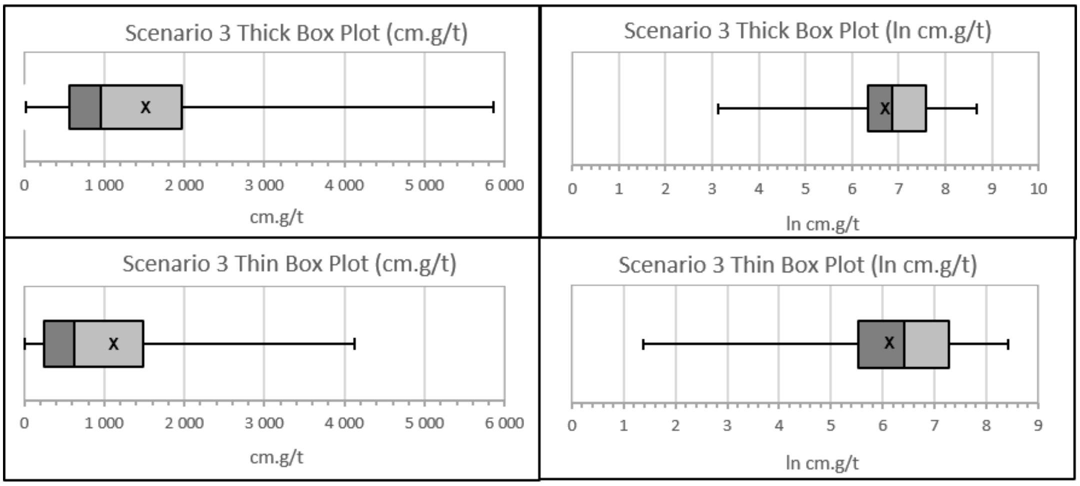

Figure 5-15: Scenario Three Thick and Thin Domain cm.g/t and ln(cm.g/t) box plots

The statistical analysis of the cm.g/t values confirmed the presence of the two geozones.

5.3.3 Scenario Three Variography

The number of data are too few and too widely spaced to create meaningful variogram models as presented in Figure 5-16. The experimental semi-variograms were calculated to investigate whether spatial grade continuity or correlation could be established. The experimental semi-variogram calculated for Scenario Three with all data (without domaining) produced a variogram with pure nugget effect with all experimental variogram points plotting along the sill, or statistical population variance.

The experimental semi-variograms for the Thick and Thin Domains produced variograms that also indicated pure nugget effect, the variograms were “noisy” as the experimental semi-variogram points plotted erratically above and below the sill due to a reduction in the number of data pairs.

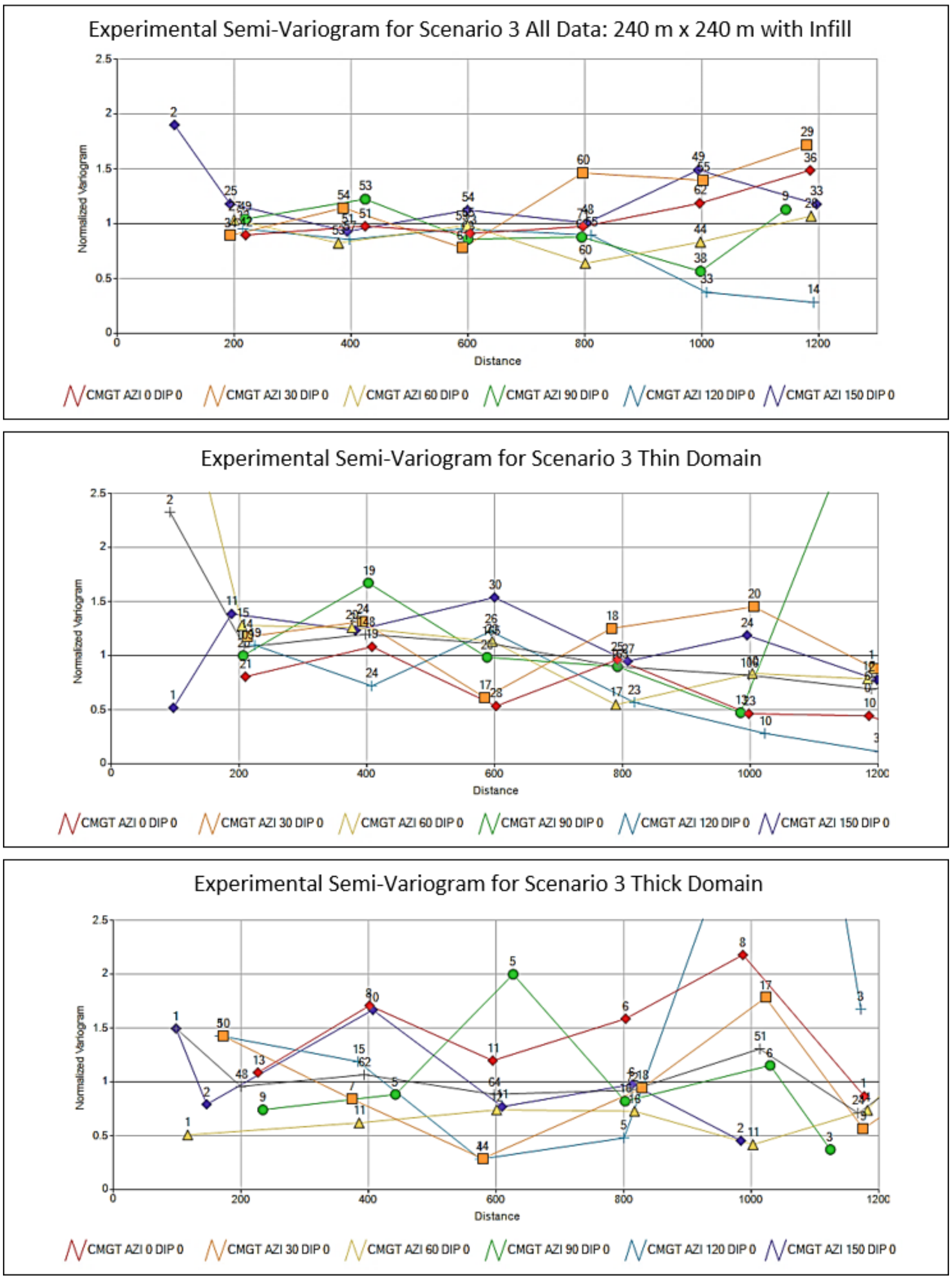

Figure 5-16: Scenario Three experimental semi-variograms

All three variograms were calculated using a lag of 200 m, a lag tolerance of 100 m, in 6 directions at 30° angle increments with a 15° angle tolerance and a bandwidth of 1000 m.

5.3.4 Scenario Three Global Value (cm.g/t) Estimates

A statistical global estimate is appropriate for Scenario Three as the variograms do not indicate spatial correlation. Table 5-6 presents three global estimates for Scenario Three. The first estimate (All data) excludes domaining, the second estimate is for the Thick Domain only and the third estimate is for the Thin Domain only. The global estimate for the Thick Domain was calculated using the Sichel t estimator for n < 40. The other two estimates were calculated using a LN(2) distribution for n > 40.

Table 5-6: Scenario Three global Gold estimates

SCENARIO 3 GLOBAL Gold Value (cm.g/t) ESTIMATE			
Domain	**TOTAL**	**THICK**	**THIN**
n	66	20	46
Arithmetic Mean (cm.g/t)	1284	1540	1118
Estimator	LN(2)	Sichel t	LN(2)
Log-mean ξ	6.412716	6.776555	6.176221
Sichel's biased sample variance, V		1.630440	
Equation	$\tau = e^{\xi+\frac{1}{2}\sigma_L^2}$	$t = e^{\xi}\gamma(v)$	$\tau = e^{\xi+\frac{1}{2}\sigma_L^2}$
Variance (ln(cm.g/t)), σ_L^2	2.366580		2.711724
Global Estimate (cm.g/t)	**1990**	**1936**	**1867**
90% Confidence Lower Limit for the mean estimate (cm.g/t)	1458	1230	1217
90% Confidence Upper Limit for the mean estimate (cm.g/t)	2718	4018	2865

The global mean estimates for the un-domained scenario produced a similar result to the global mean estimate of the Thick Domain and is within 123 cm.g/t of the Thin Domain global mean estimate. All three global mean estimates for Scenario Three are higher than for Scenario One (1523 cm.g/t) and Scenario Two (1722 cm.g/t).

The arithmetic mean is below the lower limit of the global mean estimate for the LN(2) calculations indicating that the results are likely to be over-estimated. This over-estimation is expected as the cm.g/t log-transformed distribution is not log normal as observed in the box plots (Figure 5-15) and the log variance values are relatively high.

5.3.5 Scenario Three Exploration Target

The estimate for Scenario Three is reported as an Exploration Target as there is still insufficient data to estimate Mineral Resources even with the additional infill drilling. The estimate without domains for Scenario Three identified an Exploration Target of between approximately 3.1 million tonnes and 6.5 million tonnes with an average gold value between 1450 cm.g/t and 2700 cm.g/t. Values have been rounded to reflect a lower level of confidence (refer to Table 5-7).

Table 5-7: Scenario Three Exploration Target without Domaining

Scenario Three Exploration Target without Domaining					
	Area (m^2)	**CW (m)**	**Tonnage (Mt)**	**Value (cm.g/t)**	**Grade (g/t)**
Minimum	1 771 500	66	3.18	1458	22.02
Maximum	2 822 400	84	6.46	2718	32.18

The estimate with domains for Scenario Three identified an Exploration Target of between approximately 2.8 million tonnes and 5.5 million tonnes with an average gold value between 1220 cm.g/t and 3730 cm.g/t using a fixed in-situ density of 2.71 t/m^3 (refer to Table 5-8). The grade ranges presented are wider than those of the estimate without domaining due to the Sichel t estimator utilised for the Thick Domain.

Table 5-8: Scenario Three Exploration Target with Domaining

Scenario Three Exploration Target with Domaining						
Domain		**Area (m^2)**	**CW (m)**	**Tonnage (Mt)**	**Value (cm.g/t)**	**Grade (g/t)**
Thin	Minimum	1 329 856	41	1.46	1 230	30.33
	Maximum	2 118 762	54	3.08	4 018	74.96
Thick	Minimum	441 644	114	1.36	1 217	10.69
	Maximum	703 638	124	2.36	2 865	23.16
Total Minimum		**1 771 500**	**59**	**2.82**	**1 227**	**20.86**
Total Maximum		**2 822 400**	**71**	**5.44**	**3 731**	**52.48**

The global estimates lower and upper 90% confidence limits were used to calculate the minimum and maximum grades. The minimum and maximum areas were the same as those utilised for Scenario Two. A fixed in-situ density of 2.71 t/m^3 was used.

The estimate of the Exploration Target for Scenario Two (2.9 to 6.2 million tonnes) was between the domained and un-domained estimates for Scenario Three. The range for the Scenario Two estimate, however, was more similar to the un-domained Scenario Three estimate (the domained Scenario Three estimate had a narrower range).

5.3.6 Scenario Three Summary

An indicator kriging exercise was utilised to determine channel width trends in the widely spaced data. Rough geozones may be delineated but channel width or value continuity cannot be observed in the widely spaced data. Unfortunately, the infill drilling is still too widely spaced to demonstrate spatial mineralisation continuity and the variogram depicted pure nugget effect. A global estimate, using the 2-parameter lognormal distribution, was used to present an Exploration Target with value ranges. The global estimate is presented for both the domained and un-domained deposit.

5.4 Scenario Four

Scenario Four represents an advanced drilling phase at a grid spacing of 120 m x 120 m. The aim of the additional drilling was to prove mineralisation continuity. An additional 33 diamond drilling boreholes resulted in a total of 99 datapoints as presented in Figure 5-17.

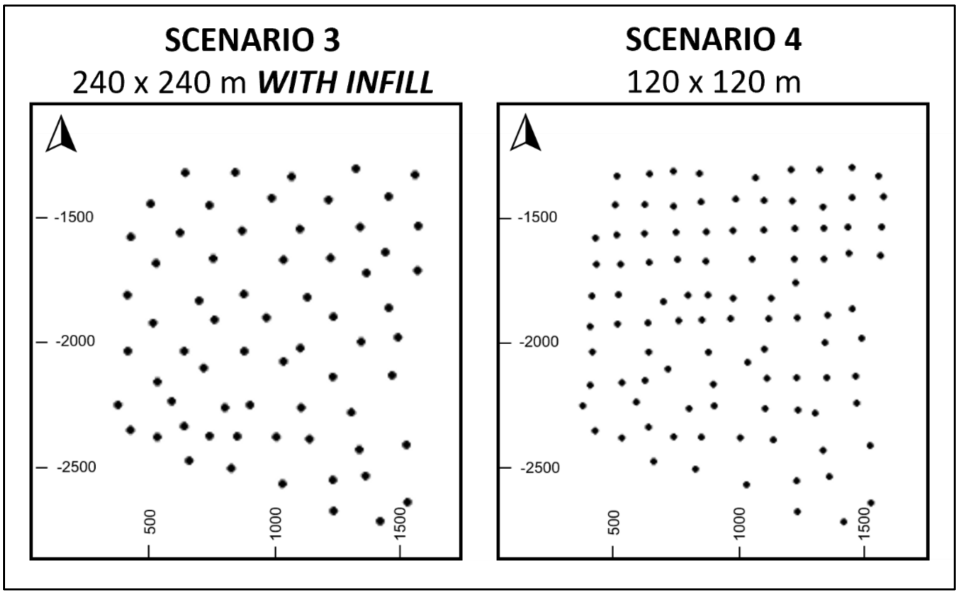

Figure 5-17: Scenarios Three and Four data location

Scenario Four aims to present defined geozones and long-range spatial mineralisation continuity. Ordinary kriging is utilised to produce a local Mineral Resource estimate and value-tonnage curve.

5.4.1 Scenario Four Geozones

Geozones were delineated using indicator kriging to estimate the probabilities that a channel width value of blocks is above a certain cut-off. The probabilities for two indicator cut-off values were estimated for a block size of 60 m x 60 m (half the average drill spacing). Inflection points at 30 cm and 78 cm were highlighted using the cumulative relative frequency distribution plot as presented in Figure 5-18. However, the 78 cm indicator estimate for thick reef was adjusted to 70 cm after a review of the indicator kriging results.

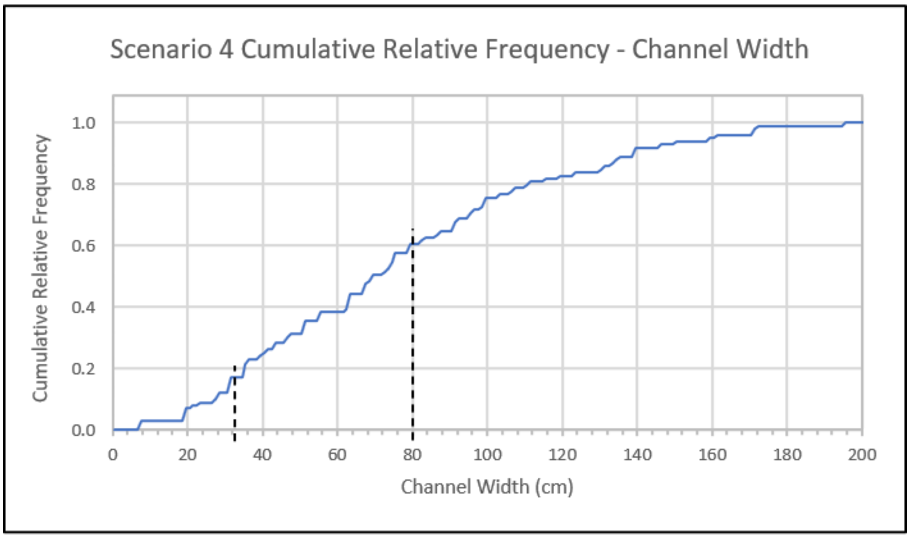

Figure 5-18: Scenario Four cumulative relative frequency distribution independent of class interval

The omnidirectional experimental indicator variograms are presented in Figure 5-19. The slope reef indicator variable at 30 cm did not produce a meaningful variogram and indicated pure nugget effect. The slope reef, which averages less than 30 cm thick (McWha, 1994), most likely occurred randomly within the data of Scenario Four and could not be delineated due to the widely spaced data.

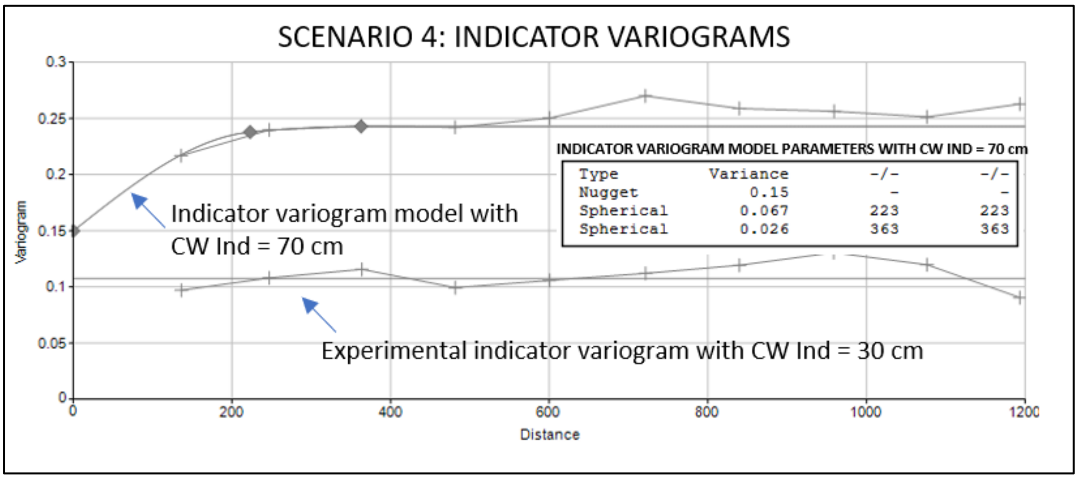

Figure 5-19: Scenario Four indicator variogram model (CW Ind = 70 cm) and experimental indicator variogram (CW Ind = 30 cm)

The results of indicator kriging for thick reef together with the CW indicators are presented for both indicator variables (78 cm in Figure 5-20 A, and 70 cm in Figure 5-20 B). The red blocks indicated a probability of 0.55 or above that channel width is greater than 78 cm and 70 cm, respectively in Figure 5-20 A and B.

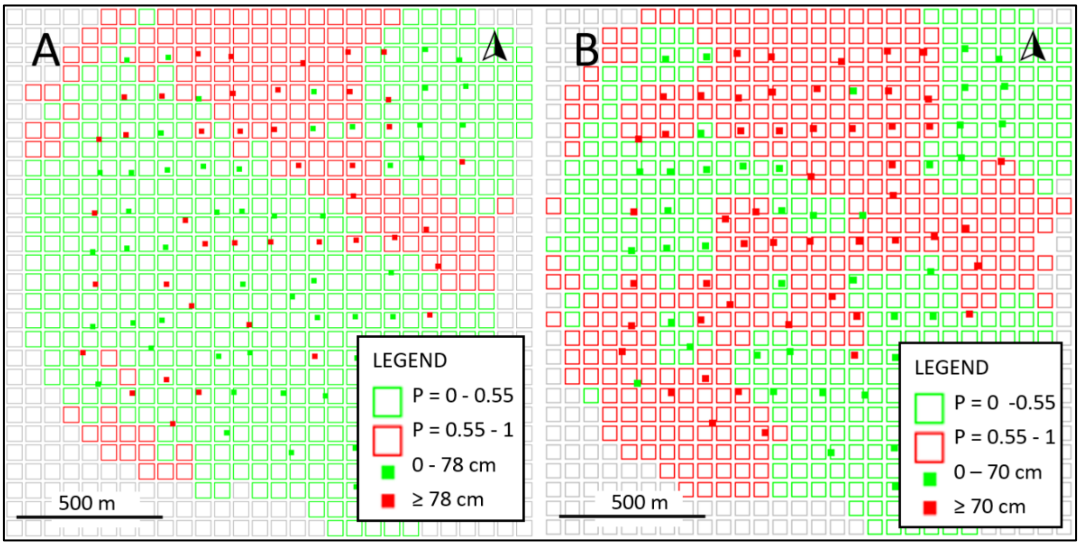

Figure 5-20: Scenario Four indicator kriging for A) CW Ind = 78 cm and for B) CW Ind = 70 cm

Indicator kriging using the 78 cm variable excluded too many thick channel width data points from the red blocks as observed in Figure 5-20 A. Figure 5-20 B shows less bias as most of the red, thick channel width data points were contained within red blocks.

The indicator kriging exercise assisted with defining a possible thicker reef geozone and the colour-coded channel width plot confirmed the presence of a Thick and Thin Domain (Figure 5-21).

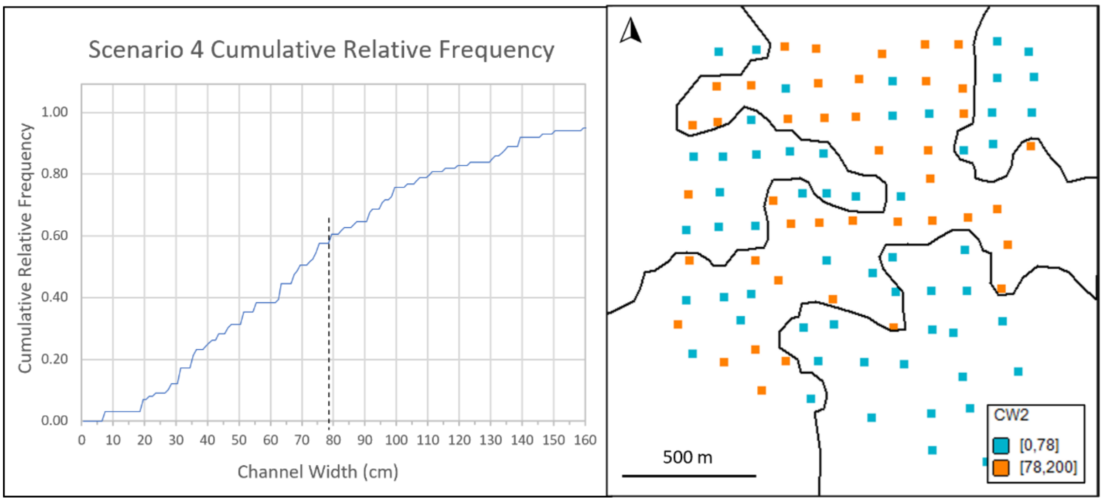

Figure 5-21: Scenario Four cumulative relative frequency distribution graph and colour-coded CW plot

The colour-coded gold value plot (cm.g/t), as presented in Figure 5-22, does not highlight an obvious high-grade domain. The Thick Domain does contain most of the high-grade values, however, it also includes a number of low-grade values. The domain boundaries were not further refined as the data is too widely spaced.

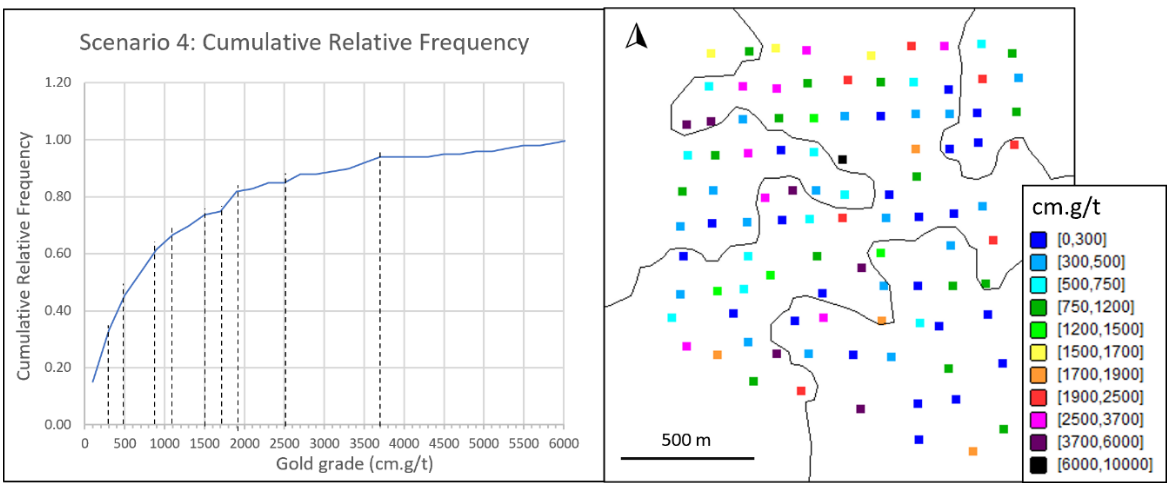

Figure 5-22: Scenario Four cumulative relative frequency distribution graph and colour-coded cm.g/t plot

The increased gold content associated with thicker, terrace reef noted by McWha (1994) was proven to show positive relationship between average gold value (cm.g/t) and channel width by Dohm (1995) during development of the Channel Width

Model. The knowledge of this relationship was accepted for Scenario Four based on a conditional expectation plot of average gold value for wide channel width intervals (30 cm, and 60 cm for the last interval) as presented in Figure 5-23.

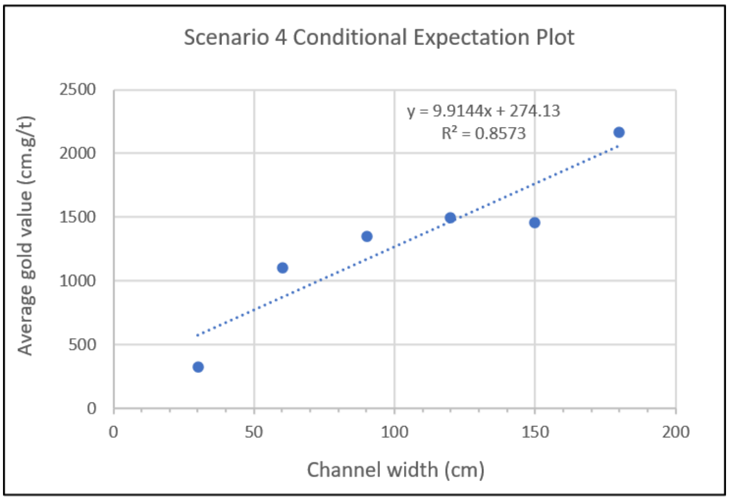

Figure 5-23: Scenario Four conditional expectation plot

5.4.2 Scenario Four Exploratory Data Analysis

The statistical summaries for Scenario Four Thick and Thin Domains are presented in Table 5-9.

Table 5-9: Scenario Four Summary Statistics

Scenario 4 Gold and Channel Width Statistics								
THICK DOMAIN			THIN DOMAIN			TOTAL		
	cm.g/t	cm		cm.g/t	cm		cm.g/t	cm
Min	23	28.00	Min	4	8.00	Min	4	8.00
Max	6 086	196.00	Max	4 525	124.00	Max	6 086	196.00
N	55	55	N	44	44	N	99	99
Range	6 063	168.00	Range	4 521	116.00	Range	6 082	188.00
Mean	1 604	103.05	Mean	851	44.34	Mean	1 255	77.03
Median	807	97.00	Median	464	41.50	Median	675	70.00
Mode	66	100.00	Mode	-	52.00	Mode	66	32.00
Q_1	433	76.00	Q_1	276	31.25	Q_1	350	41.50
Q_3	2 258	133.00	Q_3	1 043	57.75	Q_3	1 818	100.00
IQR	1 826	57.00	IQR	767	26.50	IQR	1 469	58.50
Variance	2 586 395	1 399.00	Variance	968 603	480.27	Variance	1 966 089	1 849.00
Std Dev	1 608	37.40	Std Dev	984	21.92	Std Dev	1 402	43.00
CoV	1.00	0.36	CoV	1.16	0.49	CoV	1.12	0.56

The CoV decreases for channel width (cm) in both the Thick and Thin geozone compared to the Total dataset. This decrease highlights the positive impact (variability reduced) of the geozone delineation into the Thick and Thin domains as the variability in both instances reduced.

Both geozones indicated a positively skewed distribution, as for Scenarios One, Two and Three. The box plots as presented in Figure 5-24 highlight different gold value (cm.g/t) distribution shapes, whilst both distributions are positive skewed, cm.g/t values in the Thin Domain are less variable than in the Thick Domain. The detailed lognormal data is not presented for Scenario Four as a global estimate was not determined.

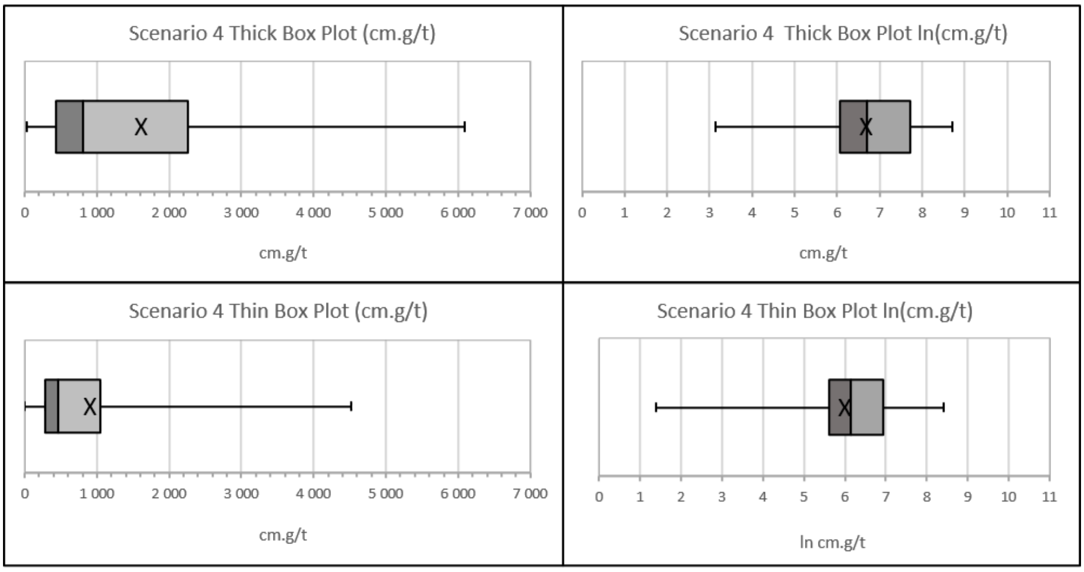

Figure 5-24: Scenario Four Thick and Thin domain cm.g/t and ln(cm.g/t) box plots

5.4.3 Scenario Four Variography

The experimental variograms were calculated using a lag of 120 m, a lag tolerance of 60 m, in 6 directions at 30° angle increments with a 15° angle tolerance and a bandwidth of 400 m. The spatial continuity at a data spacing of 120 m x 120 m is captured by the variograms of both the Thick and Thin Domains for Scenario Four which are modelled using one spherical structure. Long-range mineralisation continuity is observed up to 350 m and 471 m, respectively. This long-range spatial correlation as presented in Figure 5-25 may provide an unrealistic representation of the true gold grade variability, due to the relatively wide drilling grid.

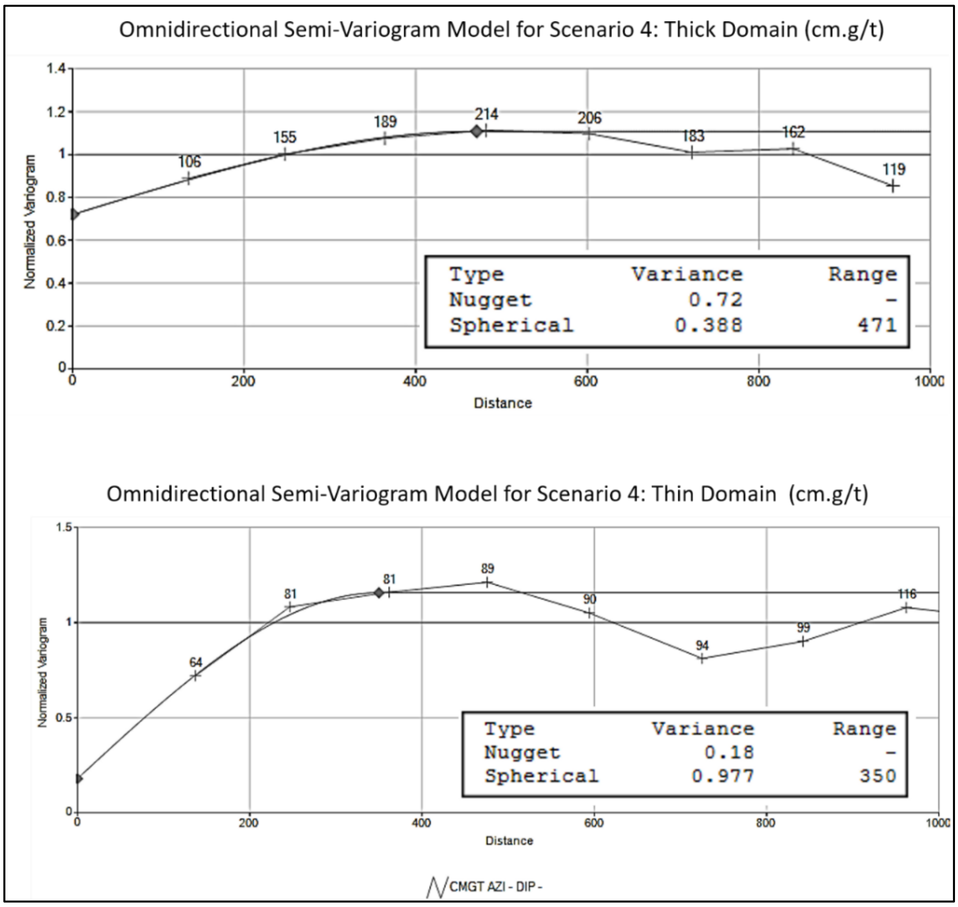

Figure 5-25: Scenario Four variogram models for the Thick and Thin Domains cm.g/t

Both variograms were modelled using one spherical structure. Both sills plateau above the standardised statistical population variance. Morgan (2011) highlighted that the experimental sill is more reliable than the population variance as the statistical population variance is likely to be incorrect when calculated using a small dataset. The variogram sill is a measure of the spatial variability and it is acceptable to have a sill that plots above or below the statistical population variance, especially for small datasets.

The Thick Domain shows a high nugget effect of 0.72 and a longer range than the Thin Domain. This is caused by the greater variability of reef within the Thick Domain, which also shows a larger statistical range with many random low values throughout the domain. Samples in the Thick Domain show spatial correlation over a longer distance than observed in the Thin Domain.

The Thin Domain shows a very low nugget effect of 0.18 and a shorter range of 350 m. The low nugget effect indicates less variability within the Thin Domain, due to a less variable thin reef and better correlation between samples closer together.

The variogram for channel width of both domains are presented in Figure 5-26. The variogram parameters are the same as those used for the gold value (cm.g/t). The spatial continuity for channel width is not as pronounced as the gold value (cm.gt) and the Thin Domain presents apparent pure nugget effect. Although it may be more appropriate to use the arithmetic mean, these variograms have been used to calculate channel width estimates for Scenario Four. The high nugget effect in the Thick Domain and the Thin nugget effect in the Thin Domain reflect the expected reef thickness variability.

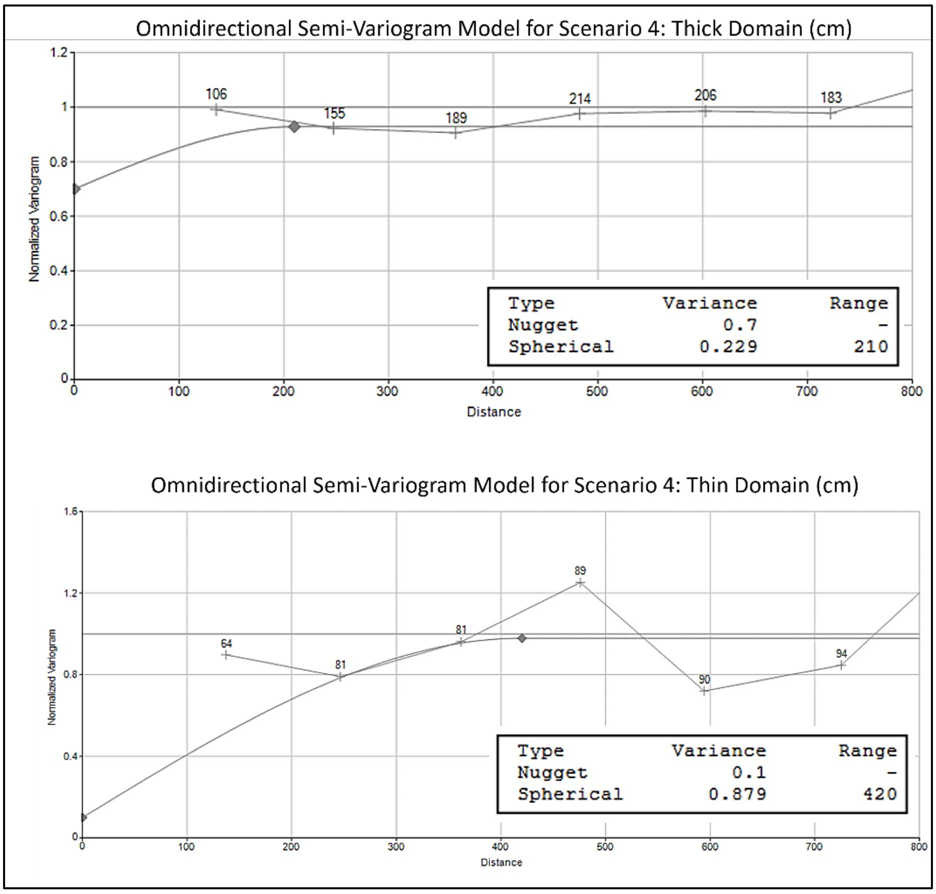

Figure 5-26: Scenario Four variogram models for the Thick and Thin Domains channel width (cm)

5.4.4 Scenario Four Local Value (cm.g/t) and CW (cm) Estimates

The additional drilling information from the advanced drilling phase allows for local block estimation based on the spatial distribution theory captured by the semi-variogram. A 60 m x 60 m block size was used for this first local estimation; the data spacing is remains relatively wide and this block size represents the mining expected within a year. Ordinary kriging is well suited to interpolation and is the local estimation technique applied to Scenario Four.

Nonetheless the extent of the conditional bias will be considered by analysing the bias measures namely the slope of regression and the kriging efficiency. Kriging variance, slope of regression, kriging efficiency and the Lagrange multiplier are presented separately for each domain in Figure 5-27 below.

.

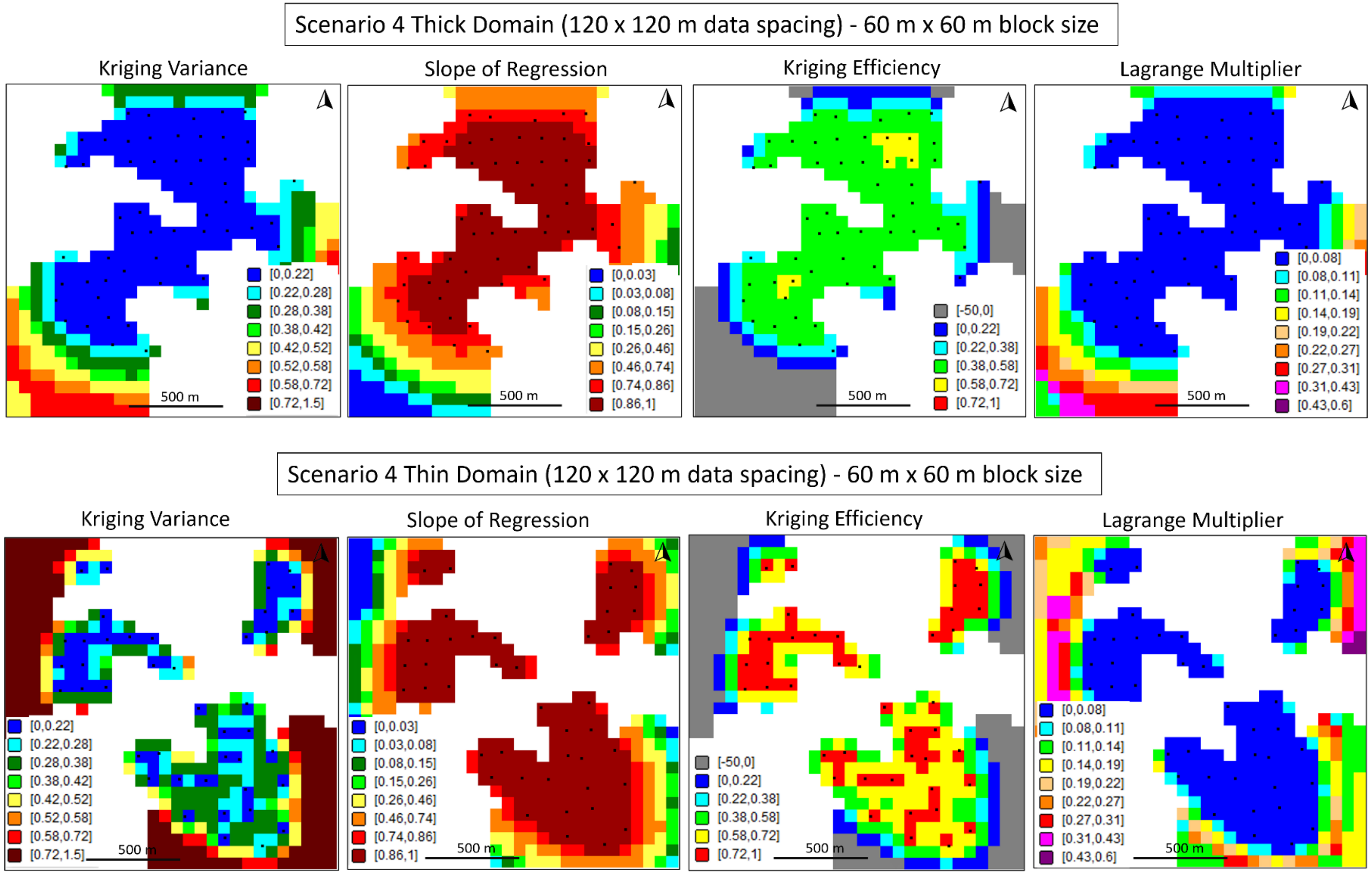

Figure 5-27: Scenario Four Thick and Thin Domain kriging performance indicators

The different nugget effects observed in the domain variograms resulted in notable differences in the kriging variances and kriging efficiencies. The high nugget effect in the Thick Domain (0.72) resulted in a low block variance of 0.35. The low nugget in the Thin Domain (0.18) resulted in a high block variance of 0.85 which resulted in the improved kriging efficiencies for the Thin Domain.

Kriging variance remains low for blocks surrounded by data in the Thick Domain. The kriging variance for the Thin Domain increases for blocks between datapoints due to a shorter variogram range and increased data spacing of the borehole data towards the south of the deposit in this domain. The smoothed increase in kriging variance is conspicuous towards the edges of the deposit in the Thick Domain but was not as pronounced in the Thin Domain due to a lower nugget effect. The increase in kriging variance towards the edges of the model occurs due to limited data resulting in extrapolation which is also observed in an increase in the Lagrange multiplier.

The slope of regression is high for both domains for blocks surrounded by boreholes due to the long variogram ranges. The Thick Domain shows a slightly lower slope of regression at the edges of the data indicating slightly increased conditional bias in the Thick Domain due to the high nugget effect.

A good kriging efficiency is observed in blocks constrained around the data in the Thin Domain. A poor kriging efficiency is observed over most of the Thick Domain indicating poor estimation methodology due to the high nugget effect and low block variance. A negative kriging efficiency occurs where block variance is lower than kriging variance considered unacceptable by Krige (1997), who suggested the mean as a more efficient estimate in this case.

The Lagrange multiplier is low for both the Thin and Thick Domains for blocks surrounded by boreholes. It increases towards the edges of the deposit. Ordinary kriging produces better results for estimation by interpolation. A simple kriging method could be applied to improve the estimate towards the edges of the resource model where extrapolation is required. A Lagrange multiplier of greater than approximately 0.3 indicates unacceptable sample weighting and a simple kriged estimate should be considered for these areas towards the edge of the deposit. The weight of the global mean would increase towards the edges of the estimate, reducing the edge effect observed in the gold value (cm.g/t) estimate.

The combined results of both domains for the ordinary kriged value (cm.g/t) estimate and channel width estimates are presented in Figure 5-28.

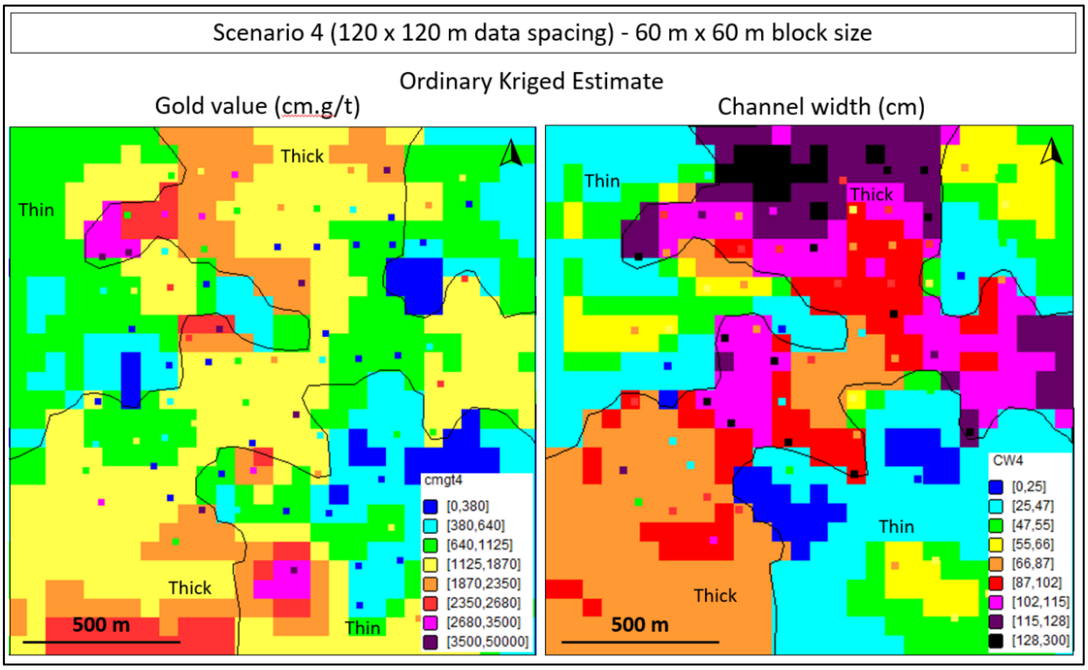

Figure 5-28: Scenario Four kriging estimates for cm.g/t and CW (cm)

The high nugget effect produced a smoother estimate within the Thick Domain due to more equal sample weighting. The edge effect is especially apparent in the southwest corner of the Thick Domain where values increase towards the edge of the model due to insufficient data. The edge effect is also apparent in the Thin Domain especially in the northwest corner but may not be as visually pronounced as observed in the Thick Domain due to the colour coding intervals, insufficient drilling information.

5.4.5 Scenario Four Estimate Validation

Table 5-10 presents a comparison of the estimate statistics and the data statistics. The Thick Domain mean estimate is 21 cm.g/t (1.3%) higher than the sample mean, and the Thin Domain estimate is 20 cm.g/t (2.3%) higher than the sample mean, both indicating acceptable estimation results.

Table 5-10: Scenario Four statistical comparison between block estimates and sampling data

SCENARIO 4 THICK DOMAIN STATISTICS				SCENARIO 4 THIN DOMAIN STATISTICS			
ESTIMATE		SAMPLES		ESTIMATE		SAMPLES	
	cm.g/t		cm.g/t		cm.g/t		cm.g/t
Min	720	Min	23	Min	76	Min	4
Max	3125	Max	6086	Max	3313	Max	4525
N	375	N	55	N	409	N	44
Mean	1 626	Mean	1 604	Mean	871	Mean	851
Variance	225 886	Variance	2 586 395	Variance	279 575	Variance	968 603
Std Dev	475	Std Dev	1 608	Std Dev	529	Std Dev	984
CoV	0.29	CoV	1.00	CoV	0.61	CoV	1.16

The relative frequency distributions presented in Figure 5-29 highlight the support effect by comparing the shape of the data distribution to the block estimate distribution. Although the means of the distributions are similar, the relative frequency polygons of the 60 m x 60 m block estimates show decreased variance and tends towards symmetry as expected due the change of support effect.

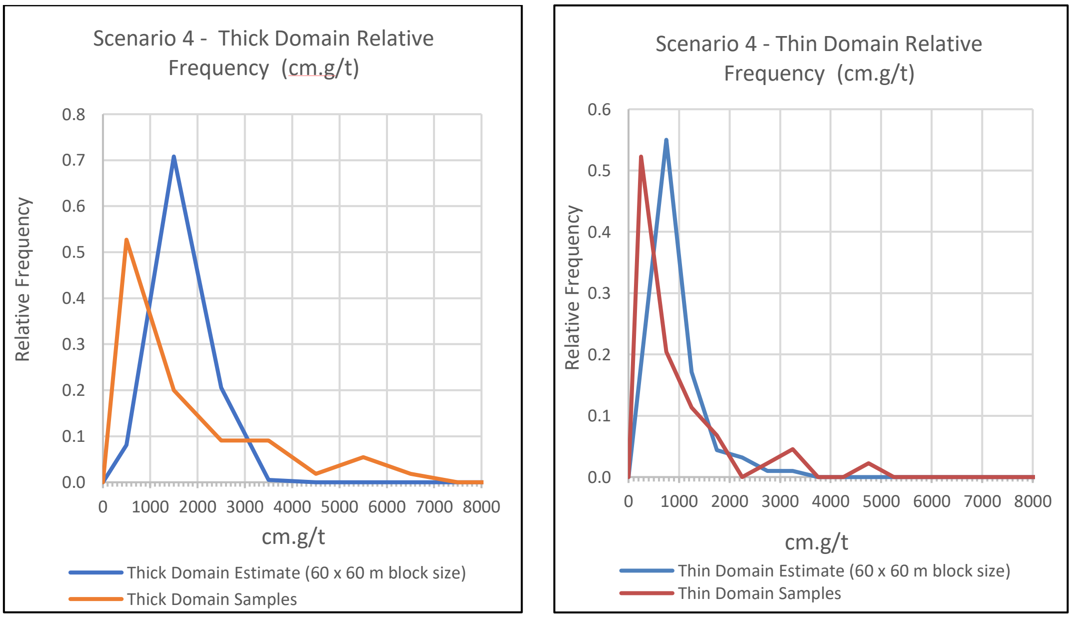

Figure 5-29: Relative frequency distributions for the Thick and Thin Domain block estimates and samples

Swath plots were generated in a north-south and east-west direction for Scenario Four. The results of the swath plots indicated acceptable estimates as the model value lies within the 90% confidence limit of the sample data. The broad confidence limits are due to the limited amount of data per swath. The estimate values (model) indicate the smoothing effect of kriging. The swath plots for the Thick and Thin Domains in a north-south direction only are presented in Figure 5-30 and Figure 5-31.

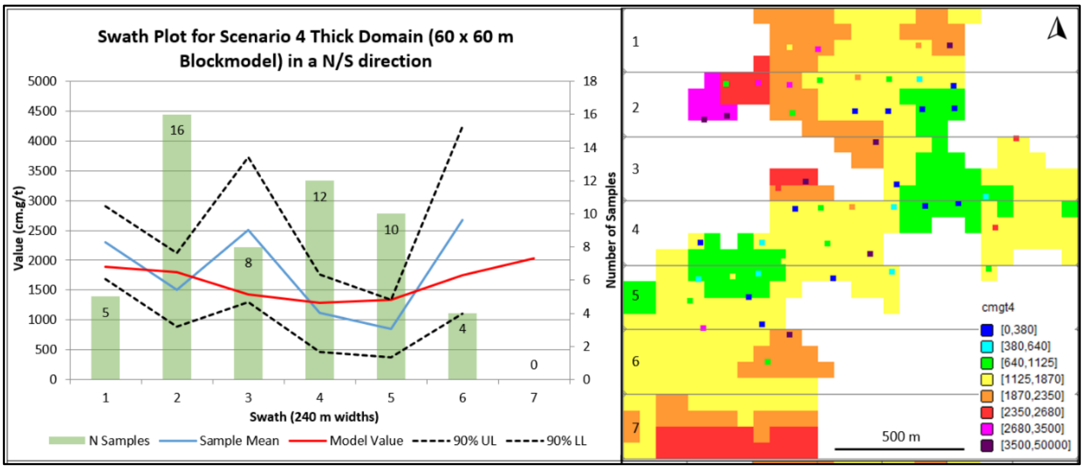

Figure 5-30: Scenario Four swath plot for the Thick Domain in a north-south direction

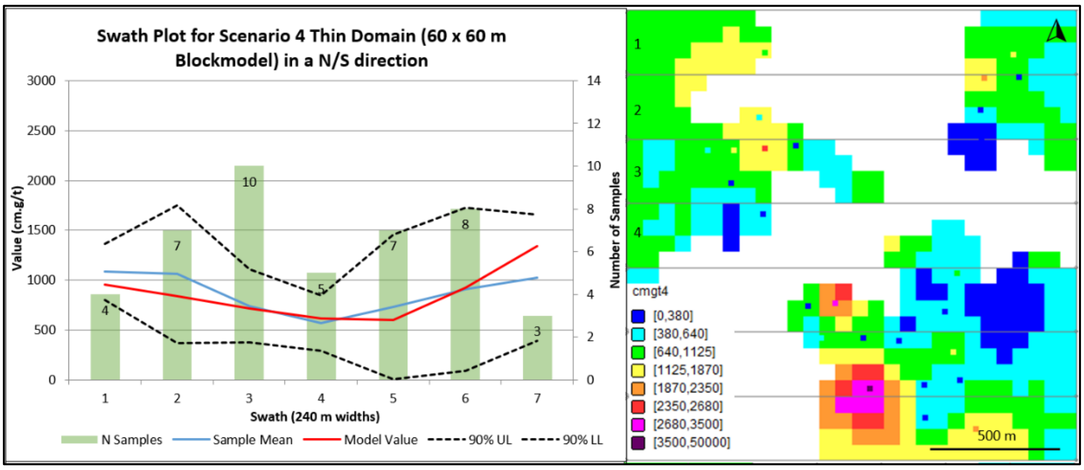

Figure 5-31: Scenario Four swath plot for the Thin Domain in a north-south direction

5.4.6 Scenario Four Mineral Resource Estimate

The long-range mineralisation continuity is not representative of typical gold grade variability and should be reflected in the confidence of the Mineral Resource classification. The Mineral Resource was classified using a simplistic methodology at the advanced drilling stage of the project development. Blocks estimated within the first search radius (the spatial correlation range) were classified at the Indicated level of confidence under the assumption of RPEEE. Blocks estimated within the second search radius (twice the range of the variogram) were classified at the Inferred level of confidence. Due to the long-range spatial correlation, most blocks fell into the Indicated category as presented in Figure 5-32.

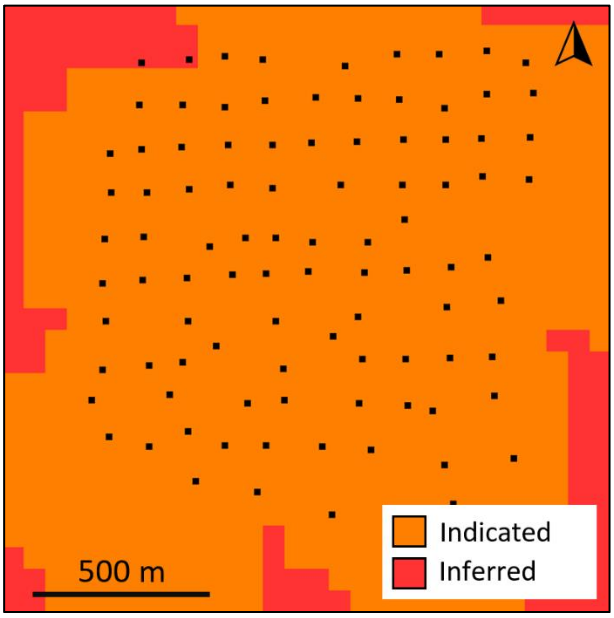

Figure 5-32: Scenario Four proposed Mineral Resource classification for the combined Thick and Thin domains

Figure 5-32 presents the proposed classification for the combined Thick and Thin domains. The Thick domain contains more datapoints and a longer variogram range allowing for the additional Indicated blocks within that domain. However, the Competent Person would use experience and expert opinion to manually override the classification for specific blocks as deemed appropriate.

The Mineral Resource tabulation for Scenario Four is presented in Table 5-11.

Table 5-11: Scenario Four Mineral Resource estimate

Scenario Four Mineral Resource Estimate								
		Area (m^2)	CW (m)	Tonnage (Mt)	Value (cm.g/t)	90 % Lower Limit (cm.g/t)	90 % Upper Limit (cm.g/t)	Grade (g/t)
Indicated Mineral Resource	Thick Domain	1 342 800	98	3.56	1 619	1 598	1 640	16.94
	Thin Domain	1 144 800	44	1.35	869	841	897	21.21
Total Indicated		2 487 600	73	4.92	1 274	1 249	1 298	18.90
Inferred Mineral Resource	Thick Domain	18 000	81	0.04	1 663	1 635	1 690	20.51
	Thin Domain	316 800	43	0.37	882	841	922	21.17
Total Inferred		334 800	45	0.41	924	884	963	21.13

5.4.7 Scenario Four Value-Tonnage Estimates

A value-tonnage curve is a graphical representation of an idealistic scenario predicting the available in-situ tonnage with an associated average grade above a specified cut-off grade. Value-tonnage curves are widely used in the mining industry and are important tools for assessing a project's overall financial and economic viability.

The value-tonnage curve for Scenario Four is presented in Figure 5-33 for the Indicated Mineral Resource blocks at point scale and 60 m x 60 m block scale. This graph illustrates the volume-variance effect. As an example, using an arbitrary cut-off value of 500 cm.g/t, the point data indicates that 2.6 Mt can be mined at an average value above cut-off of approximately 3000 cm.g/t. At the same 500 cm.g/t cut-off value, mining at a block size of 60 m x 60 m an estimated 4.3 Mt can be mined at an average value of 1800 cm.g/t.

Local estimates at a block size of 60 x 60 m may only be used for medium- to long-term planning as these blocks represent an area that will be mined over six months. The 60 m x 60 m blocks may suit some mining methods, but present lower ore/waste block selectivity due to lower variability resulting from the long range of the variogram of Scenario Four data configuration.

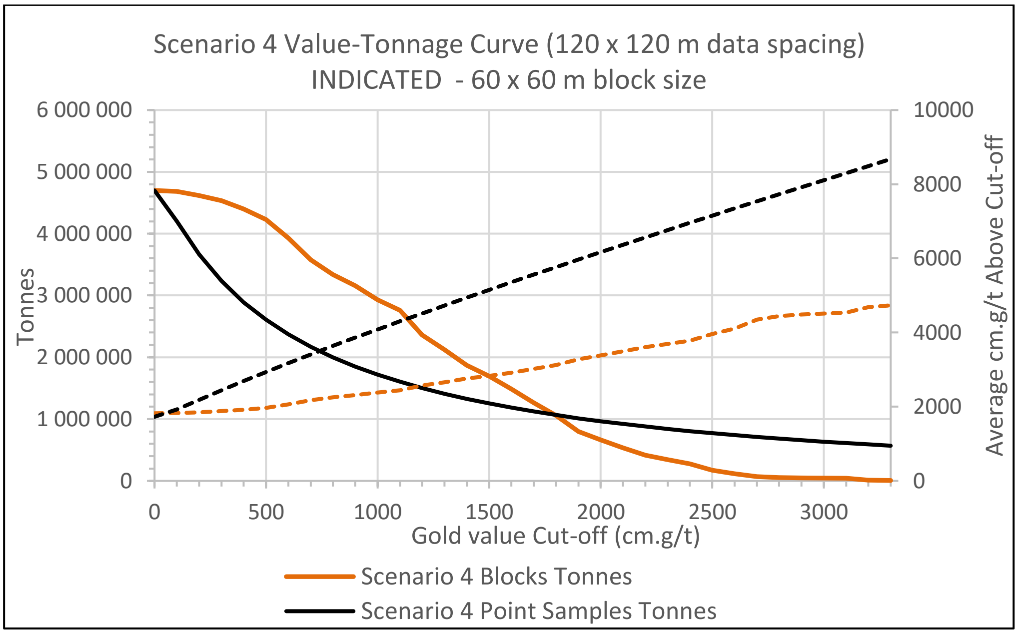

Figure 5-33: Scenario Four value-tonnage curve at for 60 m x 60 m indicated blocks.

The value-tonnage curve for Scenario Four is presented in Figure 5-33 for the Indicated Mineral Resource blocks at point scale and 60 m x 60 m block scale.

5.4.8 Scenario Four Summary

The geozoning is still a challenge as geological or grades trends are not observed and the data to too widely spaced to provide precise domains, however there is an improvement when compared to Scenario Three.

Long-range spatial mineralisation continuity is captured by the semi-variogram using one spherical structured variogram. The Thick Domain indicates a high nugget effect (0.72), and the Thin Domain indicates a low nugget effect (0.18). The spatial continuity captured by the variogram is unrealistic and is not a true representation of the gold grade mineralisation. The variogram models for channel width suggest that local estimates are not appropriate for channel width at this data spacing.

Local estimation using ordinary kriging has been produced for a block size of 60 m x 60 m. Overall, the interpolated kriging performance indicators show a low kriging variance, high slope of regression and low Lagrange multiplier. The kriging efficiencies especially in the Thick Domain are low. The value estimate results depict edge effect and smoothing, especially for the Thick Domain with a high nugget effect, but this smoothing is most likely due to limited data. The support effect presented in the value-tonnage curve indicates that cognisance must be taken of the volume-variance effect for long-term planning or overall resource estimation.

5.5 Scenario Five

Scenario Five is a representation of the project development that combines underground development sampling from all raises and reef drives with the advanced drilling grid at a data spacing of approximately 120 m x 120 m from Scenario Four. The development sampling is at a spacing of approximately 2 m and there are a total of 3591 datapoints over the project area as presented in Figure 5-34.

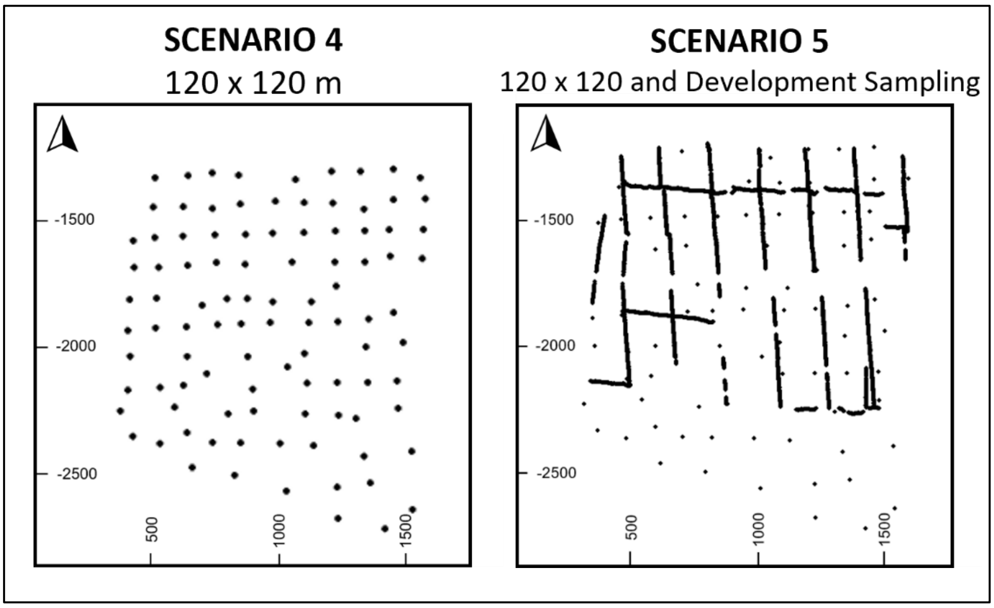

Figure 5-34: Scenarios Four and Five data locality

The challenges with Scenario Five resulted from attempting to identify the long-range mineralisation continuity observed in the widely spaced borehole data, as well as the short-range spatial structure observed in the closely spaced development data.

A cumulative frequency distribution comparing the drillhole samples from Scenario Four and the development sampling is presented in Figure 5-35. Although the amount of data differs, it can be assumed that the datasets represent similar distributions.

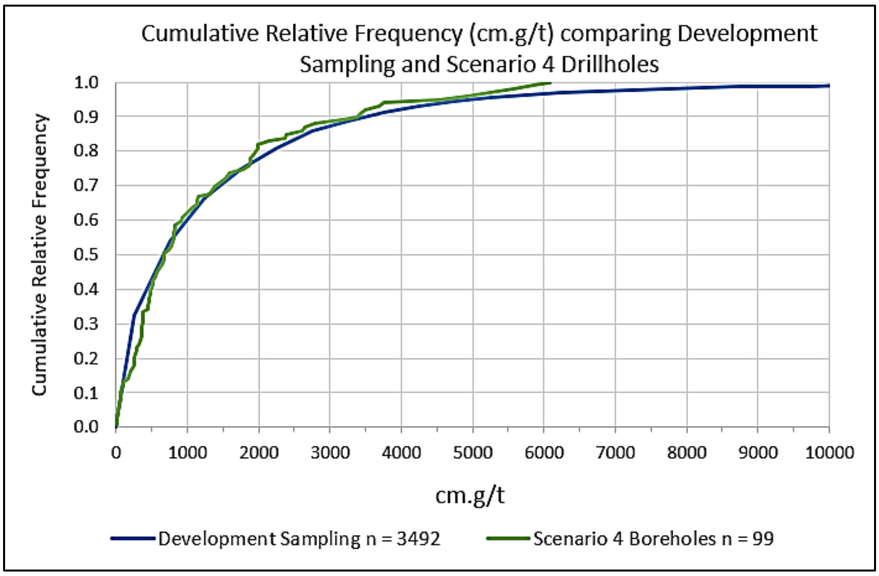

Figure 5-35: Cumulative frequency distribution plot comparing drillholes and development sampling

5.5.1 Scenario Five Geozones

A similar indicator kriging exercise as before was completed to define geozones. The aim of this exercise was to refine the domain boundaries identified in Scenario Four, and to identify a possible slope reef domain. Indicator cut-offs were obtained from inflection points (at 20 cm, 30 cm, and 75 cm) on the relative frequency distribution plots for channel width.

Indicator variograms for the 75 cm indicator variable presented long-range spatial structure at a lag distance of 120 m, which corresponds to the borehole data spacing. The short-range structure near the origin was defined using a lag distance of 2 m, which corresponds to the development sample spacing. A combination of these two variograms was created to provide definition for both the long-range continuity (up to approximately 250 m) as well as the short-scale structure near the origin (Figure 5-36). The experimental semi-variograms using indicator variables at 20 cm and 30 cm produced variograms without spatial structure indicating that slope reef occurs randomly within the data.

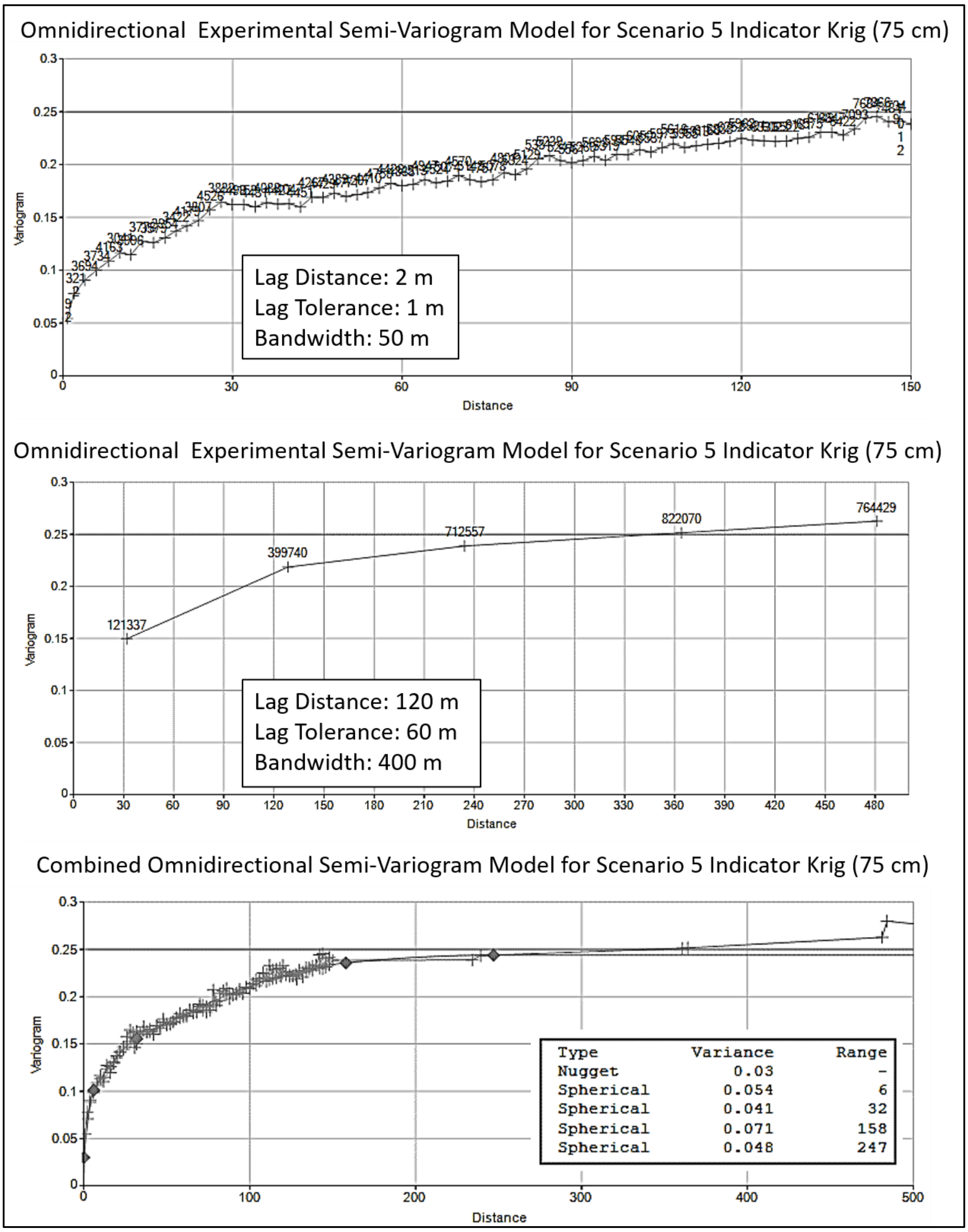

Figure 5-36: Scenario Five combined indicator variograms

A Thick Domain was delineated by red 60 m x 60 m blocks with a greater than 0.65 probability for reef width to be greater than, or equal to, 75 cm (Figure 5-37 A). The Thick Domain boundaries were adjusted using the colour-coded channel width plot as presented in Figure 5-37 B. The final geozone boundaries were further refined using the closely spaced development data in the colour-coded gold value (cm.g/t) plot as presented in Figure 5-37 C.

The domaining for Scenario Five reflects Thick and Thin Domains that are more clearly defined and show an improvement compared to the Scenario Four boundaries, which were delineated using only borehole data, and continuity is observed in a northwest to southeast direction.

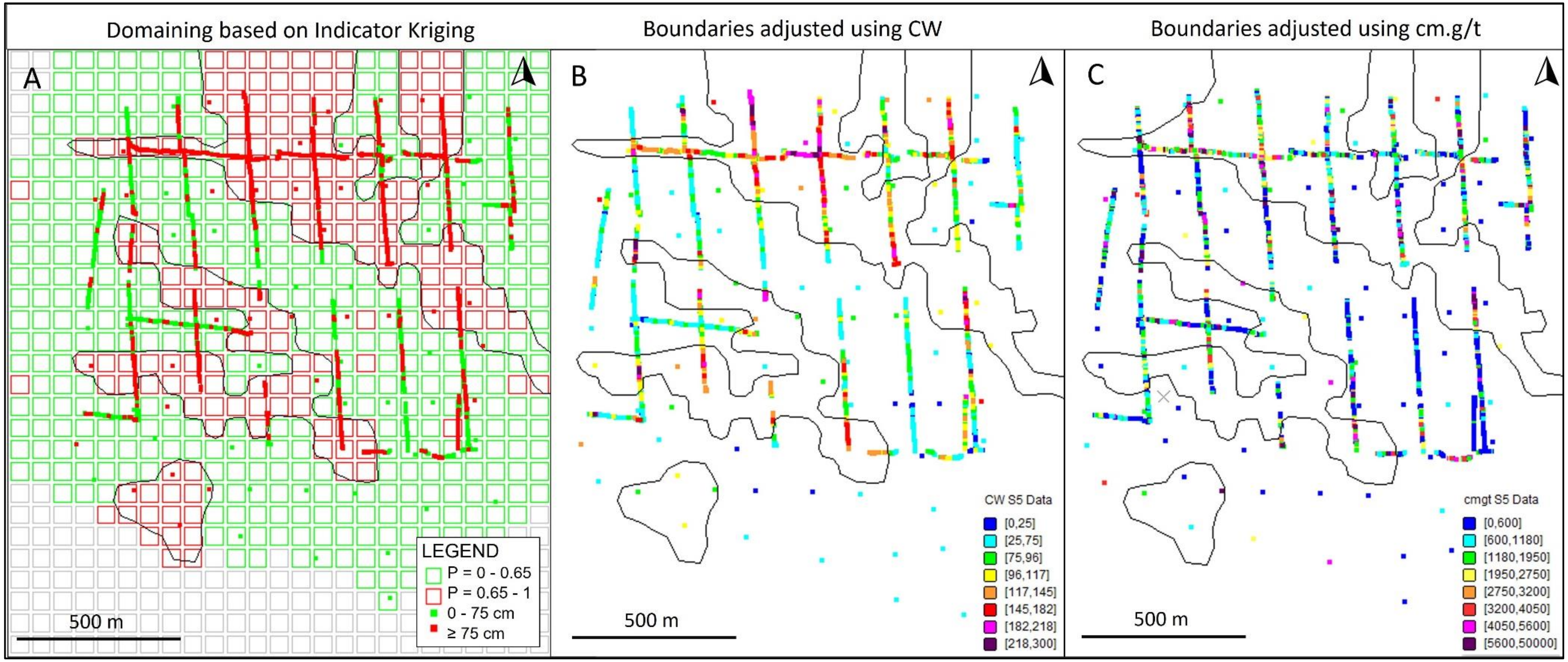

Figure 5-37: Scenario Five domaining

The conditional expectation plots of channel width verses gold value (cm.g/t), as presented in Figure 5-39, show a positive linear relationship between gold value (cm.g/t) and channel width. For class intervals of both 12 cm and 24 cm, there is a strong positive linear relationship up to a channel width of approximately 160 cm, whereafter the relationship plateaux as observed in Figure 5-39 and Figure 5-39. This positive linear relationship between average gold value (cm.g/t) and channel width supports the geozoning method based on channel width.

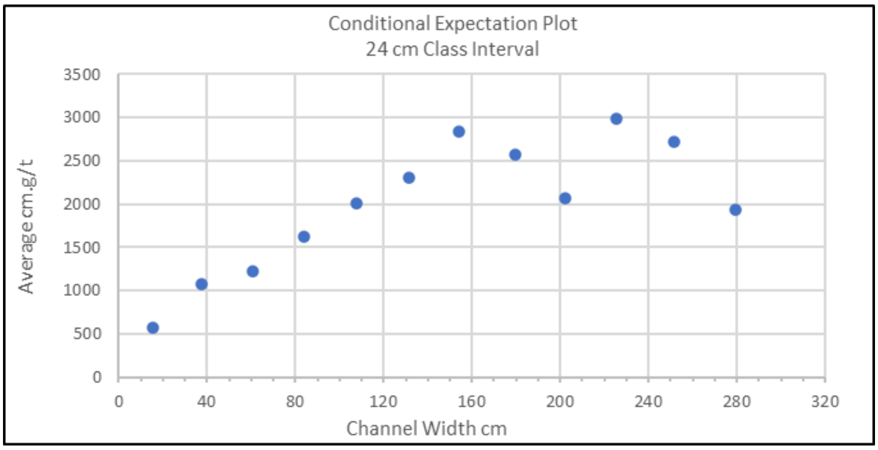

Figure 5-38: Conditional expectation plot of channel width (cm) vs average value (cm.g/t) using 24 cm class intervals

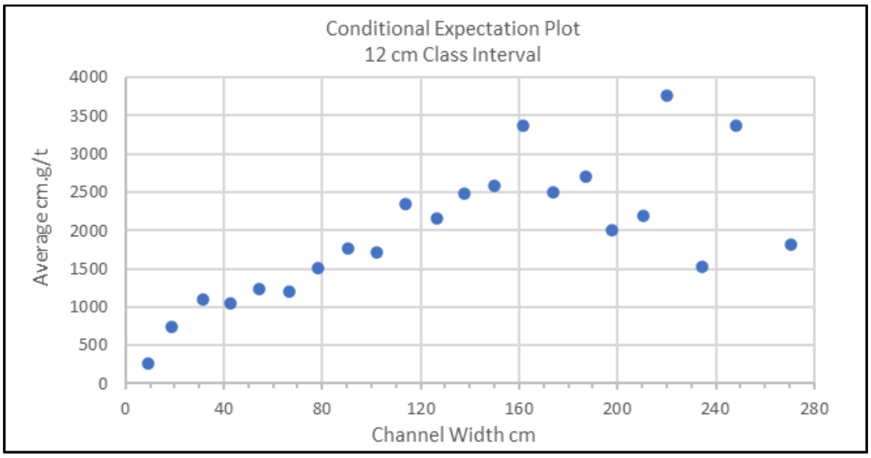

Figure 5-39: Conditional expectation plot of channel width (cm) vs average value (cm.g/t) using 12 cm class intervals

5.5.2 Scenario Five Exploratory Data Analysis

The summary statistics for the Thick and Thin Domains are presented in Table 5-12.

Table 5-12: Scenario Five Summary Statistics

Scenario 5 Gold and Channel Width Statistics					
THICK DOMAIN			THIN DOMAIN		
	cm.g/t	cm		cm.g/t	cm
Min	9	20.00	Min	1	7.00
Max	22 988	285.00	Max	25822	287.00
N	1 380	1 380	N	2211	2211
Range	22 979	265.00	Range	25 821	280.00
Mean	2 243	119.53	Mean	1 147	58.00
Median	1 461	114.00	Median	627	54.00
Mode	1 082	112.00	Mode	53	52.00
Variance	6 035 197	1 677.09	Variance	2 745 752	925.97
Std Dev	2 457	40.95	Std Dev	1 657	30.43
COV	1.10	0.34	COV	1.44	0.52
Skewness	2.82	0.66	Skewness	5.23	1.43
Kurtosis	14.77	3.62	Kurtosis	54.80	8.03

The frequency distribution models, or histograms, for gold value (cm.g/t) highlighted the different shapes of the Thick and Thin Domain cm.g/t distributions (Figure 5-40). The cumulative relative frequency distributions emphasise the cm.g/t value differences between domains for the same proportion of data.

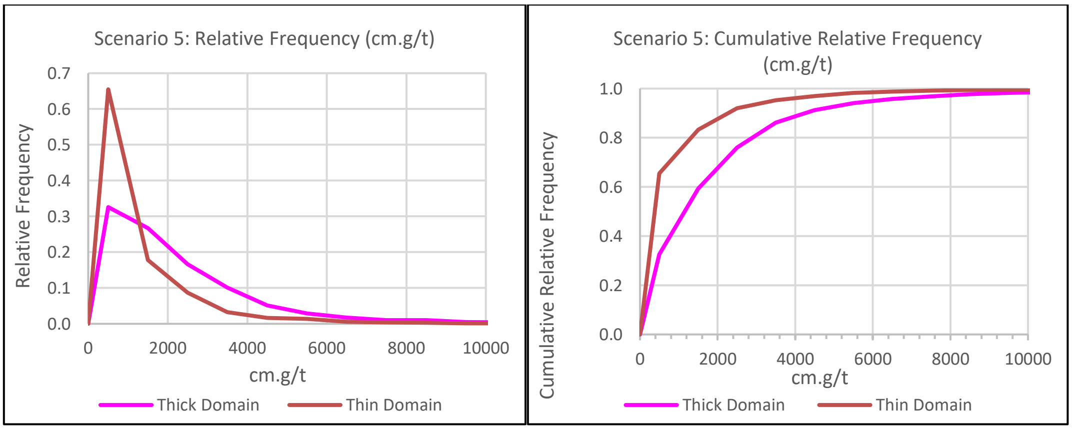

Figure 5-40: Scenario Five relative frequency distributions for gold value (cm.g/t)

The summary statistics and frequency distribution models confirmed two different populations, and the data was therefore split into the Thick and Thin Domains.

5.5.3 Scenario Five Variography

Figure 5-41 depicts the spatial variogram contour plot and omnidirectional semi-variogram model for the Thick Domain. The variogram contour plot indicates slight preferential continuity in an east-west direction due to the data orientation of a dominant east-west development drive within the Thick Domain. The preferential continuity is therefore an artefact of data configuration along the development drives. The omnidirectional semi-variogram model is therefore appropriate for modelling the spatial structure of the Thick Domain. A variogram combining the 5 m and 10 m lag distances was created to capture the short-scale spatial structure near the variogram origin. The experimental variogram calculated at smaller lag distances along the development drives provides better definition of the nugget effect, which decreased from 0.72 in Scenario Four to 0.5 in Scenario Five.

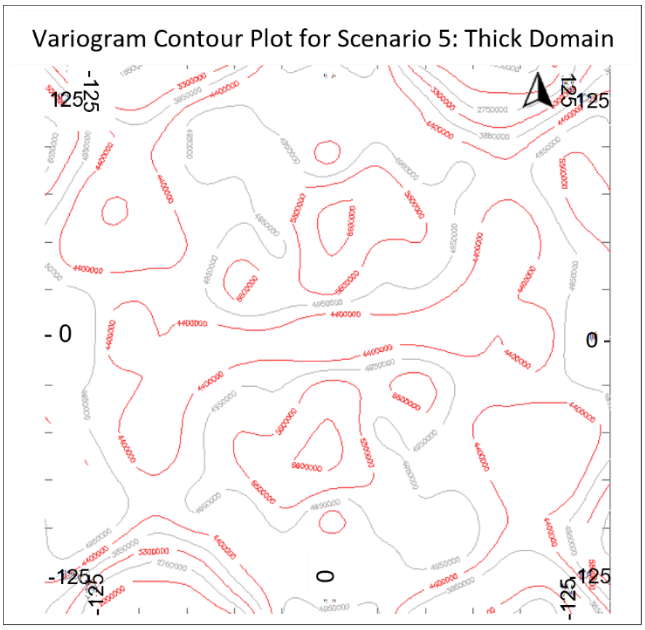

Scenario 5: Thick Domain

Exp. Semi-Variogram

Parameters

Angle: 30° increments

Angle Tolerance: 15°

Lag Length: 5 and 10 m

No. of Lags: 10

Lag Tolerance: 2.5 and 5 m

Bandwidth: 50 m

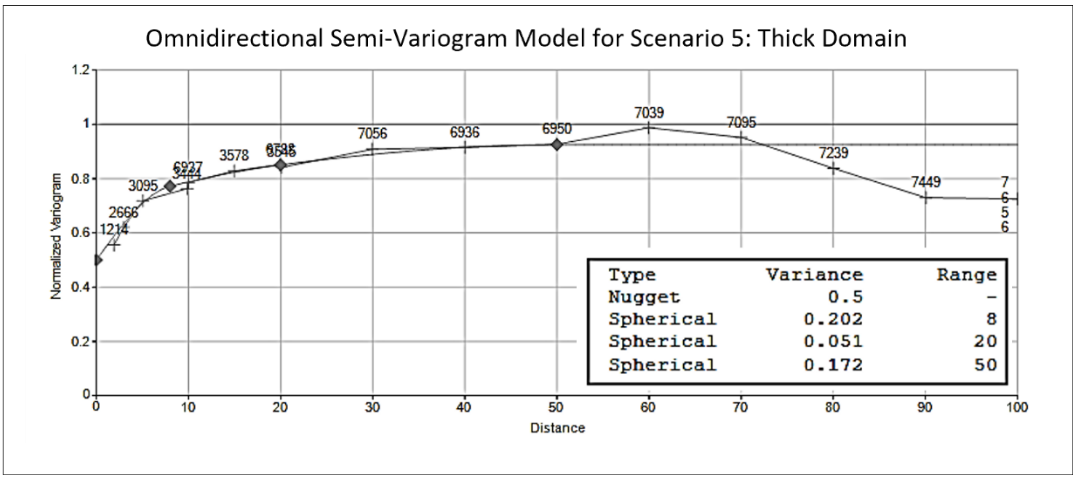

Figure 5-41: Scenario Five variogram for the Thick Domain

The closely spaced development sampling (at 2 m intervals) provides an indication of the close spaced variability and is a guide for improving the nugget effect estimation similar to a downhole variogram in a 3D environment. The range decreased from 471 m to 50 m in Scenario Four which is a better reflection of the distance of true mineralisation continuity.

Figure 5-42 presents the variogram contour plot and omnidirectional semi-variogram model for the Thin Domain. The variogram contour map depicted preferential continuity in a northwest-southeast direction which aligned with the overall data orientation within the domain and was therefore considered an artefact of data orientation. An omni-directional variogram was modelled for the Thin Domain.

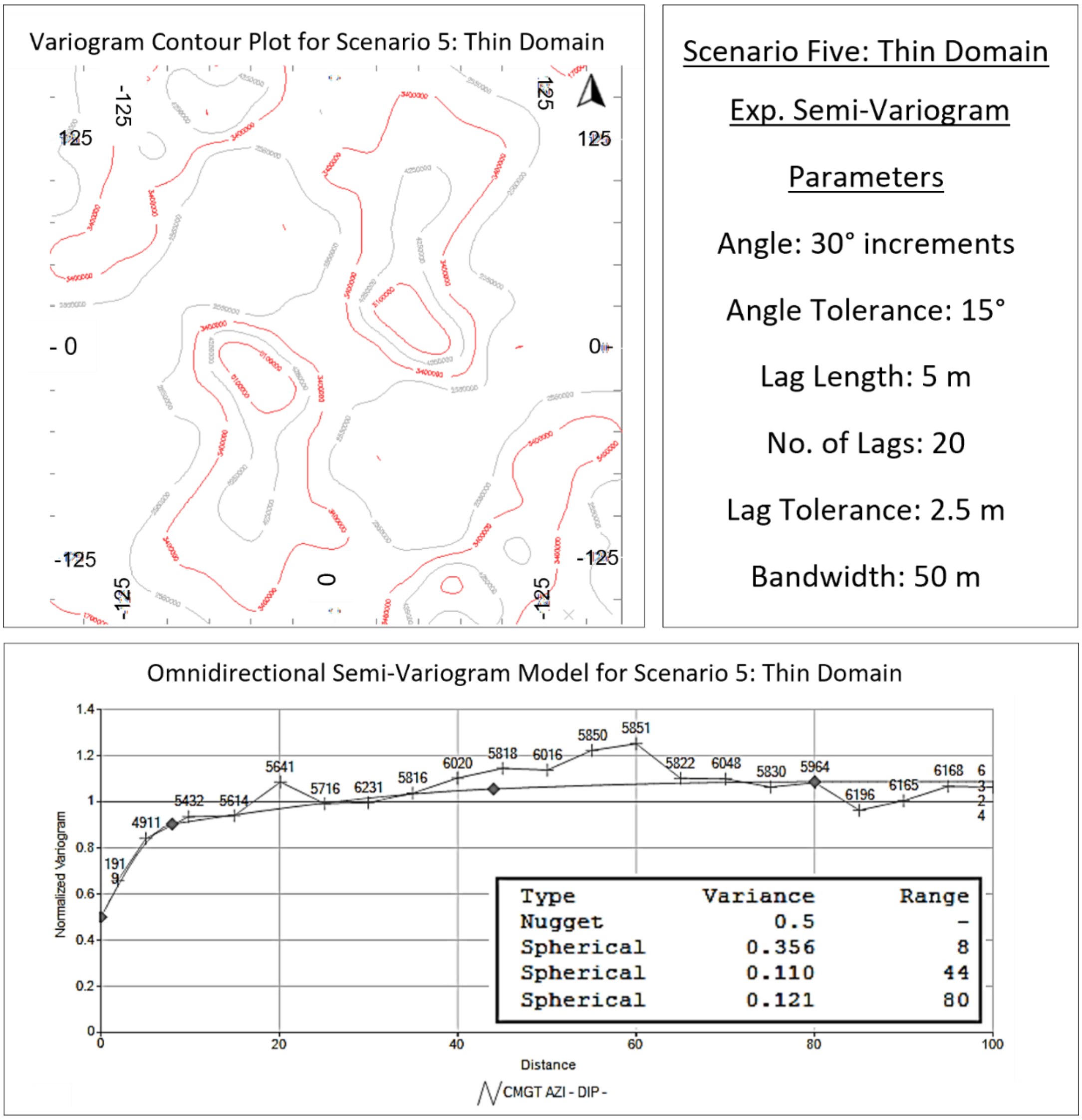

Figure 5-42: Scenario Five variogram for the Thin Domain

The nugget effect increased from 0.18 in Scenario Four to 0.5 in Scenario Five. This increased nugget effect reflects the greater variability of the data within the Thin Domain due to the increased amount of data. The range decreased from 350 m in Scenario Four to only 80 m in Scenario Five, which is a more realistic reflection of the true mineralisation continuity distance.

The long-range mineralisation continuity distance observed in Scenario Four was not observed in Scenario Five. A lag distance at 120 m and a wider bandwidth does not indicate any spatial correlation in either the Thin or Thick Domains, and a pure nugget effect was observed at this lag distance. This highlights the increased variability due to the increased amount of data, and only samples closer together show correlation.

The variograms for channel width of both domains are presented in Figure 5-43. The variogram parameters are the same as those used for the gold value (cm.g/t).

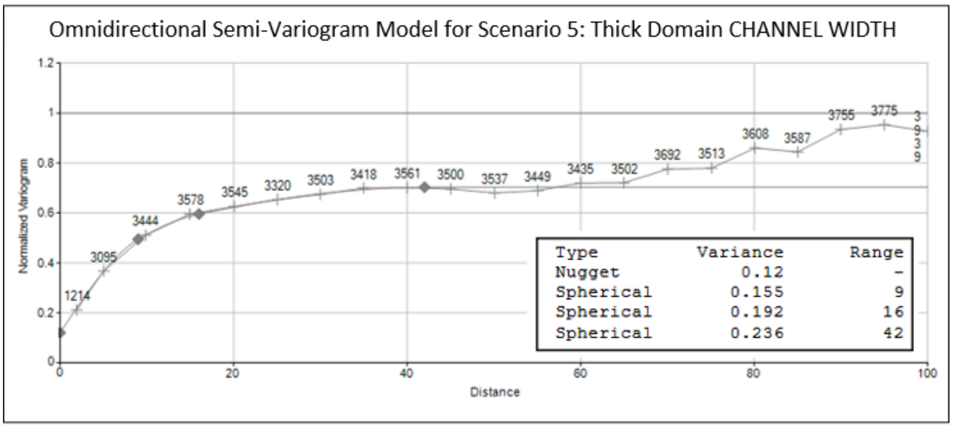

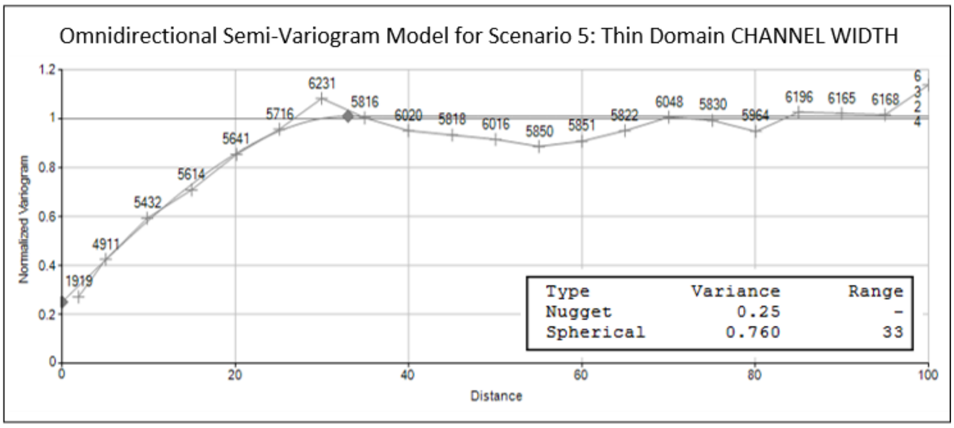

Figure 5-43: Scenario Five Thick and Thin Domain variograms for channel width (cm).

5.5.4 Scenario Five Local Value (cm.g/t) and CW (cm) Estimates

A local geostatistical estimate was generated for Scenario Five to reflect the spatial correlation captured by the variogram models. The challenge with estimating Scenario Five was to extrapolate estimates into areas with less data density.

Kriging performance indicators for the 10 m x 10 m blocks are presented in Figure 5-44 (Thick Domain) and Figure 5-45 (Thin Domain). The kriging performance indicators indicate that ordinary kriging into a block size of 10 m x 10 m is only acceptable for a narrow strip, or column, surrounding the data (20 m to 50 m) due to the short variogram range (50 m to 80 m) and data configuration along raise lines at approximately 180 m apart. Samples towards the end of the variogram range tend towards equal weighting and result in a worse estimate with a higher kriging variance, low slope of regression and negative kriging efficiencies.

Block variance for the Thick and Thin Domains is fairly low (0.23 and 0.29 respectively) due to the nugget effect of 0.5 for both domains, and a range of 50 m and 80 m for the Thick and Thin Domains, respectively.

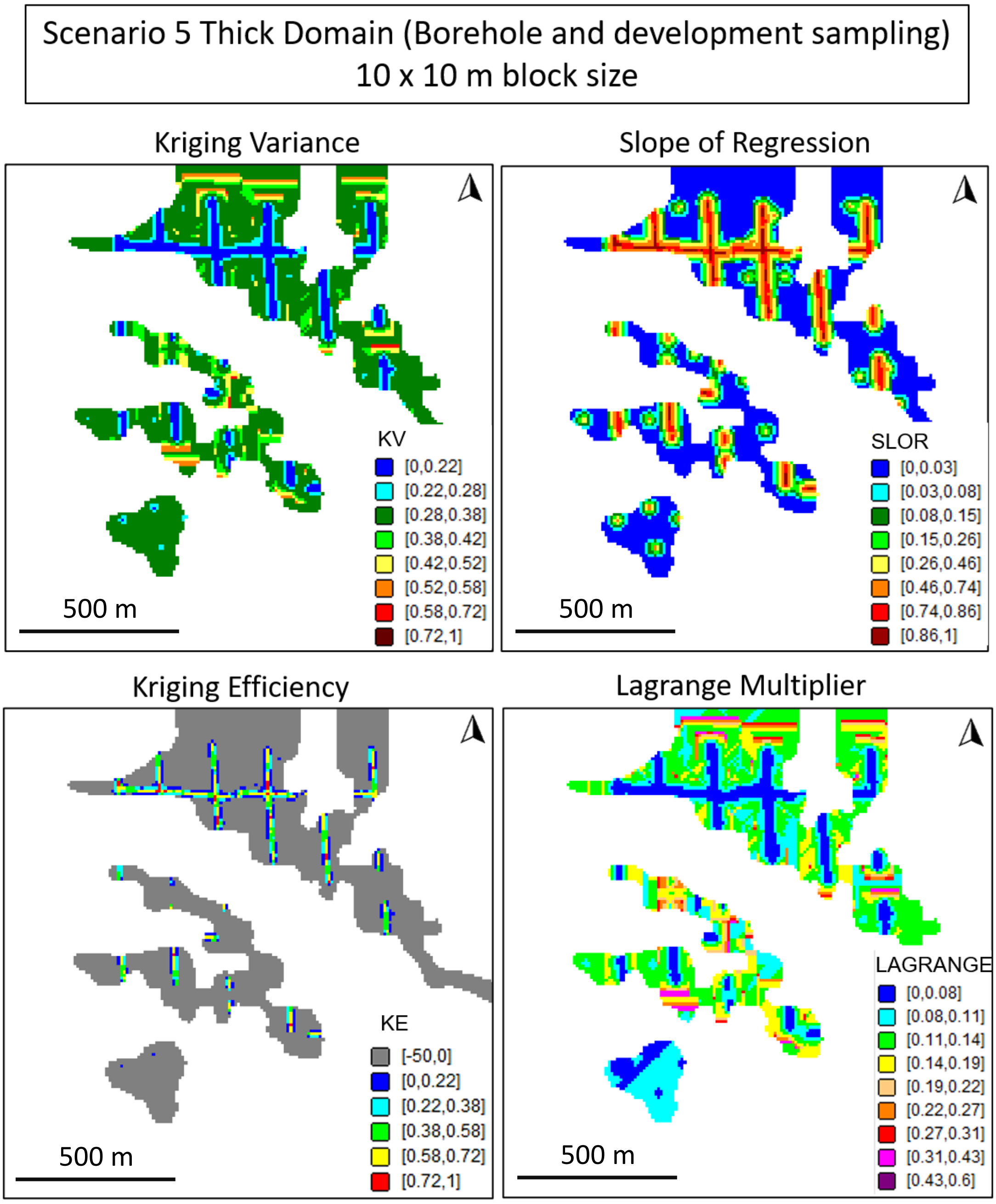

Figure 5-44: Scenario Five Thick Domain kriging performance indicators

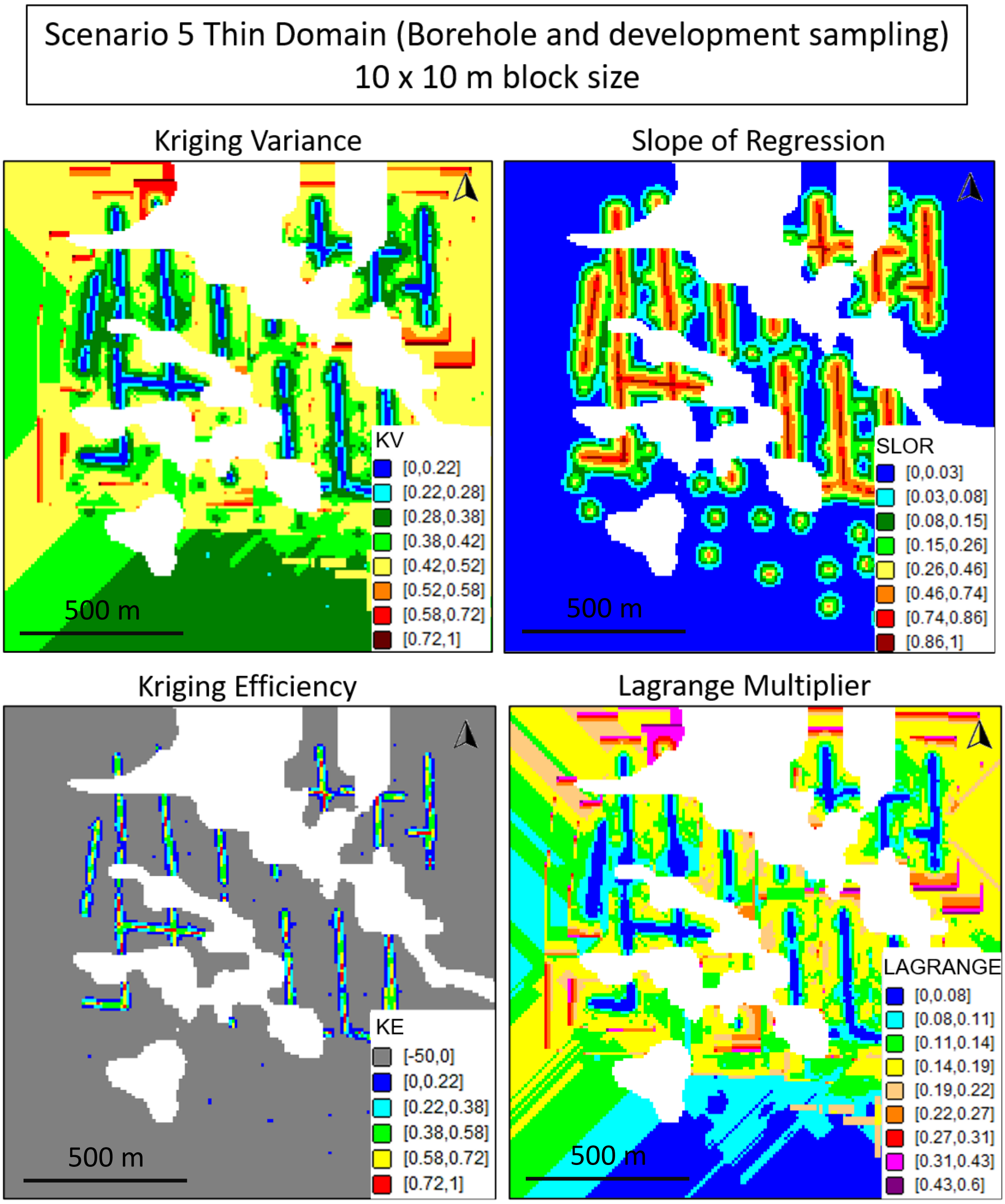

Figure 5-45: Scenario Five Thin Domain kriging performance indicators

A suitable alternative method to improve the estimation results beyond the narrow range of acceptable 10 m x 10 m blocks is to utilise the long-range variograms modelled using the borehole data in Scenario Four. The widely spaced boreholes captured a long-range spatial structure that would result in acceptable estimates further from the data. The Scenario Four variogram models and the data from Scenario Five were used to generate an improved estimate at a block size of 60 m x 60 as presented in Figure 5-46.

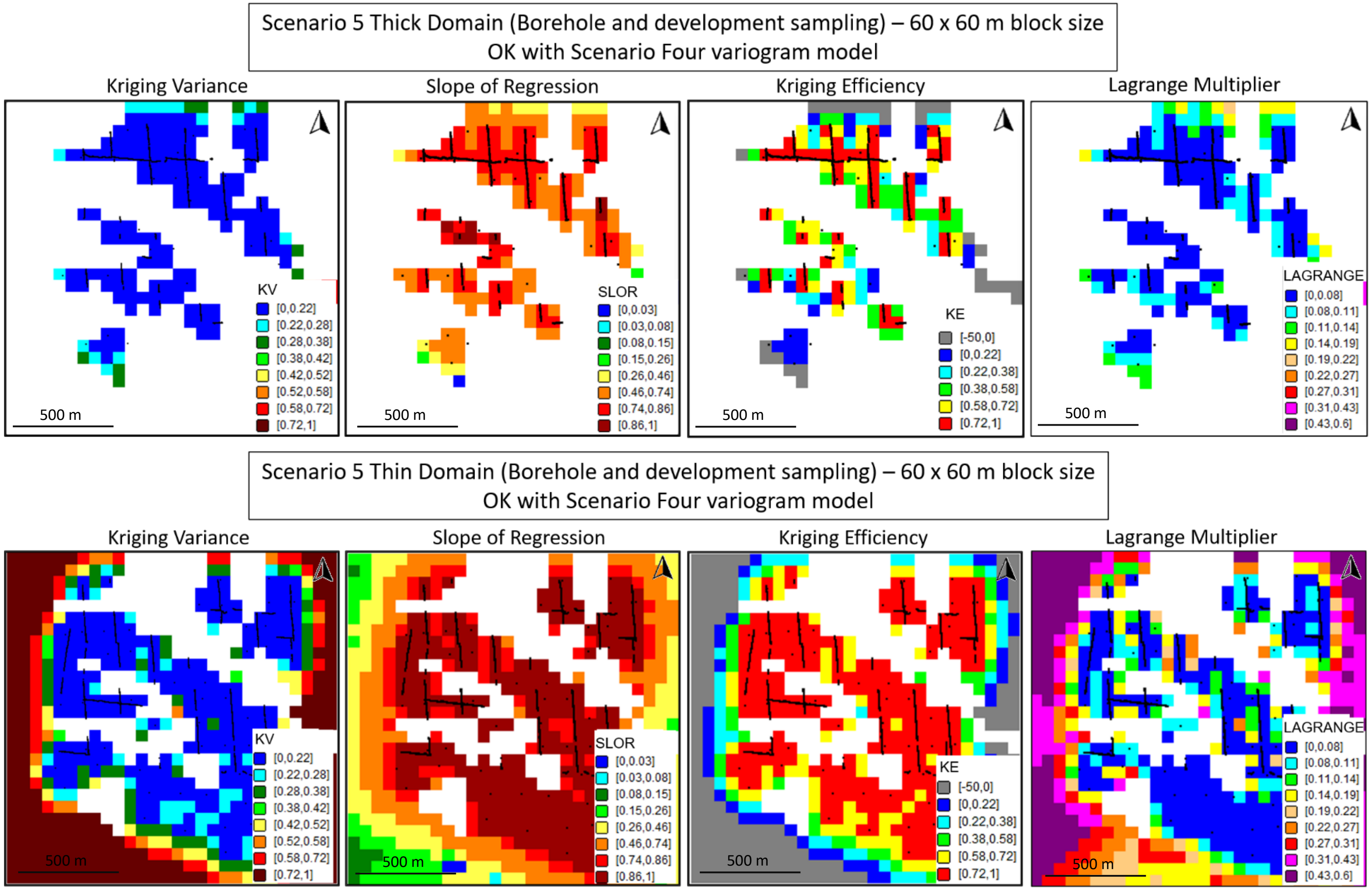

Figure 5-46: Scenario Five kriging performance indicators for 60 m x 60 m blocks using the Scenario Four variogram models

The 60 m x 60 m blocks between raise lines now present lower kriging variances, a higher slope of regression and no negative kriging efficiencies due to the long variogram range and larger block size. The Lagrange multiplier increases to a value of greater than 0.3 towards the edges of the model in the Thin Domain supporting the application of simple kriging for extrapolation beyond the data. The higher nugget effect in the Thick Domain results in a slightly poorer slope of regression and lower kriging efficiencies as observed in the results from Scenario Four.

The final estimate for Scenario Five is presented in Figure 5-47. The 10 m x 10 m estimates were constrained to blocks with a positive kriging efficiency. Constraining may, however, be based on kriging variance, slope of regression, kriging efficiency, or a combination of these results. The inclusion of the 10 m x 10 m blocks result in improved selectivity for planning surrounding raise line development. The 60 m x 60 m blocks result in an improved estimate, particularly in the Thin Domain, due to the additional data available in Scenario five.

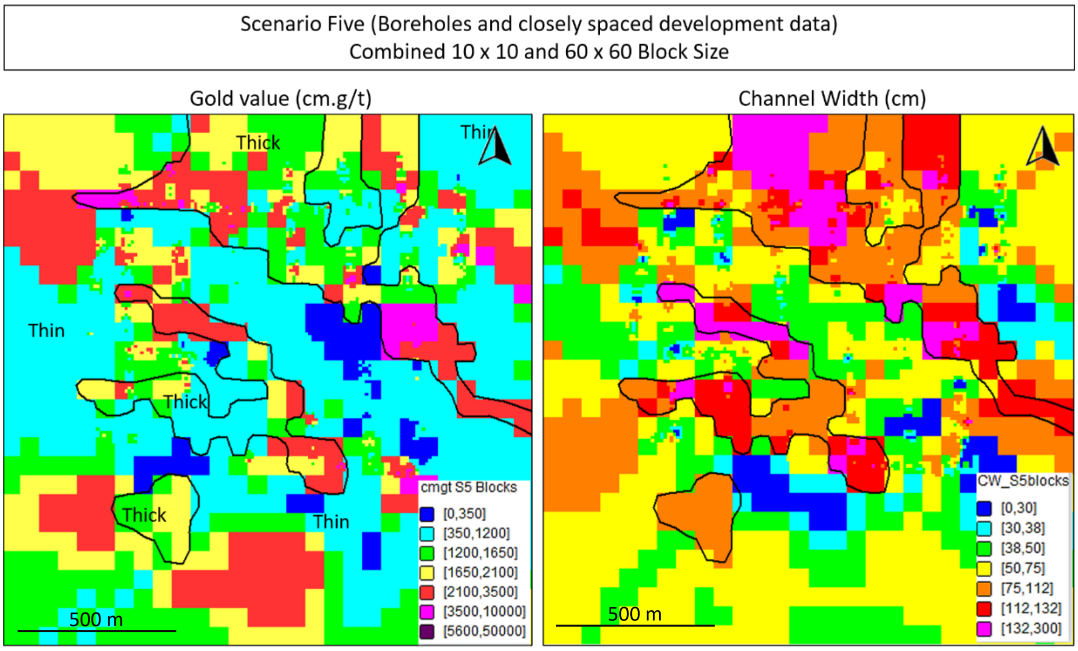

Figure 5-47: Scenario Five Thick and Thin Domain estimates for gold value (cm.g/t) and channel width (cm)

Extrapolating data using simple kriging may be useful to reduce the edge effect observed towards the Thin Domain model edges, as observed in the ordinary kriging in Figure 5-48. A simple kriged estimate is weighted using a local mean value and blocks beyond the range of the variogram are equal to the global mean value due to limited data, as observed in the simple kriging estimates in Figure 5-48 (global mean of 1147 cm.g/t).

Constraining the ordinary kriging 60 m x 60 m blocks using a low Lagrange multiplier of less than 0.3 would result in the simple kriging overwriting the ordinary kriged blocks that are displaying the edge effect.

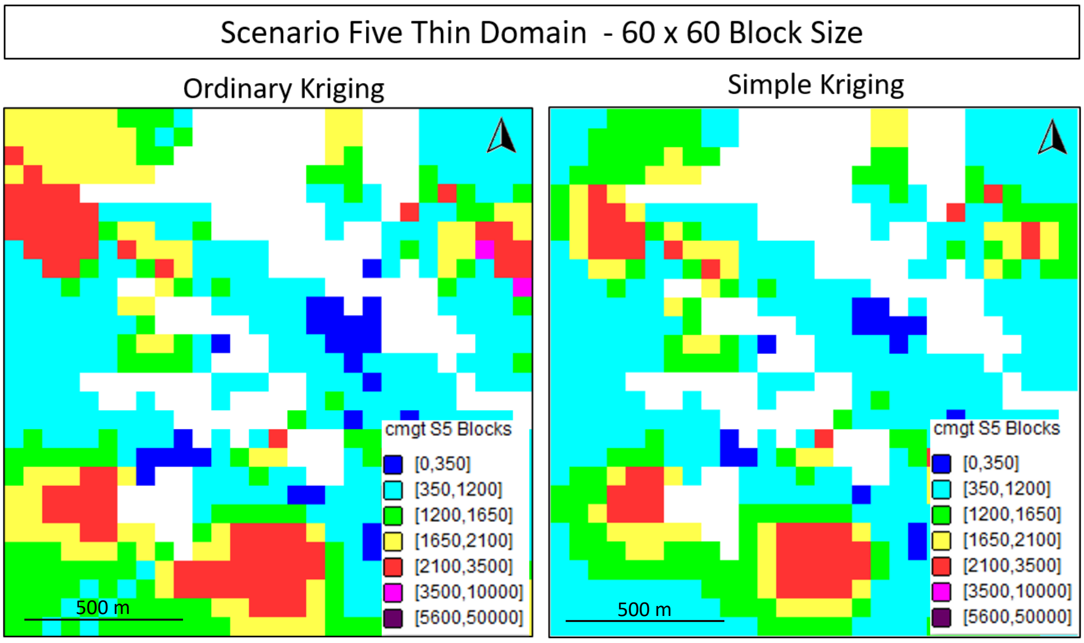

Figure 5-48: Scenario Five Thin Domain comparing ordinary and simple kriging.

5.5.5 Scenario Five Estimate Validation

Table 5-13 presents a comparison of the estimate statistics and the data statistics for Scenario Five. The Thick Domain mean estimate is 22 cm.g/t (0.9%) lower than the sample mean, and the Thin Domain estimate is 20 cm.g/t (4.0%) higher than the sample mean, both indicating acceptable estimation results.

Table 5-13: Scenario Five statistical comparison between block estimates and sampling data

SCENARIO 5 THICK DOMAIN STATISTICS				SCENARIO 5 THIN DOMAIN STATISTICS			
ESTIMATE		SAMPLES		ESTIMATE		SAMPLES	
	cm.g/t		cm.g/t		cm.g/t		cm.g/t
Min	478	Min	9	Min	19	Min	1
Max	9597	Max	22988	Max	6954	Max	25822
N	1 072	N	1 380	N	2 472	N	2 211
Mean	2 221	Mean	2 243	Mean	1 194	Mean	1 147
Variance	1 614 902	Variance	6 035 197	Variance	530 411	Variance	2 745 752
Std Dev	1 271	Std Dev	2 457	Std Dev	728	Std Dev	1 657
COV	0.57	COV	1.10	COV	0.61	COV	1.44

The relative frequency distributions for the two domains, presented in Figure 5-49 again display that the block estimate distribution shape changes and tends towards symmetry due to the variance decrease associated with larger support size estimates (support effect).

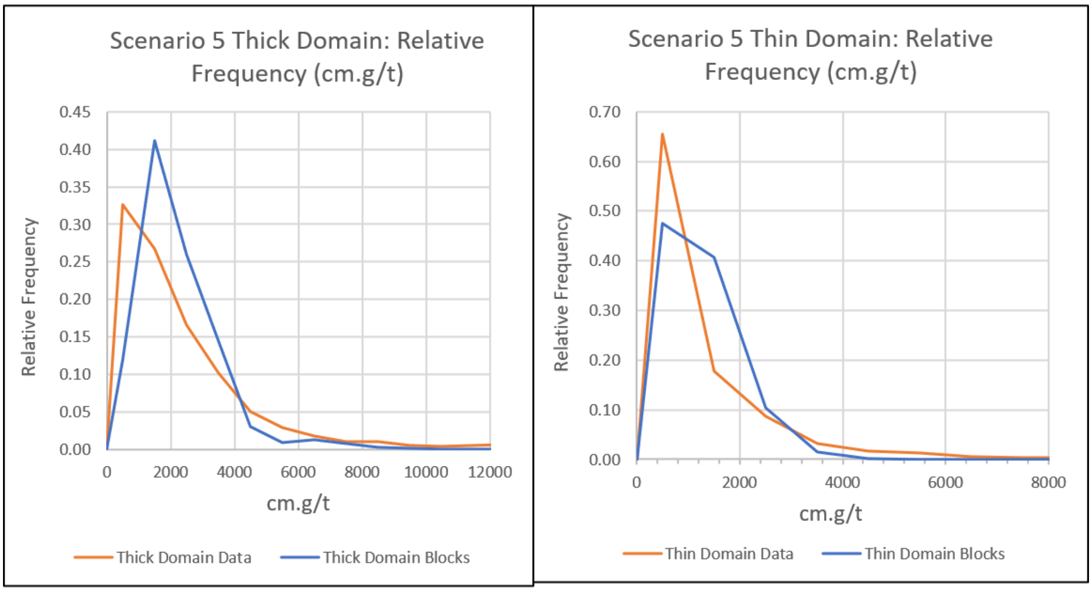

Figure 5-49: Relative Frequency distributions for the Thick and Thin Domain block estimates and samples

Swath plots were generated in a direction parallel to the observed northwest-southeast grade trend. Swath plots generated at widths of 240 m and 120 m showed similar results. Most estimate values (model) plot within the 90% confidence limit of the sample data and show less smoothing than Scenario Four. Confidence limits are narrower due to an increased number of samples. The 240 m swath plots for the Thick and Thin Domains in a northeast-southwest direction only are presented in Figure 5-50 and Figure 5-51.

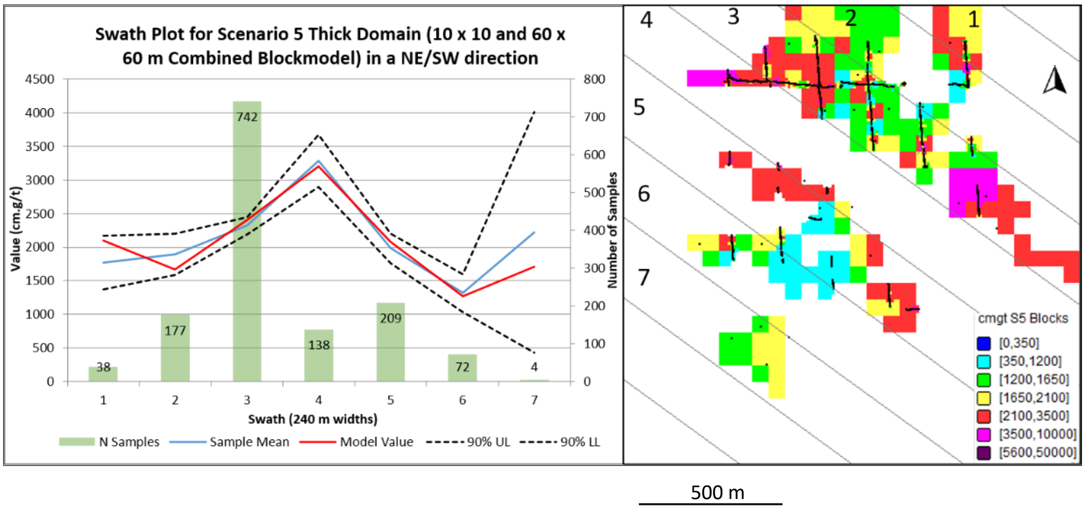

Figure 5-50: Scenario Five Thick Domain swath plot

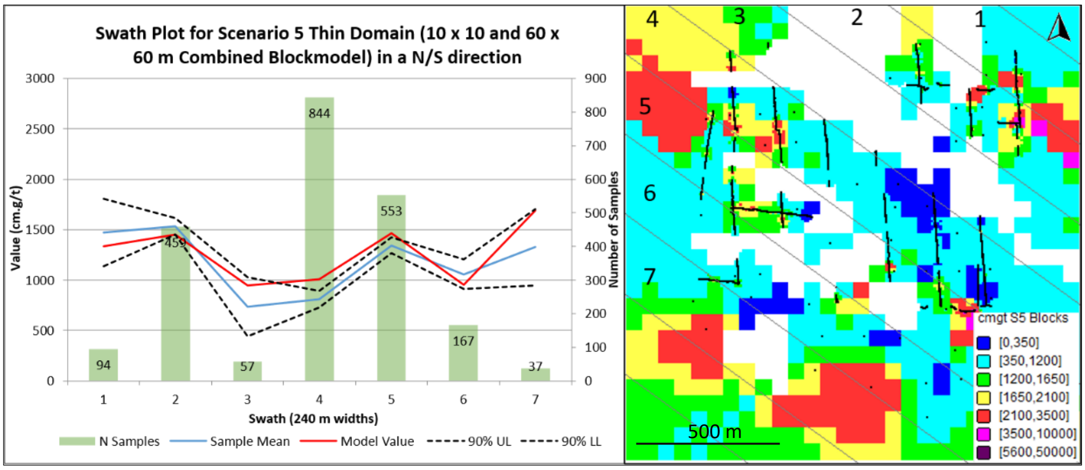

Figure 5-51: Scenario Five Thin Domain swath plot

5.5.6 Scenario Five Mineral Resource Estimate

The Competent Person on the project would use experience to provide their opinion on the Mineral Resource classification and one proposed resource classification is presented for Scenario Five. The 10 m x 10 m blocks were classified as Measured Mineral Resources. Indicated Mineral Resources were assigned to 60 m x 60 m blocks with a positive kriging efficiency, and Inferred Mineral Resources were assigned to 60 m x 60 m blocks with a negative kriging efficiency, as presented in Figure 5-52.

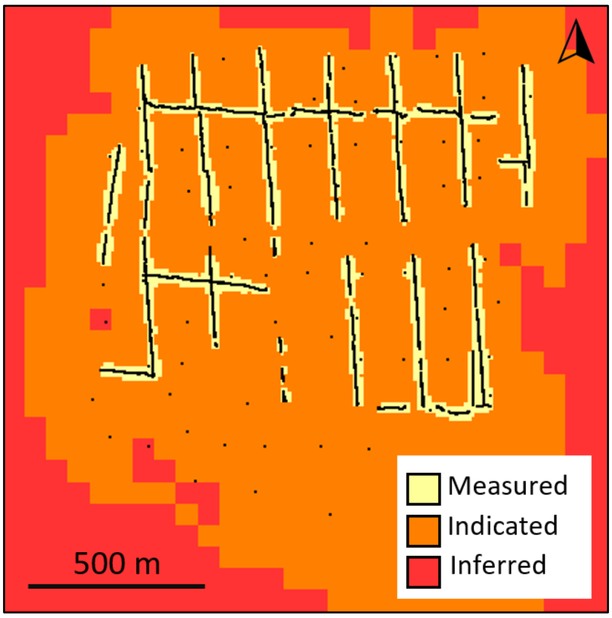

Figure 5-52: Scenario Five proposed Mineral Resource classification combined

The Mineral Resource estimate tabulation for Scenario Five is presented in Table 5-14.

Table 5-14: Scenario Five Mineral Resource estimate

Scenario Five Mineral Resource Estimate								
		Area (m^2)	CW (cm)	Tonnage (Mt)	Grade (cm.g/t)	95 % Lower Limit (cm.g/t)	95 % Upper Limit (cm.g/t)	Grade (g/t)
Measured	Thick Domain	79 100	120	0.26	2 241	2 180	2 302	18.73
	Thin Domain	168 300	58	0.27	1 170	1 139	1 202	20.05
Total Measured		247 400	78	0.52	1 513	1 472	1 554	19.40
Indicated	Thick Domain	435 800	121	1.43	2 178	2 116	2 240	18.02
	Thin Domain	1 490 200	57	2.31	1 196	1 167	1 225	20.95
Total Indicated		1 926 000	72	3.73	1 418	1 382	1 455	19.83
Total Measured + Indicated		2 173 400	72	6.04	1 429	1 392	1 466	19.78
Inferred	Thick Domain	100 800	122	0.33	2 009	1 949	2 070	16.53
	Thin Domain	543 600	63	0.93	1 451	1 422	1 480	22.89
Total Inferred		644 400	73	1.27	1 539	1 505	1 572	21.22

5.5.7 Scenario Five Value-Tonnage Estimates

The 60 m x 60 m blocks account for over 90% of the resource volume, so relative tonnes of the Indicated Mineral Resource blocks and Inferred Mineral Resource blocks are presented for comparison in a value-tonnage plot (Figure 5-53).

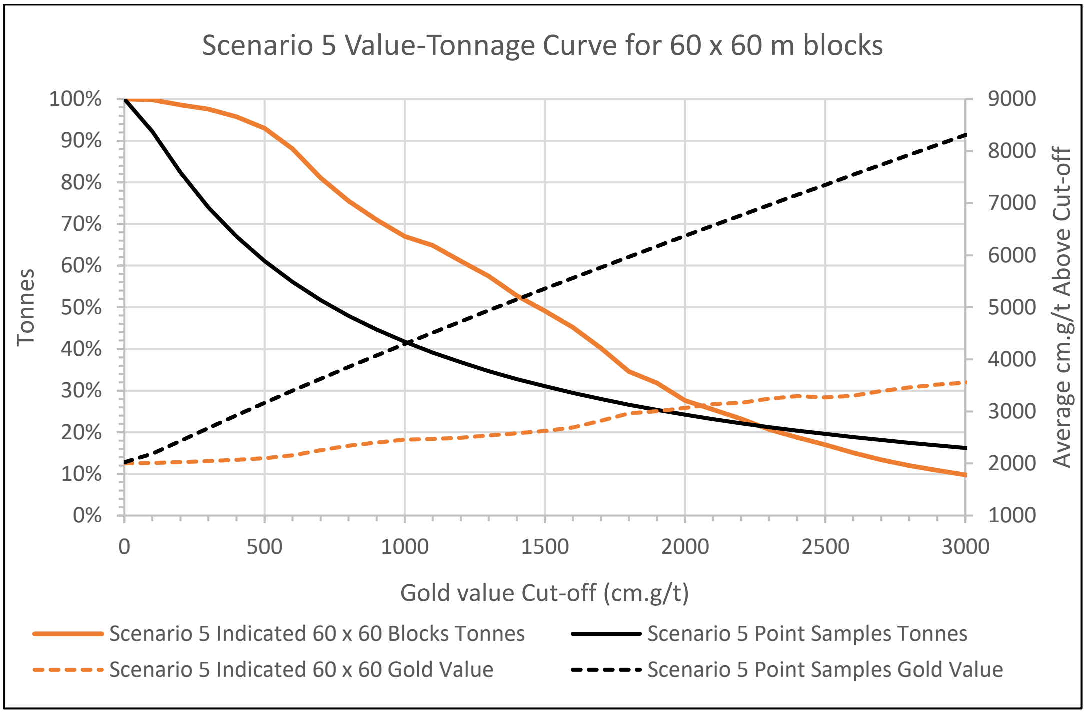

Figure 5-53: Scenario Five value-tonnage curve for the 60 m x 60 m blocks

Figure 5-53 demonstrates the support effect by comparing point samples to indicated block values. For example, at a cut-off value of 1000 cm.g/t, 68% of the indicated tonnes would have to be mined, compared to just 42% of the point samples tonnes. Inferred Resources should not be included in the mine plan.

The theoretical reduced support effect for the 10 m x 10 m blocks would provide greater selectivity for areas adjacent to raise lines. However, in a deep underground mining environment, these 10 m x 10 m blocks would be mined-out to a specific distance as a geotechnical requirement to reduce stress on the raise line, and therefore the selectivity of a limited strip, or column, adjacent to a raise line does not have much practical use.

5.5.8 Scenario Five Results Summary

The additional data used in the indicator kriging produced a channel width trend that aided definition of geozone boundaries for the Thick and Thin Domains. Both domains variograms were modelled using three nested spherical structures. The additional data allows for better short-scale definition and a better nugget effect estimation.

Ordinary kriging produced acceptable results for a block size of 10 m x 10 m for a narrow area surrounding the closely spaced development sampling. These blocks are classified as the Measured Mineral Resource and show increased selectivity, however they only account for less than 10% of the total Mineral Resource and, in practice, are not particularly useful.

An *a priori* variogram (from Scenario Four) was used to estimate a block size of 60 m x 60 m for extrapolation towards the edges of the deposit and for blocks between development data. 60 m x 60 m blocks with a positive kriging efficiency were classified as Indicated Measured Resource, and blocks with a negative kriging efficiency were classified as the Inferred Measured Resource.

The value-tonnage curve for the 60 m x 60 m indicated and inferred blocks indicated the decreased selectivity for the inferred blocks and although the estimate presents less smoothing, Scenario Five is most appropriate for overall resource estimation and long-term planning.

5.6 Scenario Six

Scenario Six represents the resource exploitation phase and includes the closely spaced development chip sampling, the stope face chip sampling (at a spacing of approximately 5 m x 10 m), and the surface borehole drilling data towards the south of the project area. The dataset contains a total of 10933 datapoints as spatially presented in Figure 5-54.

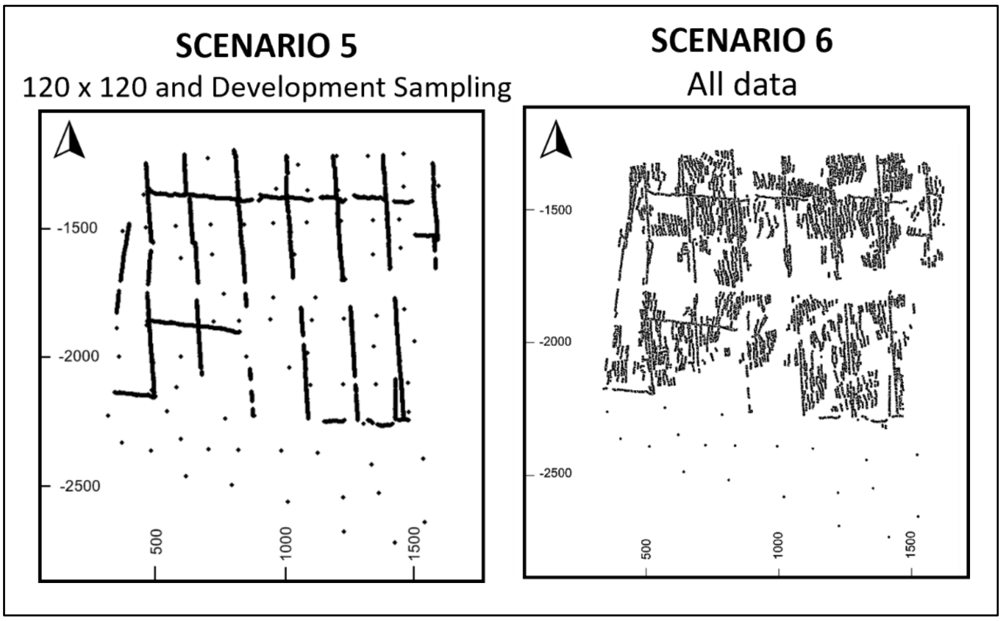

Figure 5-54: A comparison of the data location in Scenarios Five and Six

5.6.1 Scenario Six Geozones

An indicator kriging exercise using a CW indicator variable defined at 75 cm presented well-defined geozone boundaries for a smaller block size of 30 m x 30 m to represent a mining period over a quarter of the year based on a panel length of 30 m mined at an advance of 10 m per month (Figure 5-55 A). The indicator kriging channel width trends are confirmed in the colour-coded channel width plot with broad class intervals (Figure 5-55 B).

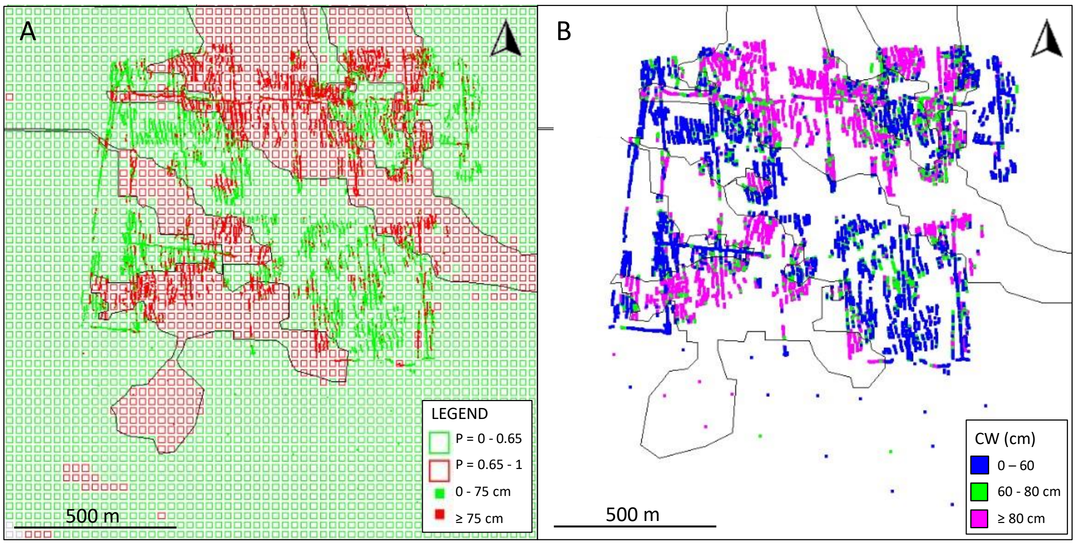

Figure 5-55: A) Scenario Six indicator kriging and B) colour-coded channel width plot

The domain boundaries identified by the indicator kriging and channel width plot are not confirmed in the colour-coded gold value (cm.g/t) plot, and sufficient data exists to consider alternative boundary positions. Relative cumulative frequency plots independent of class interval were used to identify large-scale inflection points in channel width, gold grade (g/t) and gold value (cm.g/t). Conditional expectation plots were also used to highlight large-scale inflection points in the gold value (cm.g/t) data and gold grade (g/t) data. The aim of considering these different plots was to produce broad, but meaningful, colour-coding intervals to produce spatial similar data variability in order to assist with boundary delineation. The colour-coded gold grade plot in combination with the colour-coded (cm.g/t) plot with respective thresholds at 18 g/t and at 1000 cm.g/t provided refined boundary positions.

The data were ultimately separated into two domains, a distinct Thin Domain, and a higher-grade domain with more data variability - the Mixed Domain. The final geozone boundaries are presented in Figure 5-56.

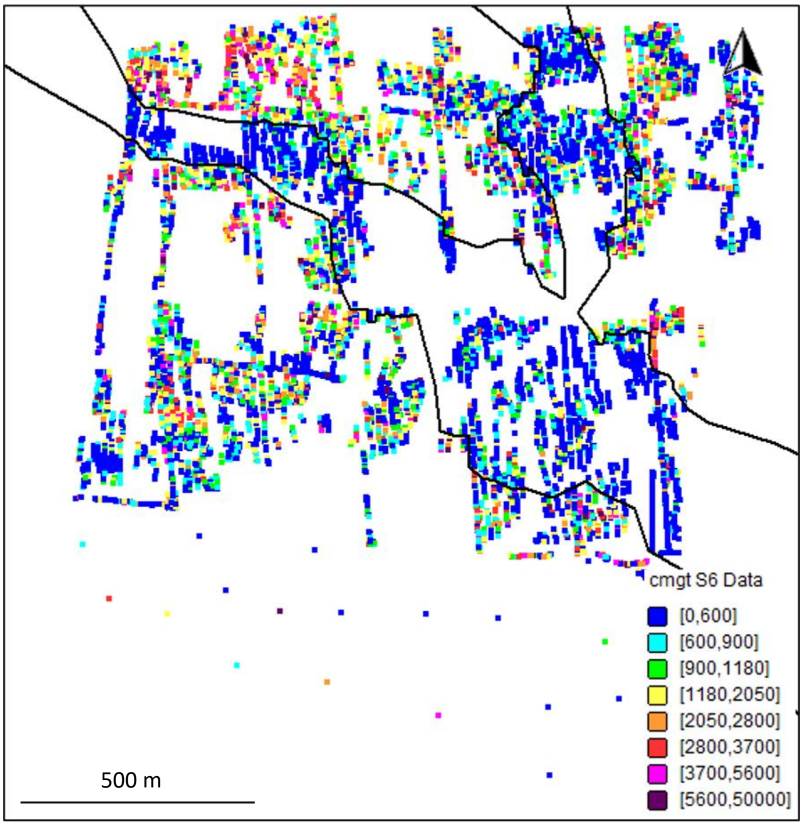

Figure 5-56: Scenario Six colour-coded cm.g/t plot with final geozone boundaries

5.6.2 Scenario Six Exploratory Data Analysis

The statistical summary for Scenario Six is presented in Table 5-15.

Table 5-15: Scenario Six statistical summary

Scenario 6 Statistical Summary					
MIXED DOMAIN DATA			THIN DOMAIN DATA		
	cm.g/t	cm		cm.g/t	cm
Min	1	52.00	Min	1	7.00
Max	32 487	297.00	Max	11 663	251.00
N	7 588	7 588	N	3 345	3 345
Range	32 486	245.00	Range	11 662	244.00
Mean	1 757	90.10	Mean	610	65.71
Median	1 122	87.00	Median	371	62.00
Mode	240	52.00	Mode	197	52.00
Variance	4 241 917	1.44	Variance	646 410	1 119.44
Std Dev	2 060	1.20	Std Dev	804	33.46
COV	1.17	0.01	COV	1.32	0.51

The relative frequency distribution and cumulative relative frequency distribution plots highlight the differences in distribution shape and cm.g/t value between the two geozones (Figure 5-57).

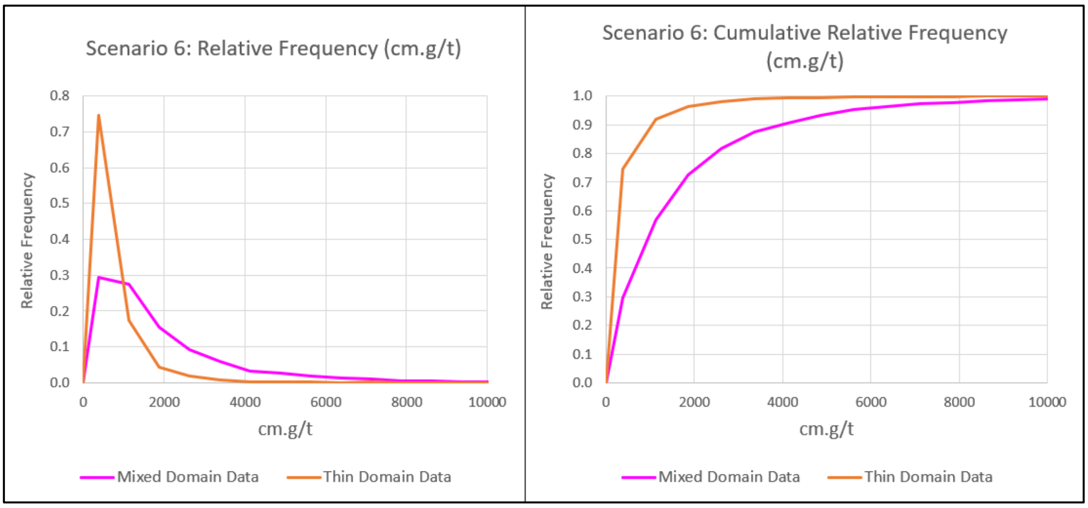

Figure 5-57: Scenario Six relative and cumulative relative frequency distributions

5.6.2.1 Data Cutting

Krige and Magri (1982) proved that outliers may hide continuity structures present in the variogram, especially when data has not been transformed. This was found to be true for Scenario Six and the data were ignored for variogram analyses (not estimation) to remove the influence of outlying high-grade values for calculation of the variogram model. The top 1% of data were removed, as indicated by the probability plot presented in Figure 5-58.

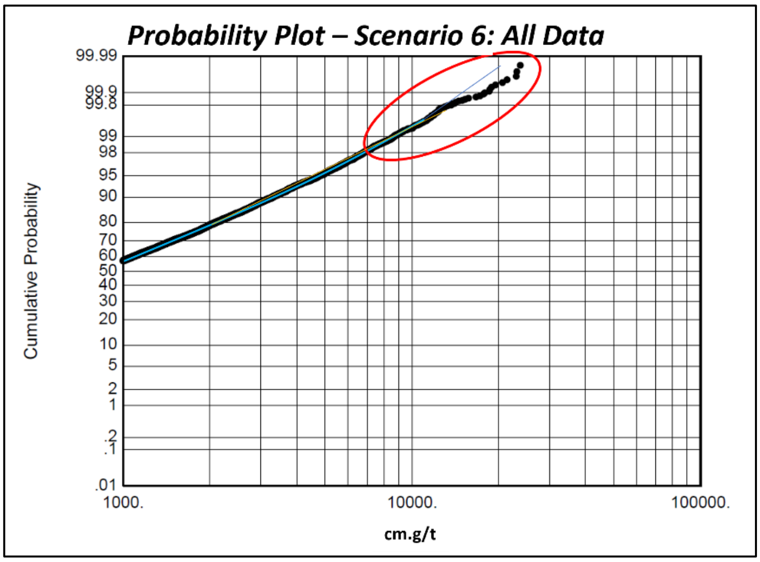

Figure 5-58: Scenario Six probability plot

5.6.3 Scenario Six Variography

The spatial structure for the Mixed Domain was modelled using three nested spherical structures. The nugget effect increased from 0.5 in Scenario Five to 0.65 in Scenario Six which highlights the increased sample variability due to additional data. The ranges are similar to those of Scenario Five, at 8 m, 22 m, and 60 m for the three structures. The Mixed Domain variogram contour map indicates preferential continuity in a northwest-southeast direction; however, this was not confirmed in the directional experimental variogram, and the omnidirectional variogram is more suitable for modelling the spatial structure of the Mixed Domain (Figure 5-59).

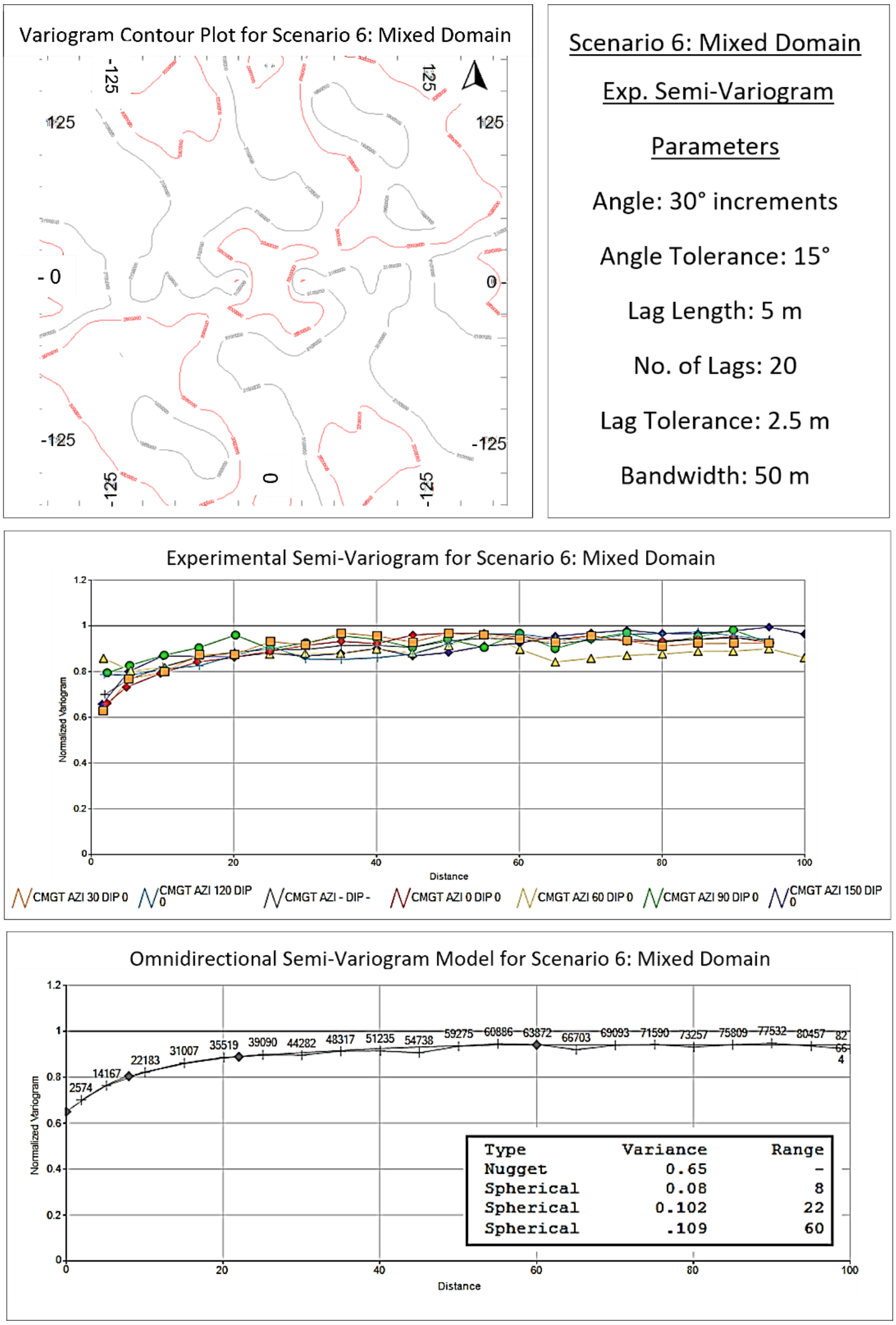

Figure 5-59: Scenario Six Mixed Domain omnidirectional variogram model

An omnidirectional variogram model is appropriate for the Thin Domain as the variogram contour plot shows a near circular shape near to the origin. The variogram model shows spatial continuity up to 9 m and only samples spaced very closely together show correlation (Figure 5-60). The nugget effect is slightly lower than for the Mixed Domain due to less data variability.

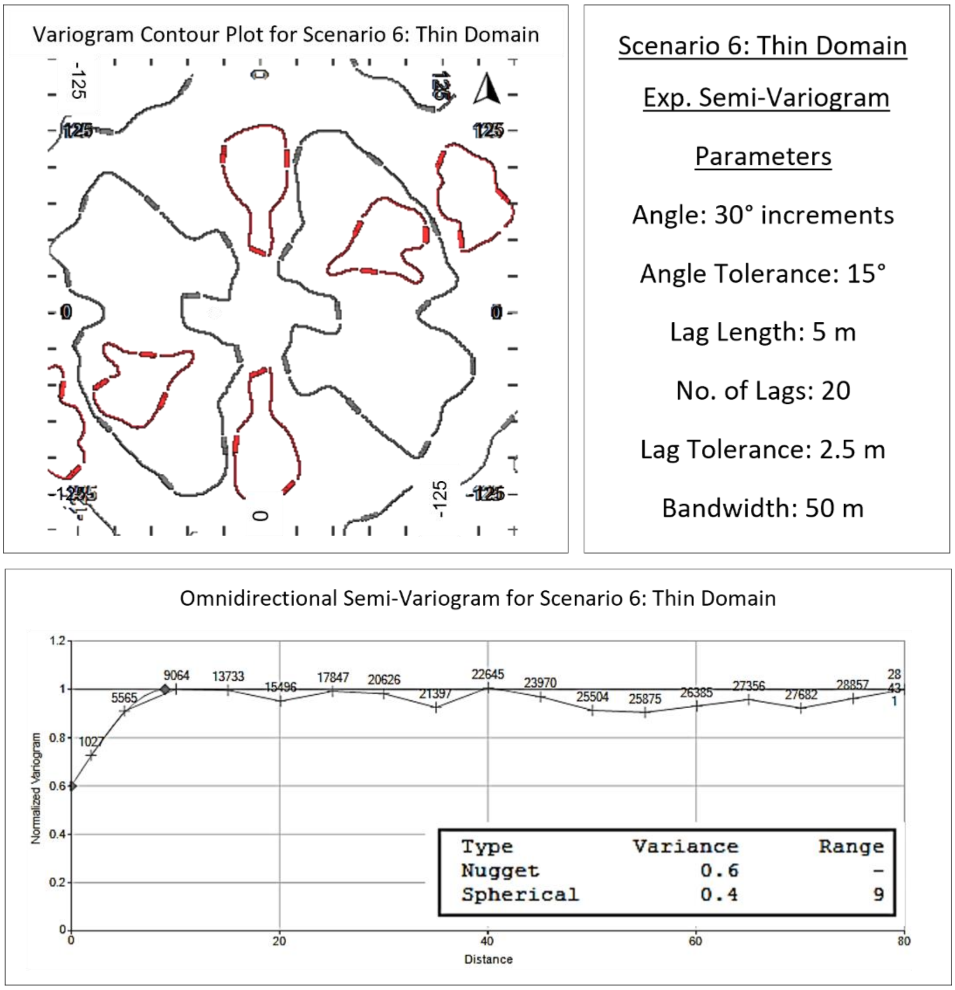

Figure 5-60: Scenario Six omnidirectional variogram models for gold value (cm.g/t)

The semi-variograms for channel width are calculated using the same parameters as those used for the value (cm.g/t) semi-variogram calculation in both domains (refer to Figure 5-61).

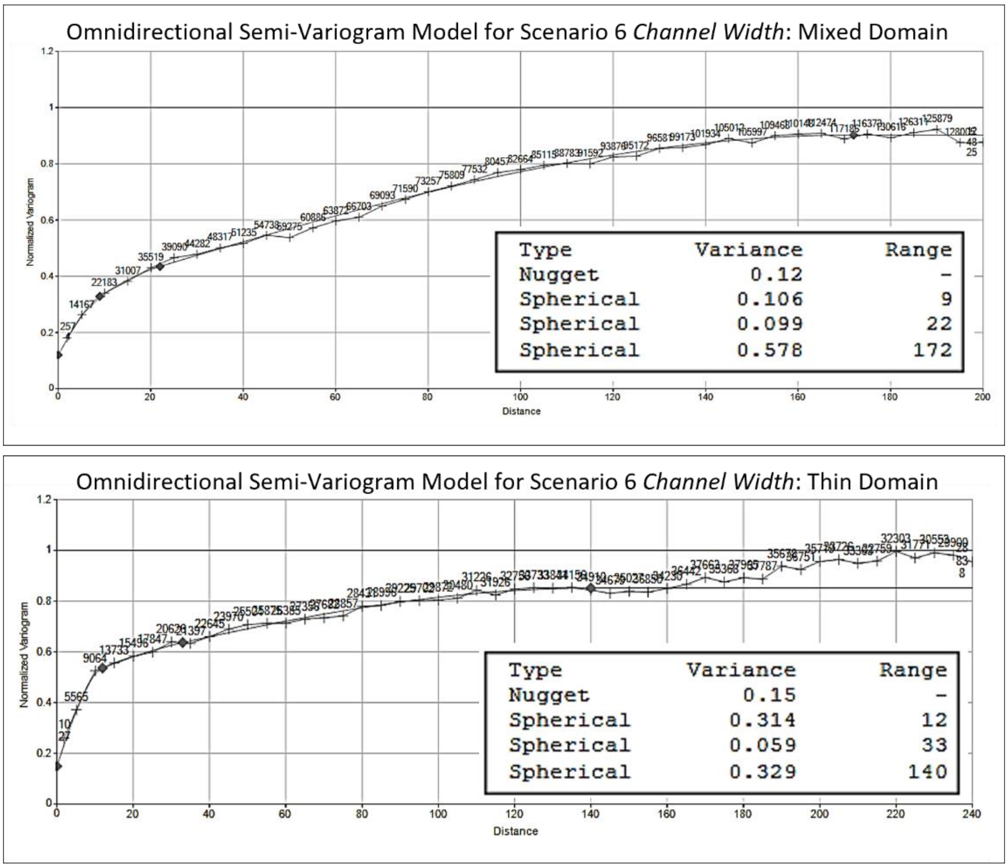

Figure 5-61: Scenario Six omnidirectional variogram models for channel width (cm)

5.6.4 Scenario Six Local Value (cm.g/t) and CW (cm) Estimates

Scenario Six Mixed Domain kriging performance indicators (kriging variance, slope of regression, kriging efficiency and the Lagrange multiplier) for the 10 m x 10 m and 30 m x 30 m blocks are presented in Figure 5-62. These results are constrained to the first search radius. The Mixed Domain block variance, a function of the variogram, is 0.18 for the 10 m x 10 m blocks which decreases to 0.09 for the 30 m x 30 m blocks worse kriging efficiencies.

The Mixed Domain 10 m x 10 m blocks show good, low kriging variances, a high slope of regression, acceptable kriging efficiencies and a low Lagrange multiplier for blocks surrounded with data. The acceptable block estimates extend over a larger area than observed in Scenario Five due to the additional stope sampling data now included. The slope of regression decreased for the 30 m x 30 m blocks indicating higher conditional bias in the larger blocks. However, the 30 m x 30 m blocks extend over a slightly larger area surrounding the data and indicate lower kriging variances than observed in the 10 m x 10 m results.

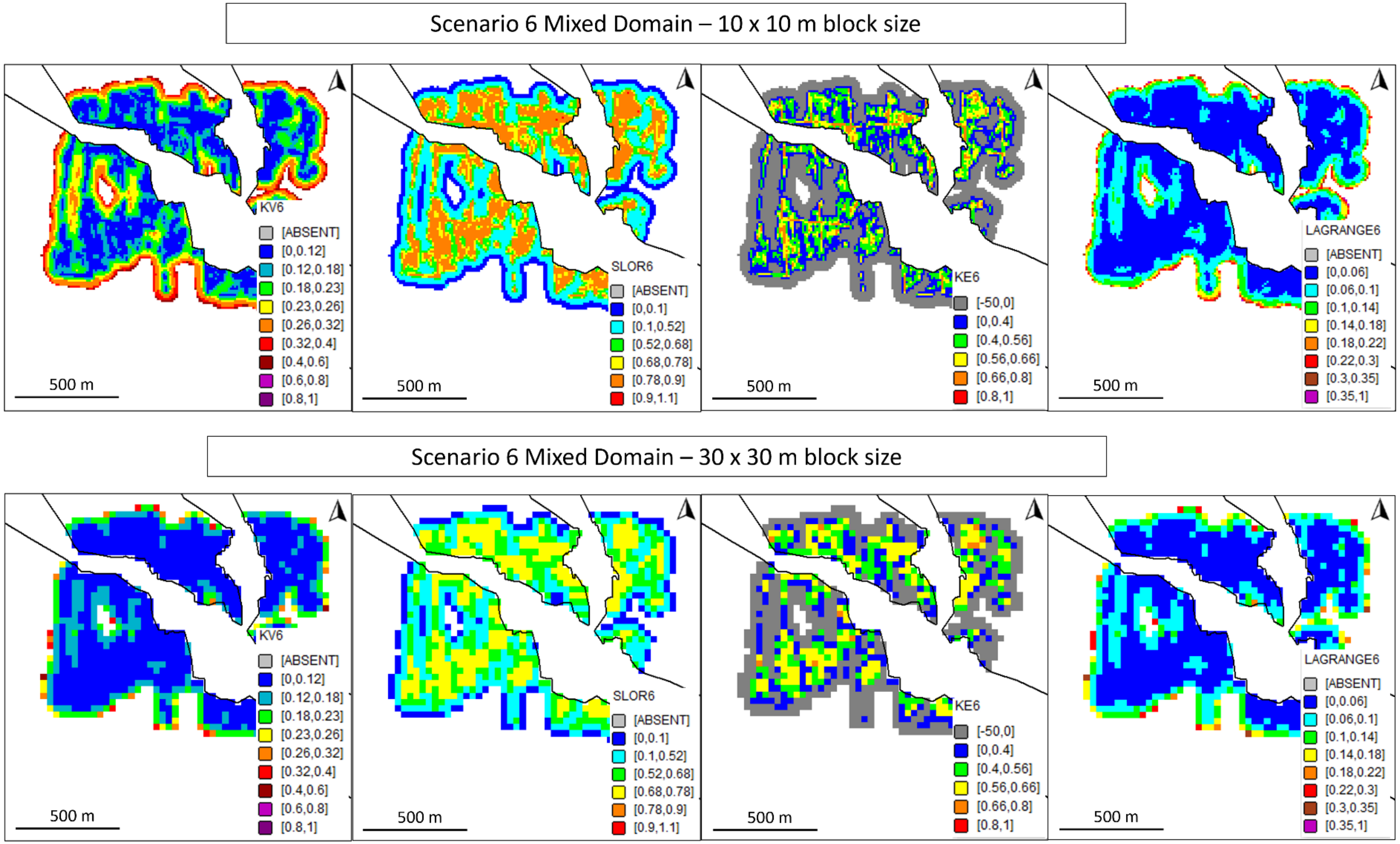

Figure 5-62: Scenario Six Mixed Domain kriging performance indicators for the 10 m x 10 m and 30 m x 30 m block sizes

Scenario Six Thin Domain kriging performance indicators for the 10 m x 10 m and 30 m x 30 m blocks are presented in Figure 5-63. Results have been constrained to the second search radius.

The block variance for the 10 m x 10 m blocks for the Thin Domain is 0.12 due to the nugget effect of 0.6 and a variogram range at a distance of just 9 m. The block variance decreased for the 30 m x 30 m blocks to 0.02, resulting in negative kriging efficiencies for all 30 x 30 m blocks because the blocks extend beyond the range of the variogram.

The kriging performance indicators for the Thin Domain are worse than the results of the Mixed Domain due to the poorly defined variogram structure and fewer data within the domain. Acceptable block estimates appear scattered (Figure 5-63). Kriging variance is low for these blocks; however, the slope of regression and kriging efficiency is poor indicating that block estimates show conditional bias and poor methodology. The Lagrange multiplier is fairly low for all constrained blocks.

For the final Scenario Six model, the blocks in the Thin Domain for the 10 m x 10 m and 30 m x 30 m blocks sizes were constrained to a kriging variance of less than 0.18 for the Thin and the Mixed Domains. The Mixed Domain block estimates were additionally constrained to the first search radius at the variogram range (60 m). The Thin Domain block estimates were additionally constrained to the second search radius at twice the variogram range (18 m).

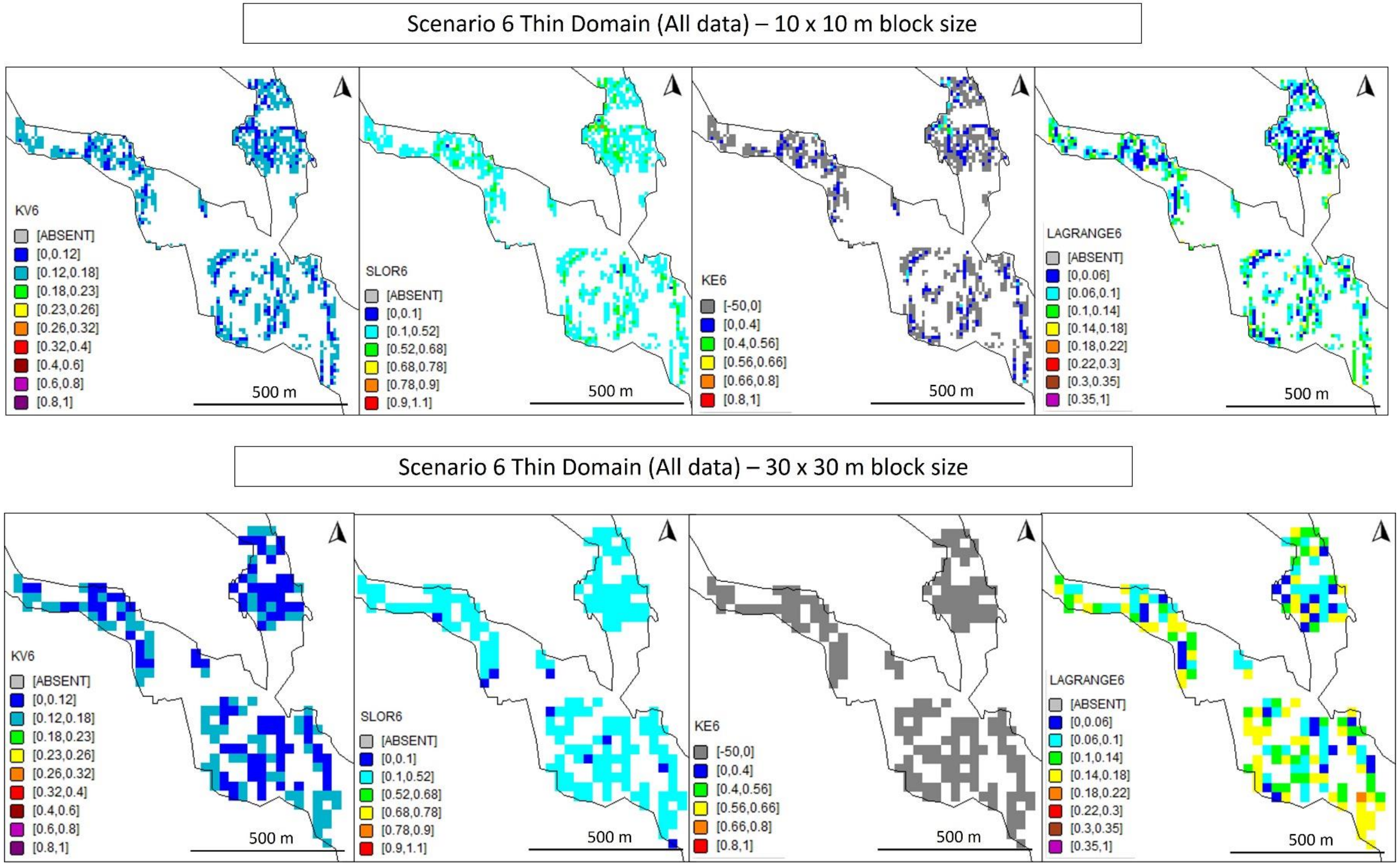

Figure 5-63: Scenario Six Thin Domain kriging performance indicators for the 10 x 10 m and 30 x 30 m blocks

5.6.4.1 Post Processing

The estimation methodology for large blocks beyond the current range of the Scenario Six variograms, utilised a technique to calculate variograms from regularised 10 m x 10 m block estimates in order to generate variograms with a long-range spatial structure and a low nugget effect. These variograms were then applied to the Scenario Six data to fill areas with insufficient data coverage.

To determine the block size and sample spacing for the large blocks, a variance size of area analysis was completed using the entire dataset for Scenario Six. A variance size of area analysis determines a block size that removes the influence of the block size on the estimation variance by analysing the within block variance for increasing block sizes from a mined-out area (Dohm, 1995; Chamberlain, 1997). This method involved calculating the weighted average lognormal variance of samples within blocks of different sizes using a meaningful minimum number of samples per block in the calculation of the combined variance for different block sizes as per Dohm (1995).

Figure 5-64 indicates the increasing within block variance as block size increases until a plateau (the population variance) is reached. This flattening out represents the block size at which the size of the area (block) no longer has an impact on the variance estimate. A change of slope is observed between the points hovering around the blue stippled line and the points within the red stippled ellipse (Figure 5-64). This slope change coincides with a logarithmic value of the block area of less than 12, or a block size of 210 m x 210 m.

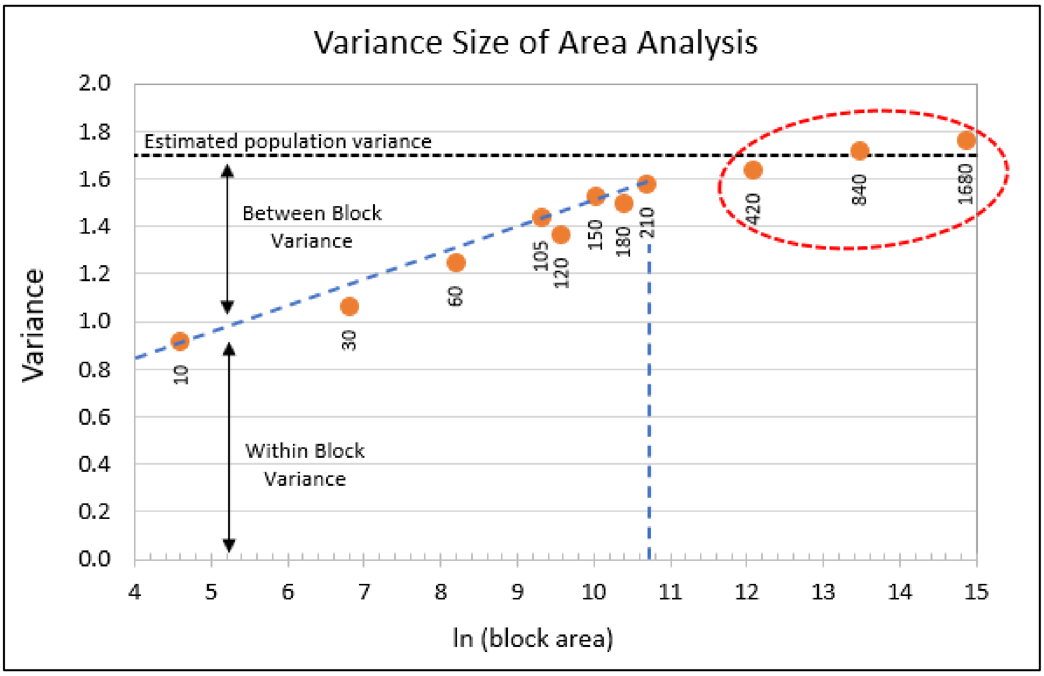

Figure 5-64: Variance size of area analysis

A new widely spaced dataset was created using the regularised, unconstrained 10 m x 10 m block estimate values at a cell size of 105 m x 105 m, as presented in Figure 5-65.

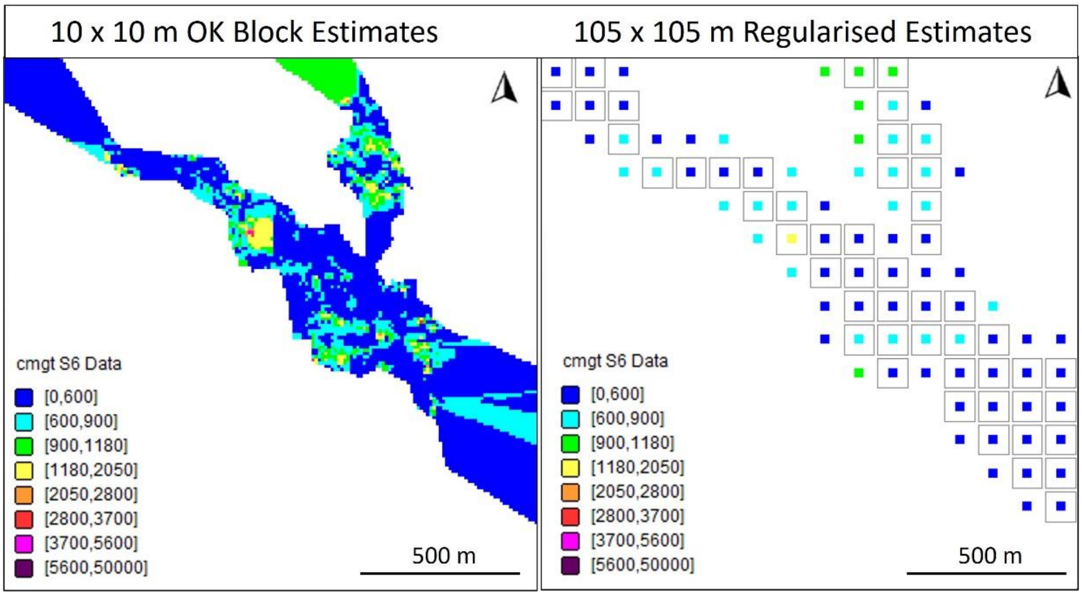

Figure 5-65: Scenario Six post-processing to generate widely spaced data

The variograms for this new 105 m x 105 m post-processed data are presented in Figure 5-66. The variograms were calculated using a lag of 105 m, lag tolerance of 52.5 m, for 6 directions with an angle tolerance of 30° and a bandwidth of 500 m.

The variogram models show a very low nugget effect, as the data was created from block estimates with a lower variability, with widely spaced data, resulting in long ranges for both domains.

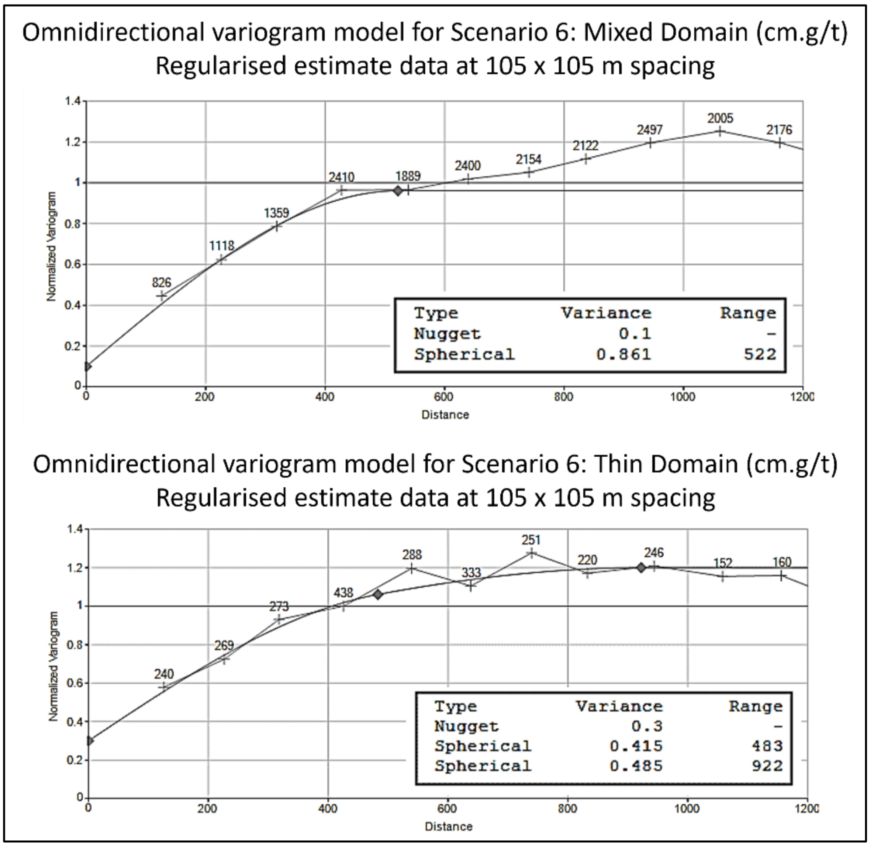

Figure 5-66: Scenario Six Mixed and Thin Domain variogram models (cm.g/t) for the regularised estimate data

The new long-range variograms for channel width were calculated using the same parameters as for gold value (cm.g/t) and are presented in Figure 5-67.

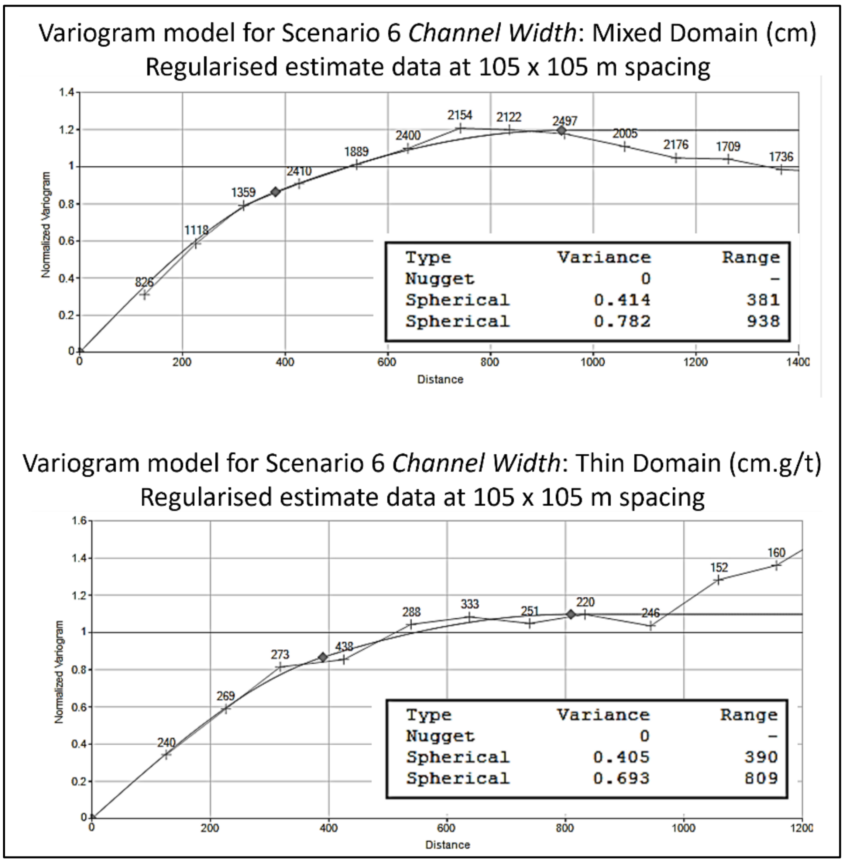

Figure 5-67:Scenario Six Mixed and Thin Domain variogram models (cm) for the regularised estimate data

This data was estimated at a block size of 210 m x 210 m (with 30 m x 30 m sub-cells), as indicated by the variance size of area analysis. The search radius is informed by the range of the semi-variogram model for each domain. A minimum number of five samples and a maximum number of 50 samples were used for both domains. The number of data was increased due to the increased number of available data within the search radius and negative sample weights may increase, however this work is not included in this research.

The ordinary kriging performance indicators of the 210 m x 210 m are presented in Figure 5-68.

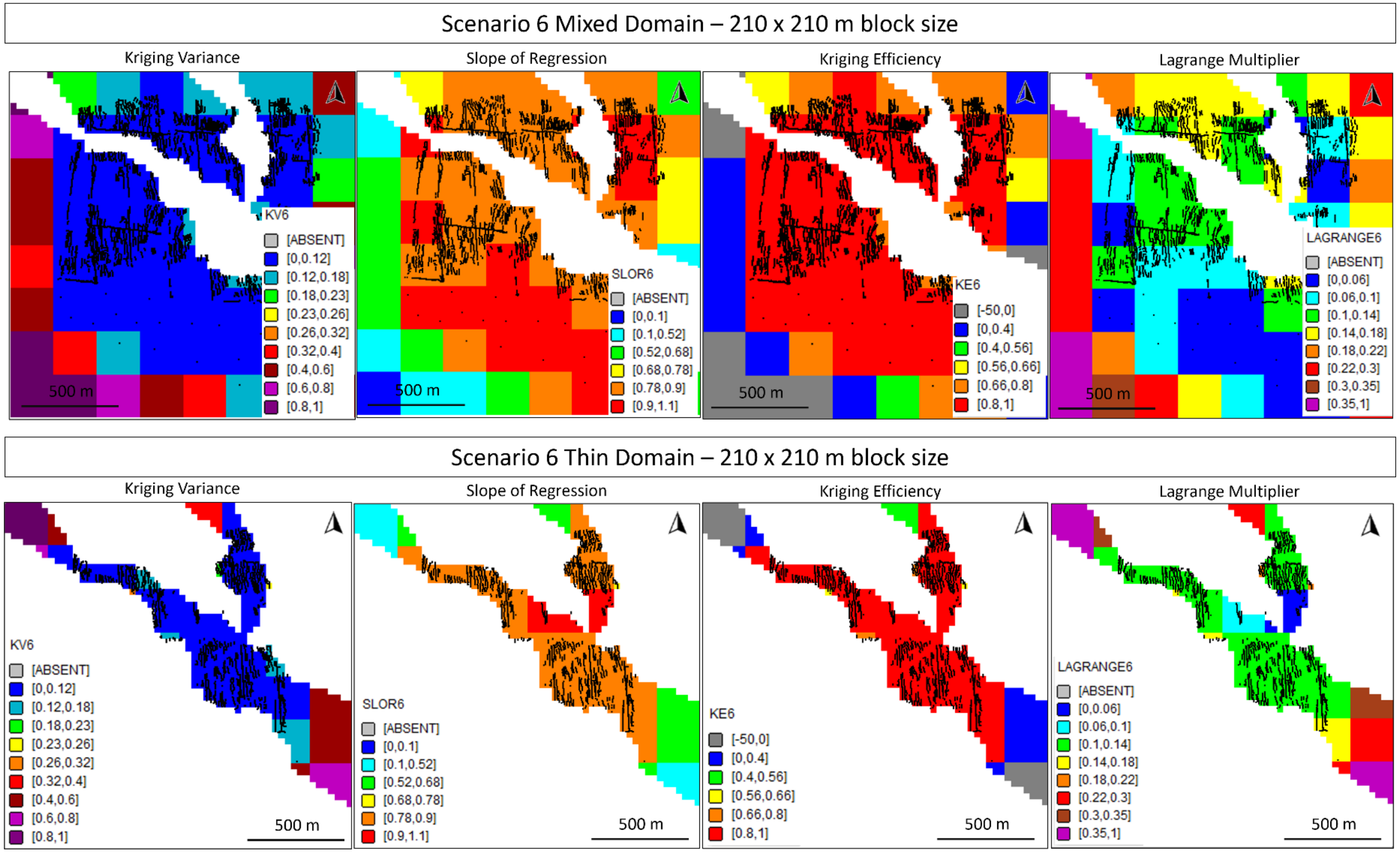

Figure 5-68: Scenario Six Mixed and Thin Domain kriging performance indicators for the 210 x 210 m block size

The block variance is 0.60 for the Mixed Domain and is 0.68 for the Thin Domain. The high block variance is a result of the low nugget effect and long ranges in the variograms for both Domains.

The kriging estimates presented in Figure 5-68 present acceptable estimates for most blocks, even with limited data and the kriging variance is low, slope of regression is high, the kriging efficiency is high, and the Lagrange multiplier is low. However, estimate results for blocks with no data show poor results, and simple kriging could be considered for the blocks around the edge of the model, as indicated by a Lagrange multiplier of approximately greater than 0.22.

The final combined estimate for variable block sizes in Scenario Six is presented in Figure 5-69. The 210 m x 210 m blocks were overwritten by the constrained 30 m x 30 m and 10 m x 10 m block estimates.

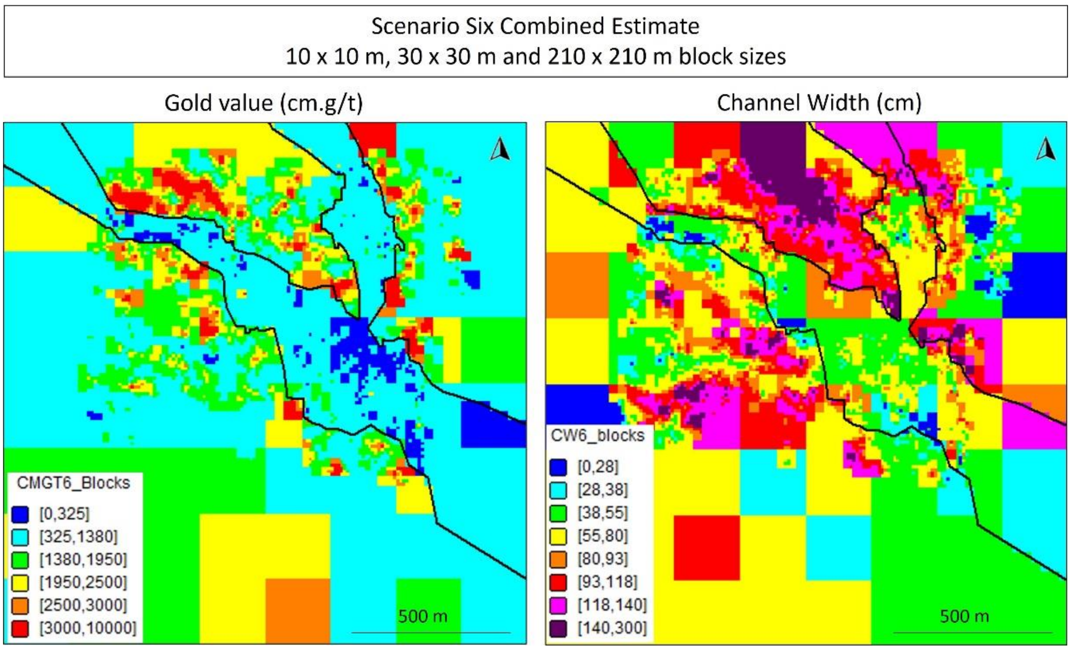

Figure 5-69: Scenario Six combined estimate with 10 x 10 m, 30 x 30 m, and 210 x 210 m combined block sizes

The 210 x 210 m estimates display an edge effect which appears to over-estimate both the gold values (cm.g/t) and the channel width (cm). To reduce the edge effect, the regularised data at a cell size of 105 m x 105 m may be generated from the constrained 10 m x 10 m block estimates.

5.6.5 Scenario Six Estimate Validation

Table 5-16 presents a comparison of the estimate and data statistics for Scenario Six. The Mixed Domain mean estimate is 70 cm.g/t (3.9%) lower than the sample mean, and the Thin Domain estimate is 7 cm.g/t (1.1%) lower than the sample mean, both indicating acceptable estimation results and no overall over-estimation.

Table 5-16: Scenario Six statistical comparison between block estimates and sampling data

SCENARIO 6 MIXED DOMAIN STATISTICS				SCENARIO 6 THIN DOMAIN STATISTICS			
ESTIMATE		SAMPLES		ESTIMATE		SAMPLES	
	cm.g/t		cm.g/t		cm.g/t		cm.g/t
Min	66	Min	1	Min	12	Min	1
Max	8724	Max	32 487	Max	3736	Max	11 663
N	5 848	N	7 588	N	1 661	N	3 345
Mean	1 687	Mean	1 757	Mean	603	Mean	610
Variance	756 665	Variance	4 241 917	Variance	122 602	Variance	646 410
Std Dev	870	Std Dev	2 060	Std Dev	350	Std Dev	804
COV	0.52	COV	1.17	COV	0.58	COV	1.32

The relative frequency distribution models, presented in Figure 5-70, indicate how the shape of the distribution of block estimates changes due to the increased in support and associated variance decrease. The Mixed Domain shows a decreased variance in the estimate distribution. The Thin Domain estimate and data distributions display similar shapes indicating a low support effect.

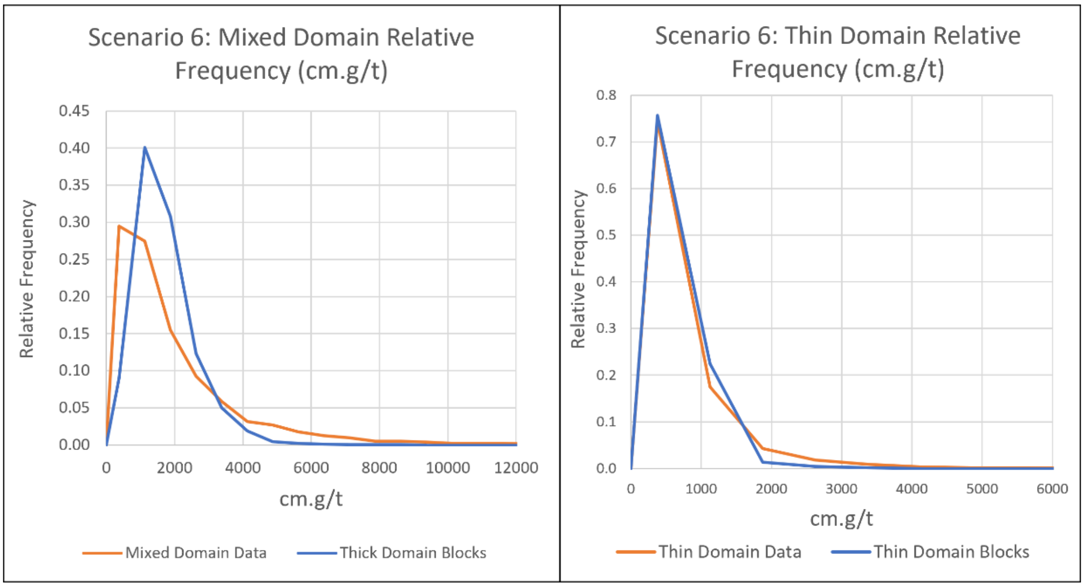

Figure 5-70: Scenario Six relative frequency distributions comparing the block estimates to the data.

Swath plots were generated at 120 m widths in a direction parallel to the observed northwest-southeast grade trend.

The Mixed Domain swath plot (Figure 5-71) indicates under-estimation for most swath widths towards the northeast. Over-estimation is indicated in the swaths situated over the widely spaced borehole data and large block estimates towards the south of the deposit.

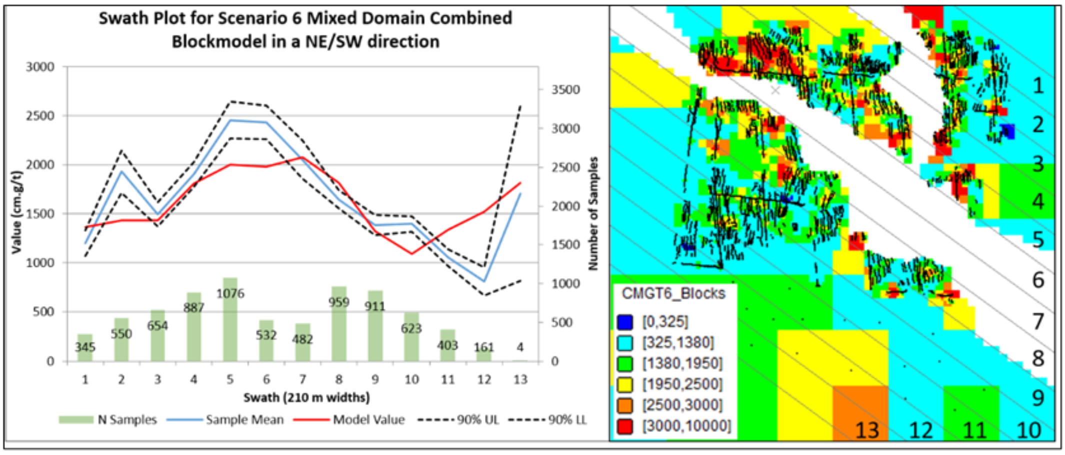

Figure 5-71: Scenario Six Mixed Domain Swath Plot

The Thin Domain swath plot in Figure 5-72 presents estimate values within the 90% confidence limits of the sample data for most swaths, except towards the edges of the domain as observed for Swath 5. Confidence limits are wider for the Thin Domain due to a lower number of samples.

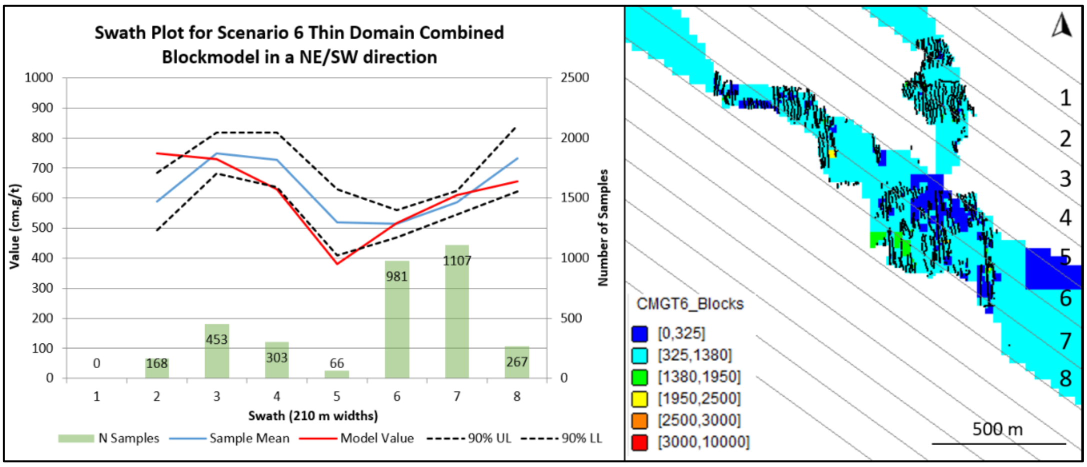

Figure 5-72: Scenario Six Thin Domain swath plot

5.6.6 Scenario Six Mineral Resource Estimate

Under the assumption of RPEEE, the 10 m x 10 m blocks were classified as Measured Mineral Resources. The Indicated Mineral Resources were assigned to the constrained 30 x 30 m blocks and the Inferred Mineral Resources were assigned to all 60 x 60 m blocks as presented in Figure 5-73.

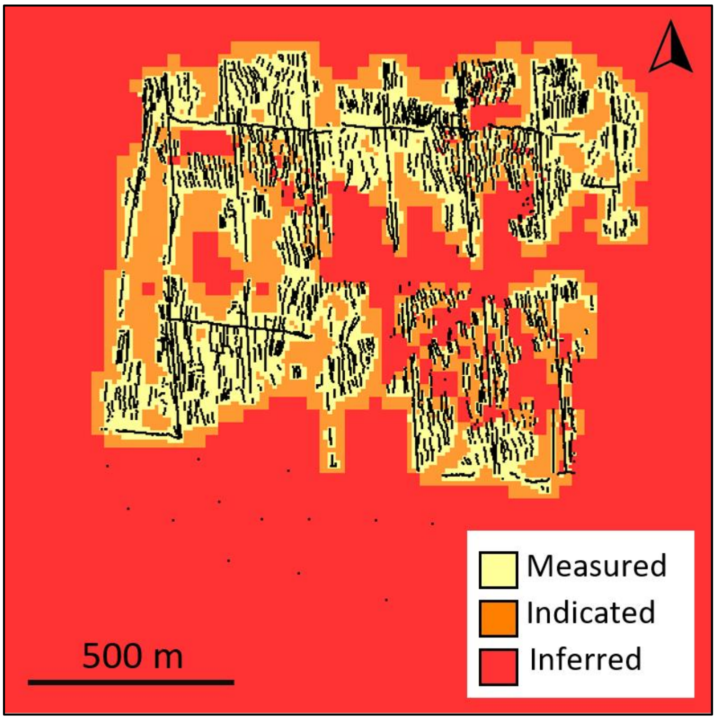

Figure 5-73: Scenario Six proposed Mineral Resource classification

The Mineral Resource estimate tabulation for Scenario Six is presented in Table 5-17.

Table 5-17: Scenario Six Mineral Resource estimate

Scenario Six Mineral Resource Estimate								
		Area (m^2)	**CW (cm)**	**Tonnage (Mt)**	**Grade (cm.g/t)**	**90 % Lower Limit (cm.g/t)**	**90 % Upper Limit (cm.g/t)**	**Grade (g/t)**
Measured	Mixed Domain	467 200	90	1.14	1 710	1 672	1 749	18.94
	Thin Domain	99 700	66	0.18	613	571	655	9.27
Total Measured		566 900	86	1.32	1 517	1 478	1 557	17.63
Indicated	Mixed Domain	276 000	83	0.62	1 591	1 556	1 626	19.08
	Thin Domain	72 200	61	0.12	599	561	638	9.78
Total Indicated		348 200	79	0.74	1 385	1 350	1 421	17.58
Total Measured + Indicated		915 100	83	2.07	1 467	1 429	1 505	17.61
Inferred	Mixed Domain	1 523 700	84	3.46	1 611	1 577	1 645	19.20
	Thin Domain	383 600	61	0.63	570	533	606	9.35
Total Inferred		1 907 300	79	4.10	1 402	1 367	1 436	17.68

5.6.7 Scenario Six Value-Tonnage Estimates

The value-tonnage curve (Figure 5-74) presents the Measured Mineral Resource 10 m x 10 m blocks and the Indicated Mineral Resource 30 m x 30 m for comparison. The graph represented tonnes and not relative tonnes. The point scale value-tonnage curve is presented to highlight the support effect.

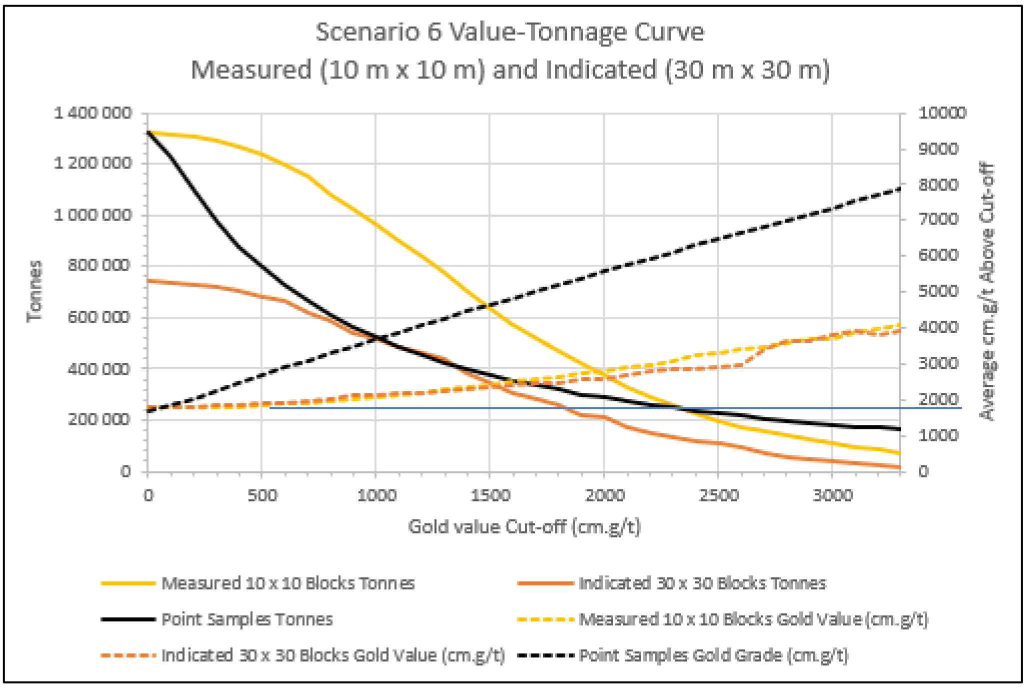

Figure 5-74: Scenario Six value-tonnage curve for the 10 m x 10 m and 30 m x 30 m blocks

The 10 m x 10 m measured blocks and 30 m x 30 m indicated blocks are more appropriate for short-term planning rather than providing an overall value-tonnage estimate of the resource. At the resource exploitation stage, the ore/waste selectivity is important for planning and the short-term resource model should aim to minimise the conditional bias (Isaaks, 2007). The 10 m x 10 m blocks show less conditional bias than the 30 m x 30 m blocks and these estimates will provide the most accurate short-term grade predictions.

5.6.8 Scenario Six Results Summary

The increased amount of data in Scenario Six resulted in greater sample variability which resulted in a more complex geozoning process. The simple indicator kriging exercise did not sufficiently represent the trend in the gold value (cm.g/t). Channel width, gold value (cm.g/t) and the gold grade (g/t) colour coded plots were proved to be more appropriate for highlighting domain boundaries.

The data were cut at the 99th percentile to remove the influence of outlying high-grade values allowing for definition of the short-range spatial structure in the variogram models. The nugget effect also increased in both domains due to the additional data. The Thin Domain produced a very short range at just 9 m which provided a challenge to produce acceptable estimation results, even for small blocks.

The additional data allowed for smaller block estimates at a size of 10 m x 10 m and 30 m x 30 m. The acceptable 10 m x 10 m estimates covered a larger area than in Scenario Five. The 10 m x 10 m blocks were classified as measured Mineral Resources as they indicate a good slope of regression appropriate for short-term planning and the best prediction of the ore/waste block selection.

The 30 m x 30 m blocks are classified as Indicated Mineral Resources as they also provide acceptable selectivity and cover a larger area than the Measured Mineral Resources.

The challenge for Scenario Six was to extrapolate estimates. A technique to generate long-range spatial structure and a low nugget effect was calculated using the regularised estimate results of the 10 m x 10 m blocks. These long-range variogram models were used to estimate a block size of 210 m x 210 m. These large blocks show limited selectivity and are not suitable for short-term planning and this is reflected in the confidence of the Mineral Resource classification.

6 SUMMARY OF FINDINGS AND RESULTS

6.1 Geozones

Domaining is an important, time-consuming exercise critical to each stage of project development. The methodology for defining homogenous domains must be refined and explored as new data becomes available. At early project stages with widely spaced data there is insufficient data to delineate meaningful geozones, as highlighted in Scenarios One and Two. Rough domain delineation was possible in Scenarios Three and Four, however, these domains were still based on widely spaced datapoints at 120 m to 240 m apart. The resultant domains did not demonstrate reef thickness or value (cm.g/t) trends, so applying the theory of alternating slopes and terraces (McWha, 1994) was difficult for Scenarios Three and Four (Figure 6-1).

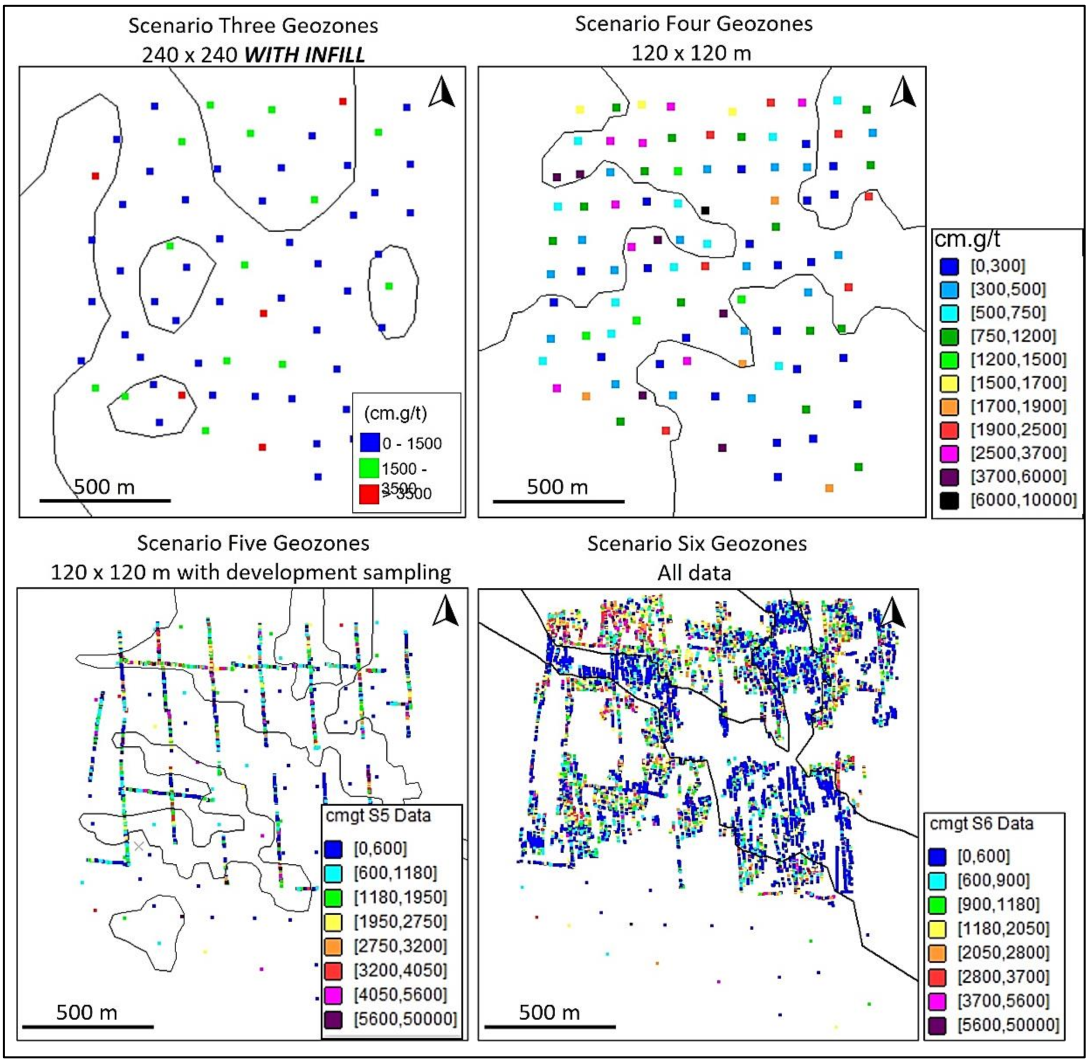

Figure 6-1: Domain boundaries with colour-coded cm.g/t data

Scenario Four shows two perpendicular continuity directions based on widely spaced data in a northeast to southwest direction and in a northwest to southeast direction. As additional data becomes available in Scenario Five and Six, a dominant northwest to southeast continuity direction is confirmed and replaces the northeast to southwest continuity direction assumed from the widely spaced data in Scenario Four.

The probabilistic methodology used in Scenario Five resulted in more meaningful geozone definition. However, in Scenario Six (all data) domain boundaries based on the channel width probabilities were refined using gold grade (g/t) and gold value (cm.g/t), ultimately including all information available for domain interpretation, as suggested by Duke and Hanna (2014).

Geozones identified in Scenario Six presented areas of thicker, high-grade reef divided by thinner, low-grade reef zones akin to alternating slope and terrace reef, as discussed in literature reviewed in Chapter 3.2. The two geozones showed different statistical distributions and hard boundaries were applied.

The presence of transitional boundaries may be confirmed by additional statistical and geostatistical techniques, such as boundary analysis, as discussed by Ortiz and Emery (2006). If validated, the use of soft boundaries may improve estimation results, especially in the case of the Thin Domain with limited data, as presented in Scenario Six. However, a boundary analysis conducted using the widely spaced data of Scenario Four would not be meaningful.

6.2 Exploratory Data Analysis

As meaningful and representative histograms cannot be generated with few samples (Sichel, 1987), the box plots for all scenarios are presented in Figure 6-2 for comparison.

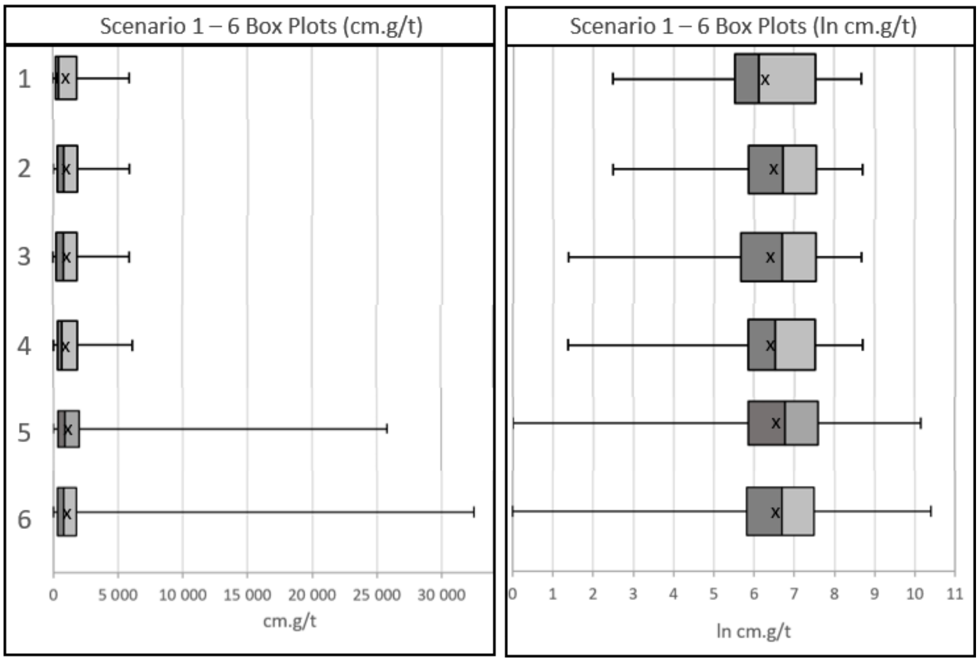

Figure 6-2: Box plots for all scenarios

The box plots for Scenario One to Scenario Six indicate a fairly constant mean value with an increasing variance as data spacing decreases. All datasets are positively skewed and become increasingly positively skewed as data spacing decreases due to the increasingly high maximum (and increasingly low minimum) values. The closely spaced sampling in Scenario Six is a good representation of the nugget effect indicating high inherent geological variability in the orebody. In 2001, Dominy *et al*., observed that high-grade outliers resulted in a high nugget effect that will increase due to the increasingly high maximum grades, as observed in the variograms for Scenarios Five and Six.

6.3 Global Estimation

A simplified graphical comparison of the global and local mean estimates for all scenarios is presented in Figure 6-3.

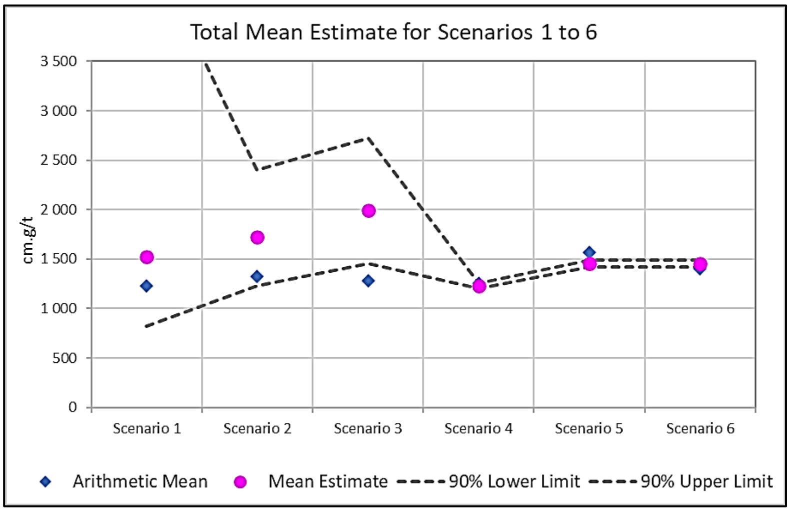

Figure 6-3: Total mean estimate for Scenarios One to Six

The Sichel-t estimator used to calculate the global estimate for Scenario One results in a mean estimate greater than the arithmetic mean, with very wide confidence limits, particularly the upper limit. Sinclair and Blackwell (2004) noted that the Sichel t estimator is useful for estimating the mean of small lognormal datasets due to the over-estimation of the mean by other estimators. However, Sichel (1987) noted that the Sichel t estimator will over-estimate the population mean if the lognormal data is negatively skewed, and the variance is not small. The box plot presented for the log-transformed data of Scenario One (Figure 6-2) indicates that the distribution is not symmetrical and therefore not lognormal. Nonetheless, with only 21 datapoints, the Sichel t is an acceptable estimator for the mean and at this early stage of resource development the methodology for Scenario One is acceptable. The arithmetic mean is above the lower confidence limit, and the upper limit may represent resource positive potential.

Even so, as the Sichel t mean estimate is greater than the arithmetic mean, and Scenario One has a positively skewed distribution, the use of the arithmetic mean would provide a valid estimate of the mean for Scenario One (Sichel, 1966; Dohm, 1995). The use of the median as an estimate of the mean would remove the influence of a small portion of high-grade outliers on the arithmetic mean (Dohm, 1995) and would also provide a valid estimate.

The 2-parameter lognormal estimator used to calculate the global estimate for Scenarios Two and Three (with no domaining), also resulted in a mean estimate greater than the arithmetic mean, with slightly narrower confidence limits. The box plots presenting the log-transformed distributions for both Scenarios Two and Three are also not symmetrical (Figure 6-2). The log-transformed data for Scenario Three is more negatively skewed than for Scenario Two (higher sample variability due to a lower minimum value) which results in a global mean estimate at 1990 cm.g/t, which is 55% higher than the arithmetic mean. The arithmetic mean also falls outside the 90% confidence limits for the 2-parameter mean estimate. The arithmetic mean or median may provide a more acceptable estimate for the mean of Scenario Three.

Figure 6-3 highlights the change in methodology from Scenario Four onwards due to the increasing amount of data. The decreased data spacing allowed for local estimation using the spatial distribution theory captured by the semi-variogram for Scenarios Four, Five and Six.

6.4 Improving the Global Mean Estimate

Improving the mean estimate with limited data is a challenge as it is difficult to determine an appropriate distribution model. The Bayesian approach relies on applying known characteristics to a virgin area to improve estimation. Complex 4-parameter distributional models are often applied to Witwatersrand gold values (Dohm, 1995; Chamberlain, 1997; Flitton and Peattie, 2016), however, information from a nearby mined-out area was not available for this research.

The log-variance estimate is an important step in the calculation of a global mean estimate. It is known that a variance typically has a positively skewed distribution, which makes it the most difficult parameter to estimate (Dohm, 1995).

In 1993, Krige showed that a poor variance estimate has a substantial effect on the global mean estimate and proved that using an *a priori* variance can improve the mean estimate for a limited dataset. Krige proved this work by using a 3-parameter lognormal distribution with an *a priori* variance. Figure 6-4 shows Krige's *a priori* variance calculated from a large underground chip sampling database.

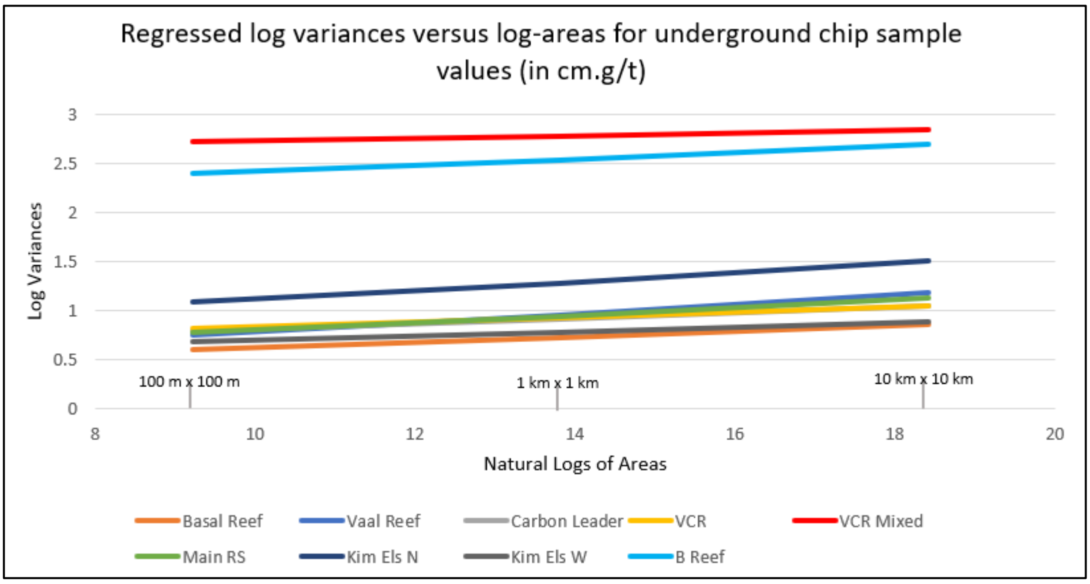

Figure 6-4: Regressed log variances verses log-areas for underground chip sampling. (after Krige,1993)

Applying Krige's *a priori* log variance value of 2.75 from the VCR Mixed Facies data (Figure 6-4) resulted in a further increase in the 2-parameter lognormal mean estimates for Scenarios Two and Three. The 3-parameter distribution model was not further explored in this research.

6.5 The Semi-Variogram

Sichel (1987) stated that variograms cannot be constructed with limited data and that geostatistical results become meaningless. Scenarios One, Two, and Three have too few, or too widely spaced, data to indicate spatial continuity and variograms show the appearance of pure nugget effect. In 1978, Journel and Huijbregts noted that the appearance of a pure nugget effect is commonly observed due to insufficient data, but true pure geological nugget effect is rare. Pure nugget effect results in equal sample weighting during kriging.

Due to the limited sampling information a pure nugget effect is expected for Scenarios One, Two and Three and therefore the application of statistical distributional theory is more suitable to value estimation in these three cases.

Spatial mineralisation continuity was captured using a single structured spherical variogram in Scenario Four with a data spacing of 120 m. While the high Thick Domain nugget effect (0.72) confirmed that thicker reef is more variable, and the low Thin Domain nugget effect (0.18) confirmed that thin reef is less variable, the nugget effect determined for Scenario Four using widely spaced datapoints may be poorly quantified.

The long-range spatial continuity that extended up to a range of 470 m in Scenario Four is not a true representation of the high variability in the gold mineralisation, but there is insufficient data to provide better results during the advanced drilling stage of the resource project.

Scenario Five provided the best estimation of the nugget effect as the dataset contains 3591 samples which are dominated by the closely spaced development sampling at a 2 m interval. A nugget effect of 0.5 was determined for both domains Guibal (2001) noted that down hole direction best estimates the nugget effect as it reflects the closest sample spacing in a 3D environment. In a 2D environment du Toit (2018) presented improved nugget effect estimates by using adjacent check samples as an additional point on the experimental variograms.

Scenario Five variograms were modelled using three spherical models and the spatial structure near the origin shows better definition, with the first range at 8 m for both domains, and a final range at 50 m for the Thick Domain and 80 m for the Thin Domain. This short-scale structure influences sample weighting during kriging (Guibal, 2001).

The increased data density in Scenario Six highlights increased variability as the nugget effect increased from 0.5 to 0.6 for the Thin Domain, and to 0.65 for the Thick Domain, indicating that thick reef is more variable than thin reef, as observed in Scenario Four. The variogram for the Thick Domain was modelled using a three structured spherical model with a range up to 60 m. The Thin Domain variogram was modelled using one spherical structure with a range at only 9 m, indicating that only very closely spaced samples show correlation, and thereafter samples will receive equal weighting, resulting in a smoother estimate.

6.6 Local Estimation

Additional data allowed for improved estimation using the spatial distribution model captured by the semi-variogram and a local estimation technique (ordinary kriging). However, Krige (1997) stated that limited data correspond with a poor spatial structure and poor kriging efficiencies. This is observed when comparing the 60 m x 60 m blocks of Scenarios Four and Five, which were estimated using the same variogram as calculated for Scenario Four.

The additional data in Scenario Five resulted in a variogram with a shorter range and nugget effect at 0.5 that more accurately reflects the grade variability within the deposit. This allowed for smaller block size estimation (10 m x 10 m) and better theoretical selectivity for these blocks.

Figure 6-5 presents the Scenario Four and Five estimates results that utilised the same variogram model from Scenario Four data. Due to additional data in Scenario Five a slightly lower kriging variance and therefore improved kriging efficiencies were observed (block variance remains similar), as presented in Figure 6-5.

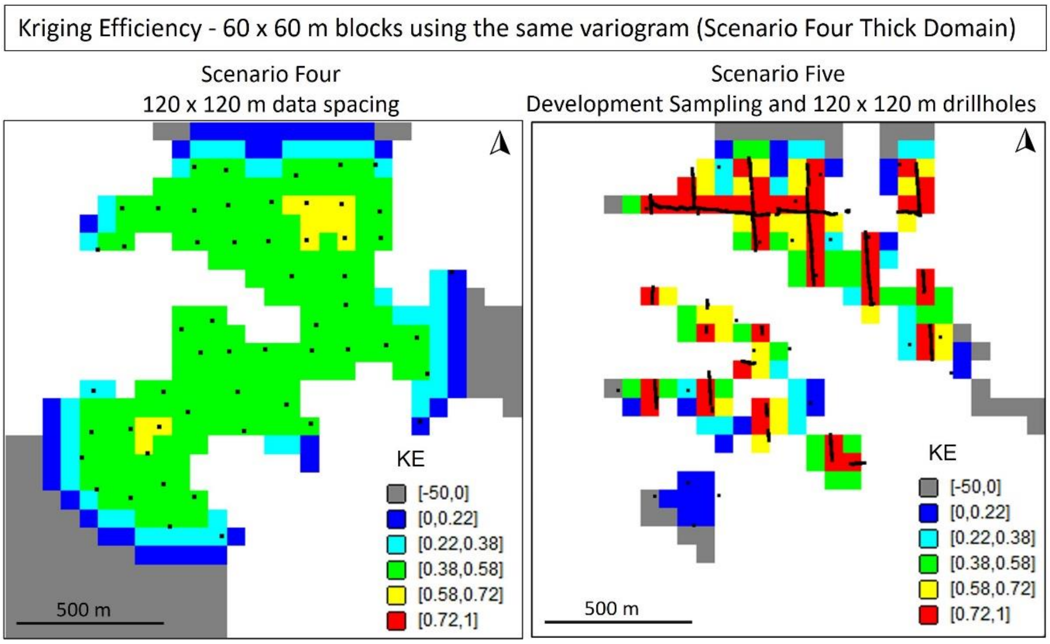

Figure 6-5: Kriging efficiency for Scenarios Four and Five Thick Domain 60 x 60 m blocks

Figure 6-6 compares the ordinary kriging performance indicators of Scenario Four 60 m x 60 m blocks to Scenario Five 10 m x 10 m blocks using the same colour-coding intervals. Robust estimates, with a low kriging variance and high slope of regression, are constrained to narrow bands surrounding the closely spaced development sampling in Scenario Five. This is because of the shorter variogram range, beyond which all samples are equally weighted.

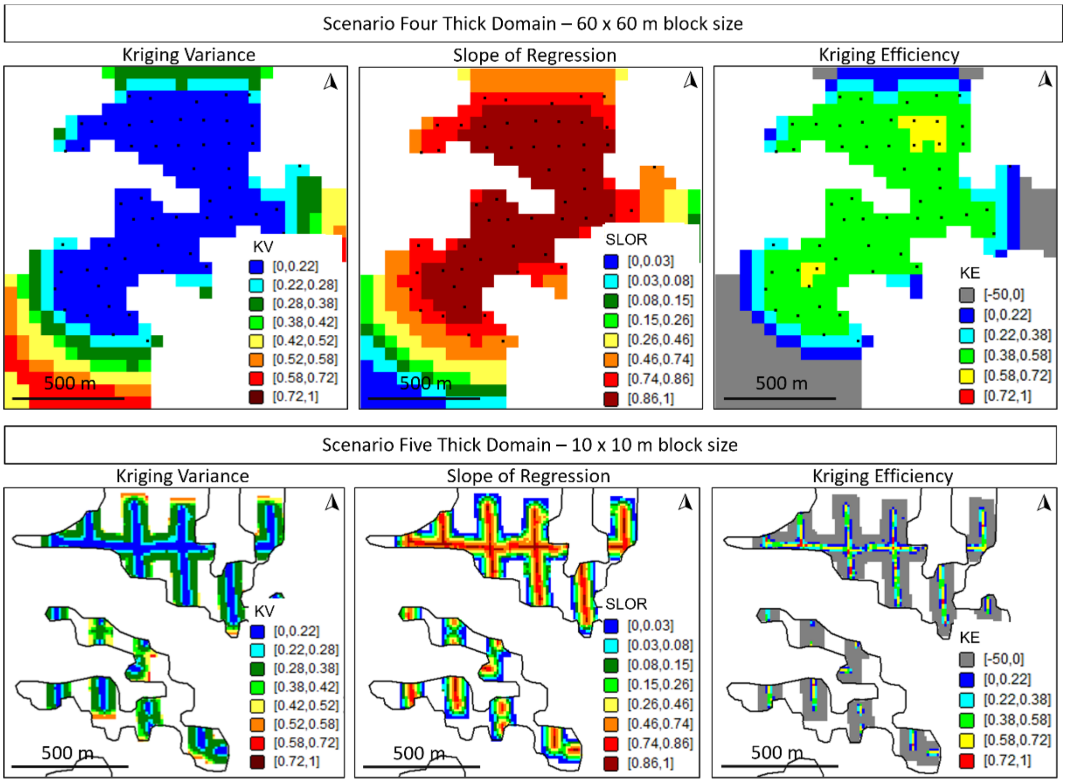

Figure 6-6: Kriging performance indicators of Scenario Four 60 x 60 m block size and Scenario Five 10 m x 10 m block size using the same colour-coding

The key difference between Scenario Four and Five is that the additional data in Scenario Five allows for estimation into smaller blocks which allow for better ore/waste selection during mining. There are too few 10 m x 10 m blocks in Scenario Five to be of practical use during mining and the estimate is most appropriate for long-term planning.

In 2004, Isaaks concluded that conditional bias is irrelevant when predicting the accuracy of long-term planning estimates, such as observed in the slope of regression and kriging efficiencies in Scenario Four but noted that long-term estimates should account for ore loss and dilution, possibly by using conditional simulation techniques such as Sequential Gaussian Simulation as presented in Deutsch and Journel (1998).

In Scenario Six, as the amount as data increases, the amount of small block estimates also increases over a larger area as presented in Figure 6-7, using the same colour-coding intervals for both scenarios. In Scenario Six, a low kriging variance, high slope of regression and positive kriging efficiency extend over a larger area due to the additional data, which can be used for short-term planning and estimation. These small blocks indicate less conditional bias (high slope of regression and improved kriging efficiencies) which is essential for accurate short-term planning estimates. The main aim of a short-term resource model is to minimise conditional bias (Isaaks, 2004) for the best possible ore/waste block selectivity at the time of mining.

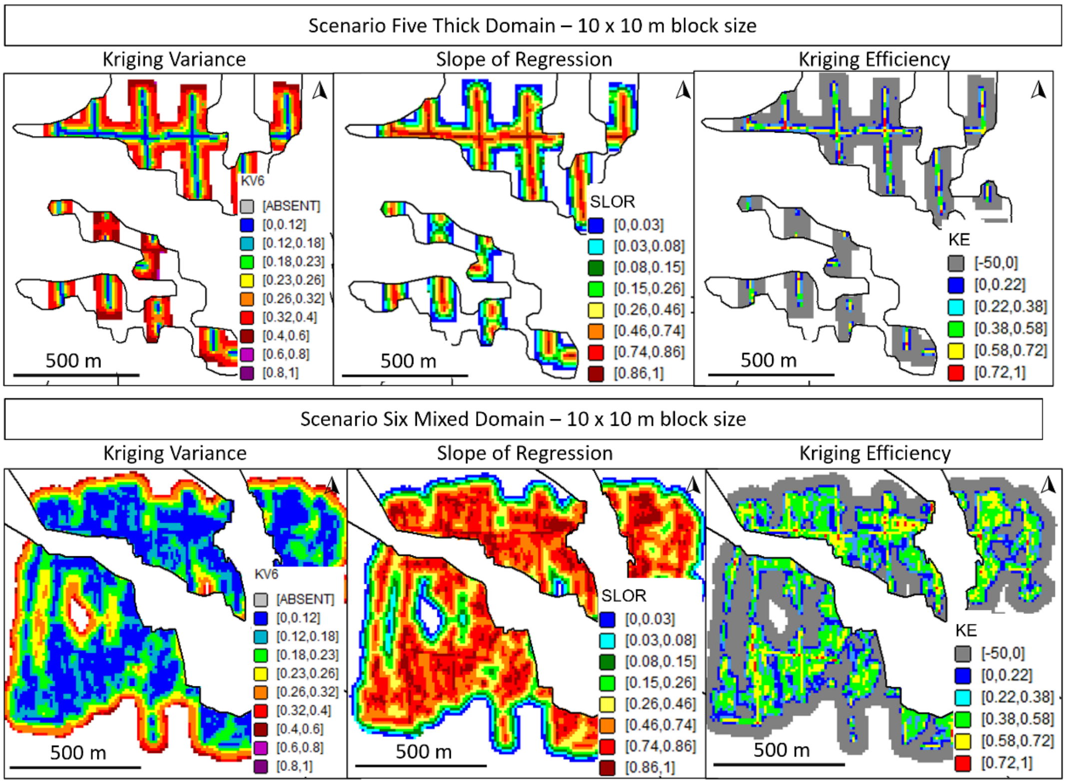

Figure 6-7: Kriging performance indicators of the Thick and Mixed Domains of Scenario Five and Scenario Six 10 x 10 m block size using the same colour-coding

The Thin Domain results for Scenario Six did not show the same improvement as noted for the Thick Domain. The variogram for the Thin Domain has a very short range at 9 m. This resulted in a low block variance of 0.12 for the Thin Domain and kriging efficiencies were mostly negative as block variance was mostly lower than kriging variance.

Scenario Six required estimates to be constrained to acceptable results based on kriging variance, slope of regression, kriging efficiency, or a combination of these results. The challenge with estimating the closely spaced data in Scenario Six was to extrapolate the results into virgin areas towards the edge of the resource.

A technique used to generate long-range mineralisation continuity utilised the regularised estimate results of the 10 m x 10 m blocks to produce long-range variogram models with a low nugget effect. These variograms were used to estimate into a block size of 210 m x 210 m. These large blocks show limited selectivity and are not suitable for short-term planning, but rather an overall value-tonnage prediction, and this is reflected in the confidence of the Mineral Resource classification.

A preferred methodology for large block estimation is discussed by Flitton and Peattie (2016). The authors describe a macro cokriging technique developed over decades that forms an essential component of Mineral Resource evaluation at AngloGold Ashanti. The AngloGold Ashanti macro cokriging technique uses the Bayesian approach to infer characteristics of a mined-out area to areas with limited borehole data. Flitton and Peattie (2016) state that "*the diagonal kriging matrix is modified to reflect different nugget effects*" allowing for the combined estimation of data at different supports (cluster and block size). Over 400,000 datapoints were log-transformed for large block estimation and back-calculated using four-parameter statistical distribution models as discussed by Dohm (1995).

6.7 The Support Effect

The support effect describes the "*relationship between the size (support) of the data and the distribution of their values*" (Isaaks and Srivastava, 1989). Small samples show more variability than block values due to the averaging of values within the blocks. The support effect is presented in the results section by comparing the point data distribution to the local estimate distribution for Scenarios Four to Six. It was observed that mean values remained similar, maximum block values decreased, block variability decreased, and the block distributions tended towards symmetry.

The challenge presented by the support effect relates to long-term mine planning, and decisions based on planned estimates, at a different support, to the selective mining unit (SMU) have serious implications on the accuracy of the predicted tonnes and gold content.

The metal tonnage selectivity plot (Figure 6-8) is a useful graphical representation highlighting the support effect, which plots the relative cumulative content (*Q*) as a function of the ore tonnage (*T*) from Rivoirard (1990).

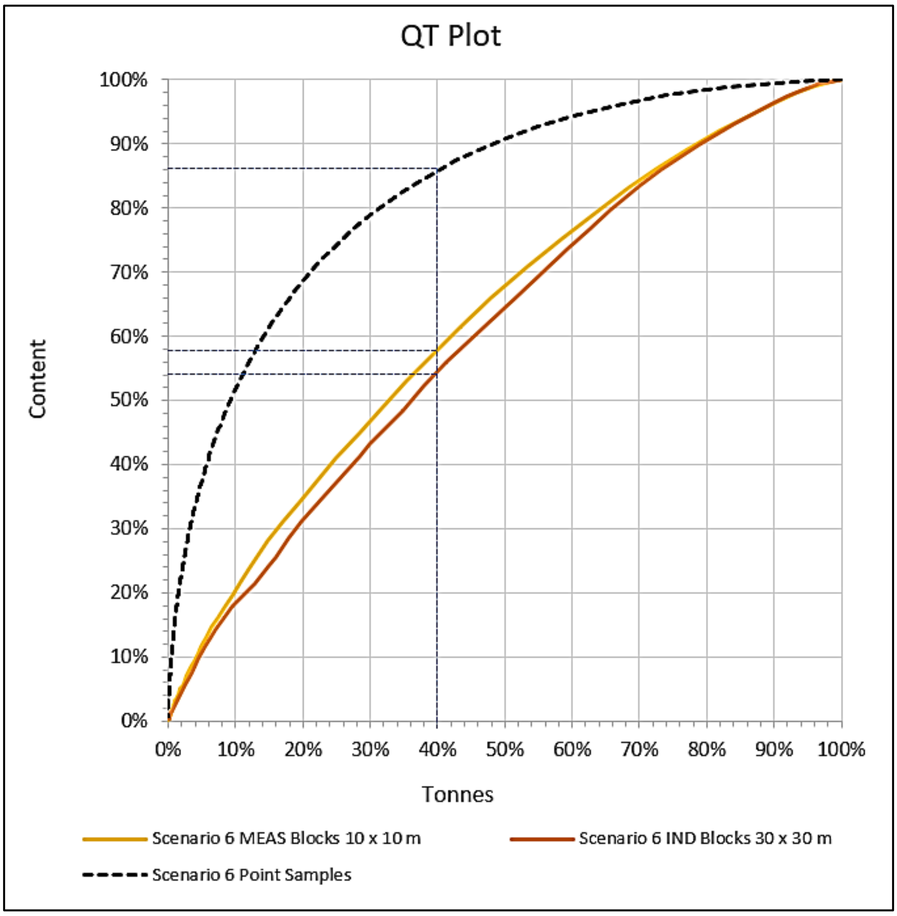

Figure 6-8: Q/T plot for Scenario Six

The support effect in Scenario Six is explained in terms of the Q/T plot in Figure 6-8.

If the mine plans to mine 40% of the tonnage within the deposit:

- At sample size support, 86% of the gold content would be recovered.
- At a 10 m x 10 m support, 58% of the gold content would be recovered,
- At a 210 m x 210 m support, 54% of the gold content would be recovered.

If the plan uses the 10 m x 10 m block estimates, but the selective mining unit is larger, the required tonnage must be increased to achieve the same gold content, directly reducing the average grade (g/t). This would have a significant financial consequence - either the same amount of gold will be mined-out over a longer period, or the mining operations would need to increase production rates.

6.8 Mineral Resource Classification

The Mineral Resource classification at each stage of project development was based on the information available at the time. Scenarios One, Two and Three are classified as Exploration Targets due to the limited amount of data available. Scenario Four was classified as Indicated and Inferred Mineral Resources based on the search radius (range of the variogram) under the assumption of RPEEE. Scenario Five was classified as Measured, Indicated and Inferred Mineral Resources based on constraining by kriging efficiency under the assumption of RPEEE. Scenario Six was classified as Measured, Indicated and Inferred Mineral Resources based on a combination of constraining by kriging variance and search radius, as presented in Figure 6-9. The results highlight a challenge for classification as the project progresses.

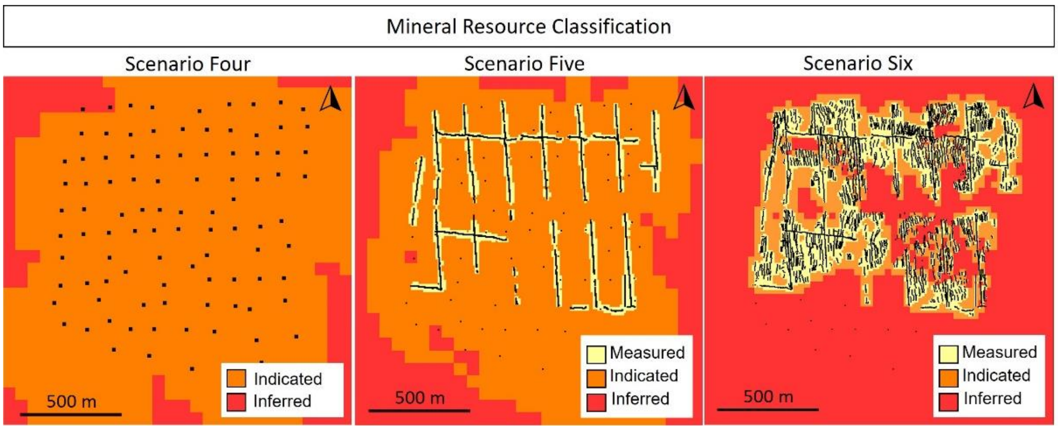

Figure 6-9: Scenarios Four, Five and Six Mineral Resource classification

The Measured Mineral Resource increased from Scenario Five to Scenario Six due to the increase in confidence associated with increasing geoscientific knowledge from additional data. However, the downgrade from Indicated Mineral Resource to Inferred Mineral Resource in areas of widely spaced data represents a decreased confidence over some areas and is a caution not to be too lenient in resource classification when the data is limited and widely spaced. This challenge may be a result of routine practice without paying attention to how data spacing may impact the estimation classification as the resource project progresses.

A possible classification revision may consider downgrading the large 60 m x 60 m blocks that represent an entire year’s mining in both Scenario Four and Five. Indicated blocks may be downgraded to Inferred blocks and Inferred blocks may be downgraded to an Exploration Target.

7 CONCLUSION

This research shows the considerable impact that the data spacing has on the entire Mineral Resource estimation approach, from geozone delineation to Mineral Resource classification. The impact also extends to mine planning due to both the information and support effect impacting the regression effect and conditional bias (Rossi and Deutsch, 2014).

During the initial resource development phases, the data are limited and widely spaced, ranging from approximately 240 m to 200 m due to infill drilling. At this spacing, spatial distribution cannot be captured by the semi-variogram and geostatistical results would be meaningless due to the appearance of pure nugget in the experimental semi-variograms.

Global estimation methodology using statistical distribution theory is appropriate for initial project phases where there is limited data, as presented for Scenarios One, Two, and Three. The Sichel t lognormal distribution and the 2-parameter lognormal distribution resulted in global mean estimates higher than the arithmetic means for all three Scenarios. This result highlights the importance of identifying an appropriate distribution model for mean estimation, which is a challenge with limited data. The use of a Bayesian approach (if available) may improve the mean estimate.

Scenario Four represented an advanced exploration phase with a data spacing of 120 m x 120 m, which allowed the spatial distribution to be modelled using the semi-variogram. Local geostatistical methodology resulted in an improved estimate. However, at this data spacing, the nugget effect is poorly estimated, and the long-range continuity does not represent the true variability of the gold grade. The Mineral Resource estimate may be used for long-term planning and overall resource assessment, however, the estimates will not be suitable for ore/waste selectivity at the time of mining.

In Scenario Five, the data was dominated by development sampling at a spacing of 2 m. The nugget effect is best defined using this closely spaced data. The estimation methodology resulted in a smaller block support being considered and thus increased theoretical selectivity, however, in practice the usefulness of narrowly constrained smaller support is limited.

Scenario Six represented the resource exploitation phase including stope sampling data at a spacing of approximately 5 m x 10 m. The additional data allow for increased acceptable small block estimates over a larger area which may be used for short-term planning due to increased selectivity. Small blocks with a high slope of regression and high kriging efficiency will present the most accurate grade estimate at the time of mining due to reduced conditional bias.

Estimating into large blocks that extend over the entire orebody area is a challenge as the spatial continuity defined by the variogram only extends to a range of up to 60 m. The estimation methodology becomes more complex and the use of the AngloGold Ashanti macro cokriging technique is recommended.

REFERENCES

Armstrong, R.A., Compston, W., Retief, E.A., Williams, I.S. & Welke, H.J. (1991). Zircon ion microprobe studies bearing on the age and evolution of the Witwatersrand triad. *Precambrian Research*, *53*, 243-266.

Chamberlain, V.A. (1997). *The Application of Macro Co-Kriging and Compound Lognormal Theory to Long Range Grade Forecasts for the Carbon Leader Reef.* (M.Sc. Thesis). Retrieved from http://wiredspace.wits.ac.za/handle/10539/22398.

Clark, I. (2015). Regression revisited (again). *The Journal of the Southern African Institute of Mining and Metallurgy, 115*, 45-50.

Clark, I. (1979). *Practical Geostatistics*. Retrieved from http://www.kriging.com/pg1979_download.html.

Clark, I. and Harper, W.V. (2000). *Practical Geostatistics 2000.* Scotland: Geostokos (Ecosse) Ltd.

David, M. (1977). *Geostatistical Ore Reserve Estimation*. Amsterdam: Elsevier Scientific Publishing Company.

Davis, J.C. (2002). *Statistics and Data Analysis in Geology* (4^{th} ed.). New Jersey: John Wiley and Sons, Inc.

Deutsch, C.V. and Journel. A.G. (1998). *GSLIB: Geostatistical Software Library and User's Guide* (2^{nd} ed.). New York: Oxford University Press.

Deutsch, C.V. (2007). *The Slope of Regression for Kriging Estimators*. Centre for Computational Geostatistics, Department of Civil and Environmental Engineering, University of Alberta.

Deutsch, C.V., Leuangthong, O., and Ortiz, J.M. (2007). *Case for geometric criteria in resources and reserves classification*. Society for Mining, Metallurgy, and Exploration 2007 Transactions, *322*, 1-11.

Deutsch, J.L., Szymanski, J. & Deutsch, C.V. (2014). *The Journal of the Southern African Institute of Mining* and Metallurgy, *114*, 223-230.

De Waele, B., Lacorde, M., Cunningham, M., and Jupp, B. (2018). *Understanding Geology and Structure: An Essential Part of Mineral Resource Estimation*, ASEG Extended Abstracts. 2018: 1, 1-8, DOI: 10.1071/ASEG2018abM2_2F.

Dohm, C.E. (1995). *Improvement of Ore Evaluation Through the Identification of Homogeneous Areas Using Geological, Statistical and Geostatistical Analyses.* (Ph.D. Thesis). University of the Witwatersrand, Johannesburg.

Dohm, C.E. (2018). *MINN7006A - Geostatistical Methods in Mineral Resource Evaluation*, Course lecture notes. Johannesburg, School of Mining Engineering, University of the Witwatersrand.

Dominy, S.C. and Annels, A.E. (2001). Evaluation of gold deposits – Part 1: review of mineral resource estimation methodology applied to fault- and fracture-related systems. *Applied Earth Science: Transactions of the Institution of Mining and Metallurgy*, Section B, 110, B145-B166.

Dominy, S.C., Johansen, G.F. and Annels, A.E. (2001). Bulk sampling as a tool for the grade evaluation of gold-quartz reefs. *Applied Earth Science: Transactions of the Institution of Mining and Metallurgy*, Section B, 110, B176-B191.

Dominy, S.C., Noppé, M.A. and Annels, A.E. (2004). Errors and Uncertainty in Mineral Resource and Ore Reserve Estimation: The Importance of Getting it Right. *Exploration and Mining Geology, 11*(1-4), 77-98.

Du Toit, R. (2018). *A Refined Resource Model for Tshepong Mine*. (Research Report). University of the Witwatersrand, Johannesburg.

Duke, J.H. And Hanna, P.J. (2014). Geological Interpretation for Resource Modelling and Estimation. *In Mineral Resource and Ore Reserve Estimation - The AusIMM Guide to Good Practice, (2nd ed.). Monograph 30*. (pp. 145-153). Melbourne: The Australasian Institute of Mining and Metallurgy.

Emery, X. and Ortiz, J.M. (2005). Estimation of Mineral Resources using Grade Domains: Critical Analysis and a Suggested Methodology. *The Journal of the South African Institute of Mining and* Metallurgy*, 105*, 247-256.

Emery, X. and Ortiz, J.M. (2006). Geostatistical estimation of mineral resources with soft geological boundaries. *The Journal of the South African Institute of Mining and Metallurgy, 106*, 577-584.

Flitton, T. and Peattie, R. (2016). Resource estimation for deep tabular orebodies the AngloGold Ashanti way. *The Journal of the Southern African Institute of Mining and Metallurgy*, *116,* 601-608.

Frimmel, H.E., Groves, D.I., Kirk, J., Rutz, J., Chesley, J., & Minter, W.E.L. (2005). The Formation and Preservation of the Witwatersrand Goldfields, the World's Largest Gold Province*. Society of Economic Geologists Inc. Economic Geology, One Hundredth Anniversary Volume*, 769-797.

Gartz, V.H. and Frimmel, H.E. (1999). Complex Metasomatism of an Archean Placer in the Witwatersrand Basin, South Africa: The Ventersdorp Contact Reef – A Hydrothermal Aquifer? *Economic Geology, 94*, 689-706.

Germs, G.J.B. and Schweitzer, J.K. (1994). A provisional model for the regional morphostratigraphy of the Venterspost Conglomerate Formation in the West Rand and Carletonville Goldfields. *South African Journal of Geology*, *97*(3), 279-287.

Gilchrist, G. (2019). Evolving estimation techniques for an evolving world class copper deposit at Kamoa-Kakula, Democratic Republic of Congo. In Muellar, C., Assibey-Bonsu, W., Baafi, E., Dauber, C., Doran, C., Jaszczuk, M.J. & Nagovitsyn, O. (Eds.), *Mining Goes Digital – Proceedings of the 39th International Symposium 'Applications of Computers and Operations Research in the Mining Industry'* (pp. 192-200). London: Taylor and Francis Group.

Guibal, D. (2001). Variography, a Tool for the Resource Geologist. In A.C. Edwards (Ed.), *Mineral Resource and Ore Reserve Estimation - The AusIMM Guide to Good Practice*, (pp. 85-90). Melbourne: The Australasian Institute of Mining and Metallurgy.

Hall, R.C.B., Els, B.G., & Mayer, J.J. (1997). The Ventersdorp Contact Reef: Final phase of the Witwatersrand Basin, independent formation, or precursor to the Ventersdorp Supergroup? *South African Journal of Geology*, *100*(3), 213-222.

Henning, L.T., Els, B.G. & Mayer, J.J. (1994). The Ventersdorp Contact Placer at Western Deep Levels South Gold Mine – an ancient terraced fluvial system. *South African Journal of Geology, 97*(3), 308-318.

Isaaks, E.H. (2004). *The kriging oxymoron: Conditionally unbiased and accurate prediction* (2nd Ed.) In Proceedings of the 2004 Geostatistics Conference, Banff Alberta (pp. 425-432). Retrieved online from http://www.isaaks.com/whitepapers.html

Isaaks, E.H. (2013). *What the Heck is a Variogram?* [Video]. Retrieved from https://www.isaaks.com/videos.html. Accessed 9 June 2019.

Isaaks, E.H. and Srivastava, R.M. (1989). *An Introduction to Applied Geostatistics*. Oxford: Oxford University Press.

Jolley, S.J., Freeman, S.R., Barnicoat, A.C., Phillips, G.M., Knipe, R.J., Pather, A., Fox, N.P.C., Strydom, D., Birch, M.T.G., Henderson, I.H.C. & Rowland, T.W. (2004). Structural controls on Witwatersrand gold mineralisation. *Journal of Structural Geology, 26*, 1067-1086.

Journel, A.G. and Huijbregts, C.H.J. (1978). *Mining Geostatistics*. London: Academic Press.

Kositcin, N., McNaughton, N.J., Griffin, B.J., Fletcher, I.R., Groves, D.I. & Rasmussen, B. (2003). Textural and geochemical discrimination between xenotime of different origin in the Archaean Witwatersrand basin, South Africa. *Geochemica et Cosmochimica. Acta, 67*(4), 709-731.

Krige, D.G. (1960). On the Departure of Ore Value Distributions from the Lognormal Model in South African Gold Mines. *The Journal of the South Africa Institute of Mining and Metallurgy, 61*(4), 231-247.

Krige, D.G. (1981). Lognormal-de Wijsian Geostatistics for Ore Evaluation. Johannesburg: South African Institute of Mining and Metallurgy.

Krige, D.G. (1993). Variability in the gold grade and spatial structures of Witwatersrand reefs: The implications for geostatistical ore valuations. *The Journal of the South African Institute of Mining and Metallurgy, 93*(3), 79-84.

Krige, D.G. (1996). A Basic Perspective on the Roles of Classical Statistics, Data and Search Routines, Conditional Biases and the Information and Smoothing Effects in Ore Block Valuations, *Conference on Mining Geostatistics, Kruger National Park, 1994, UNISA Publication 1996*.

Krige, D.G. (1997). A Practical Analysis of the Effects of Spatial Structure and of Data Available and Accessed, on Conditional Biases in Ordinary Kriging in E.Y. Baafi and N.A. Schofield (Eds.). *Geostatistics Wollongong '96*(2) (pp. 799-810. Netherlands: Kluwer Academic Publishers.

Krige, D.G. and Magri, E.J. (1982). Studies of the Effects of Outliers and Data Transformation on Variogram Estimates for a Base Metal and a Gold Ore Body. *Mathematical Geology*, *14*(6), 557-564.

McCarthy, T.S. (1994). The tectono-sedimentary evolution of the Witwatersrand Basin with special reference to its influence on the occurrence and character of the Ventersdorp Contact Reef – A review. *The South African Journal of Geology, 97*(3), 247-259.

McCarthy, T.S. (2006). The Witwatersrand Supergroup. In: Johnson, M.R., Anhaeusser, C.R. and Thomas, R.J. (Eds.), *The Geology of South Africa*. Johannesburg: Geological Society of South Africa, 150-186.

McCarthy, T.S. and Ogilvie, P. (2020). Wits Gold – 'New' insights into an old problem. A collaboration between the School of Geosciences, University of the Witwatersrand, and Shango Solutions. Presented by the Geological Society of South Africa Online Lunchtime Talks on the 3rd September 2020. Retrieved from https://www.youtube.com/watch?v=WxVfbQ1P8MI&list=PL-MPMaHidsW38tTfDVOpxByn2FGL6v-Qj&index=31&t=1s

McWha, M. (1994). The Influence of the Landscape on the Ventersdorp Contact Reef at Western Deep Levels South Mine. *South African Journal of Geology, 97*(3), 319-331.

Morgan, J.C. (2011). *Theoretical and Practical Aspects of Variography: In Particular, Estimation and Modelling of Semi-Variograms over Areas of Limited and Clustered or Widely Spaced Data in a Two-Dimensional South*

African Gold Mining Context. (Ph.D. Thesis). University of the Witwatersrand, Johannesburg.

Minnitt, R.C.A. (2014). Sampling in the South African minerals industry. *Journal of the South African Institute of Mining and Metallurgy, 114*, 63-81.

Regional VCR Working Group (1994). Some regional characteristics of the Ventersdorp Contact Reef (VCR). *South African Journal of Geology, 97*(3), 385-386.

Rendu J.-M. (1981). An introduction to Geostatistical Methods of Mineral Evaluation. *South African Institute of Mining and Metallurgy, The Monograph Series (2nd Ed.).*

Rivoirard, J. (1990). *Introduction to disjunctive kriging and nonlinear geostatistics*. C-143, Fontainebleau, Centre de Géostatistique.

Robb, L.J., Davis, D.W. & Kamo, S.L. (1991). Chronological framework for the Witwatersrand Basin and environs: towards a time-constrained depositional model. *South African Journal of Geology, 94*(1), 86-95.

Robb, L.J. and Robb, V.M. (1998). Gold in the Witwatersrand Basin. In: M.G.C. Wilson and C.R. Anhaeusser (Eds.). *The Mineral Resources of South Africa Handbook* (pp. 294-239). Pretoria: Council for Geoscience.

Rossi, M.E., Deutsch, C.V. (2014). *Mineral Resource Estimation*. Dordrecht: Springer.

SAMREC (2016). South African Mineral Resource Committee. The South African Code for the Reporting of Exploration Results, Mineral Resources and Mineral Reserves (the SAMREC Code). 2016 Edition. Retrieved from: https://www.samcode.co.za/news/201-the-samrec-code-march-2000-to-march-2020-marking-20-years-of-samcode-compliance.

Sichel, H. S. (1966) The Estimation of means and associated Confidence Limits for Small Samples from Lognormal Distributions, *Journal of the South African Institute of Mining and Metallurgy, 66*, 106-122.

Sichel, H.S. (1987). Some Advances in Lognormal Theory. APCOM87: Proceedings of the Twentieth International Symposium on the Application of

Computers and Mathematics in the Mineral Industries, Geostatistics. *Journal of the South African Institute of Mining and Metallurgy, 3*, 3-8.

Silva, C.J.E., Bassani, M.A.A. & Costa, J.F.C.L. (2019). Influence of drilling spacing on the mineral resources uncertainty. In Muellar, C., Assibey-Bonsu, W., Baafi, E., Dauber, C., Doran, C., Jaszczuk, M.J. & Nagovitsyn, O. (Eds.), *Mining Goes Digital – Proceedings of the 39th International Symposium 'Applications of Computers and Operations Research in the Mining Industry'* (pp184-191). London: Taylor and Francis Group.

Simmonds, S.J. (2009). *The Nugget Effect: In describing the variability of an ore deposit.* (M.Sc. Thesis). Rhodes University, Grahamstown.

Sinclair, A.J. (1998). Exploratory Data Analysis: A Precursor to Resource/Reserve Estimation. *Exploration and Mining Geology, 7*(1-2), 77-90.

Sinclair A.J. & Blackwell, G.H. (2004). *Applied Mineral Inventory Estimation.* United Kingdom: Cambridge University Press.

Smits, G. (1994). Note on the mineralogy of the Ventersdorp Contact Reef at Kloof Gold Mine. *South African Journal of Geology, 97*(3), 357-364.

Storrar, C.D. (1977). *South African Mine Valuation.* Johannesburg: Chamber of Mines of South Africa.

Tucker, R.F., Viljoen, R.P. & Viljoen, M.J. (2016). A Review of the Witwatersrand Basin – The World's Greatest Goldfield. In: Fareeduddin and Krishna, B.R. (Eds.), *The Great Mineral Fields of Africa. International Union of Geological Sciences, Episodes, 39*(2), 105-134.

Van der Westhuizen, W.A., de Bruiyn, H. and Meintjies, P.G. (2006). The Ventersdorp Supergroup. In: Johnson, M.R., Anhaeusser, C.R. and Thomas, R.J. (Eds.), *The Geology of South Africa* (pp. 187-208). Johannesburg: Geological Society of South Africa.

Vann, J., Jackson, S. & Bertoli, O. (2003). Quantitative Kriging Neighbourhood Analysis for the Mining Geologist – A Description of the Worked Method with Worked Case Examples. 5th International Mining Geology Conference, (pp.215 – 223). The Australian Institute for Mining and Metallurgy, Victoria.

Vann, J., Stephenson. P.R., Jackson, S., & Pilger, G. (2014). Common Sense and Good Communication – Effective Team-Based Estimation and Classification of Mineral Resources and Reserves. *In Mineral Resource and Ore Reserve Estimation – The AusIMM Guide to Good Practice, (2nd ed.). Monograph 30*, (pp. 19-30). Melbourne: The Australasian Institute of Mining and Metallurgy.

Viljoen, M.J. and Reimold, W.U. (1994). The Ventersdorp Contact Revisited – An Introduction. *The South African Journal of Geology, 97*(3), 234-237.

Zhao, B., Meyer, F.M., Robb, L.J., & McWha, M. (1994). A preliminary study of alteration associated with the Ventersdorp Contact Reef at Western Deep Levels South Mine, Witwatersrand Basin, South Africa. *South African Journal of Geology*, *97*(3), 348-356.

APPENDIX A

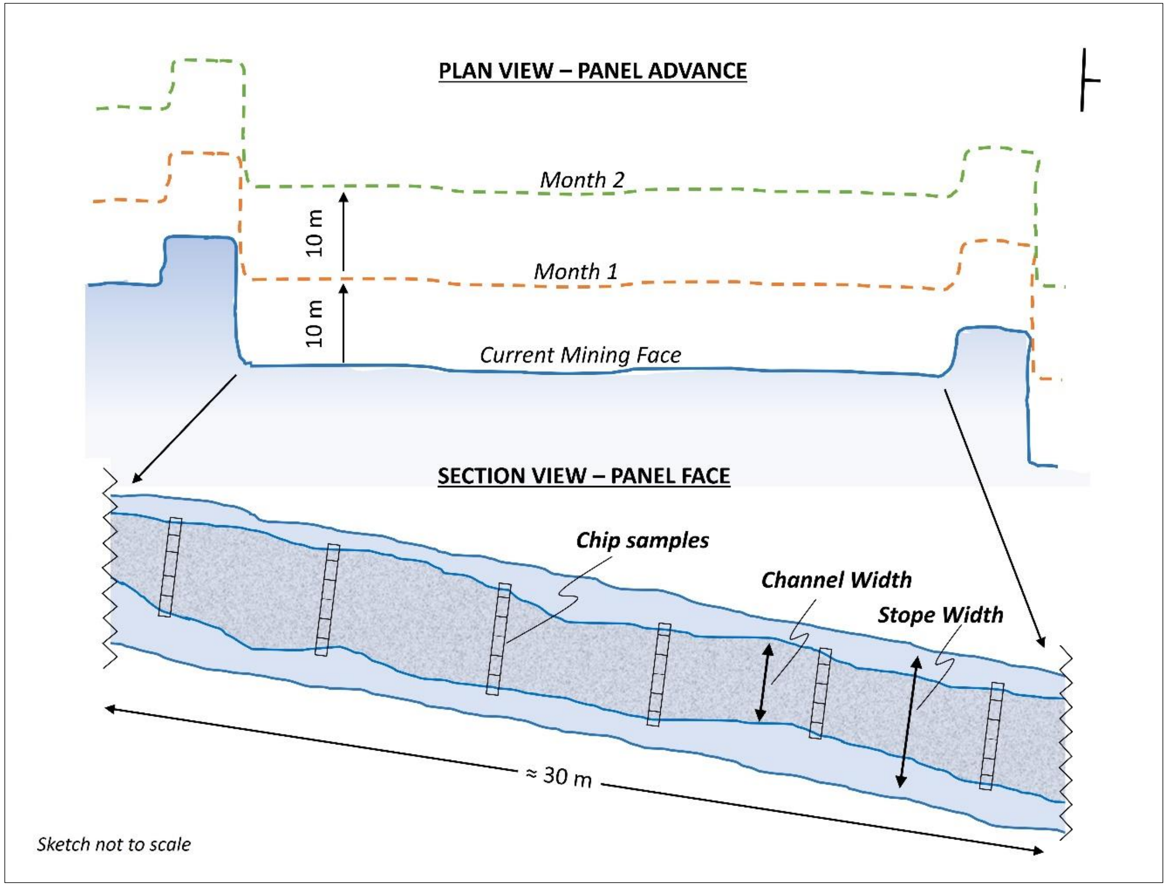

Figure A-1: Conceptual presentation of a panel in plan and section view depicting advance, panel length, channel width and stope width.

APPENDIX B

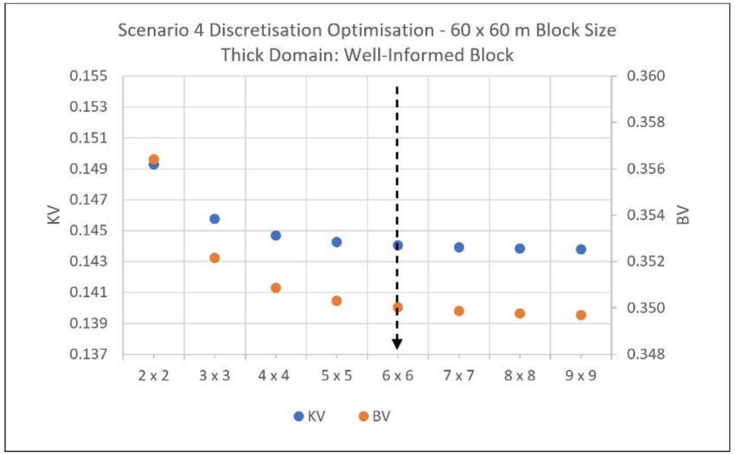

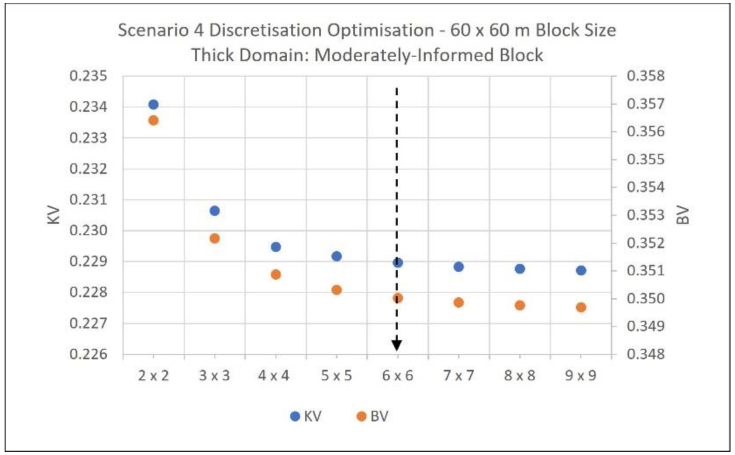

Figure B-1: Scenario Four discretisation exercise

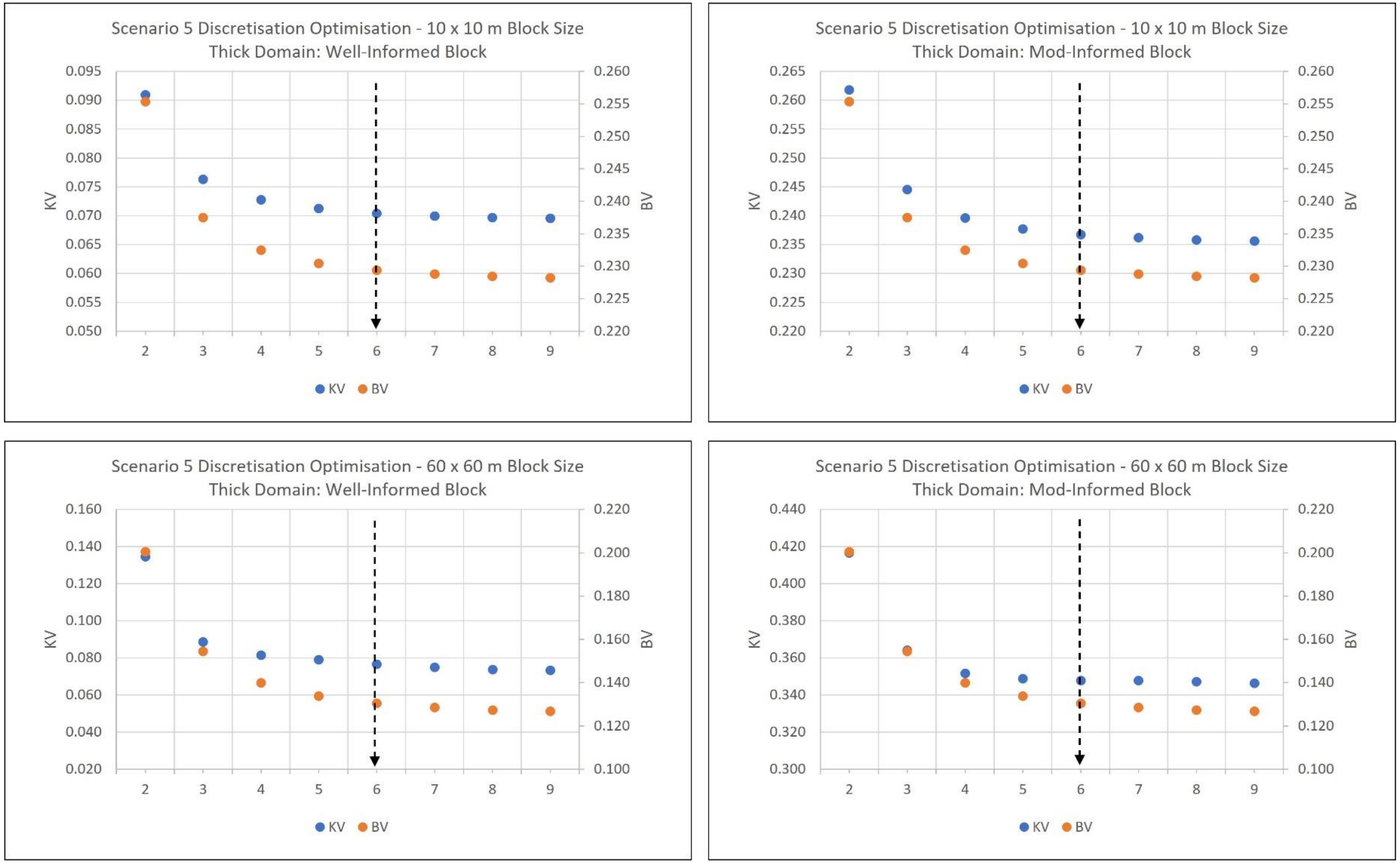

Figure B-2: Scenario Five discretisation exercise

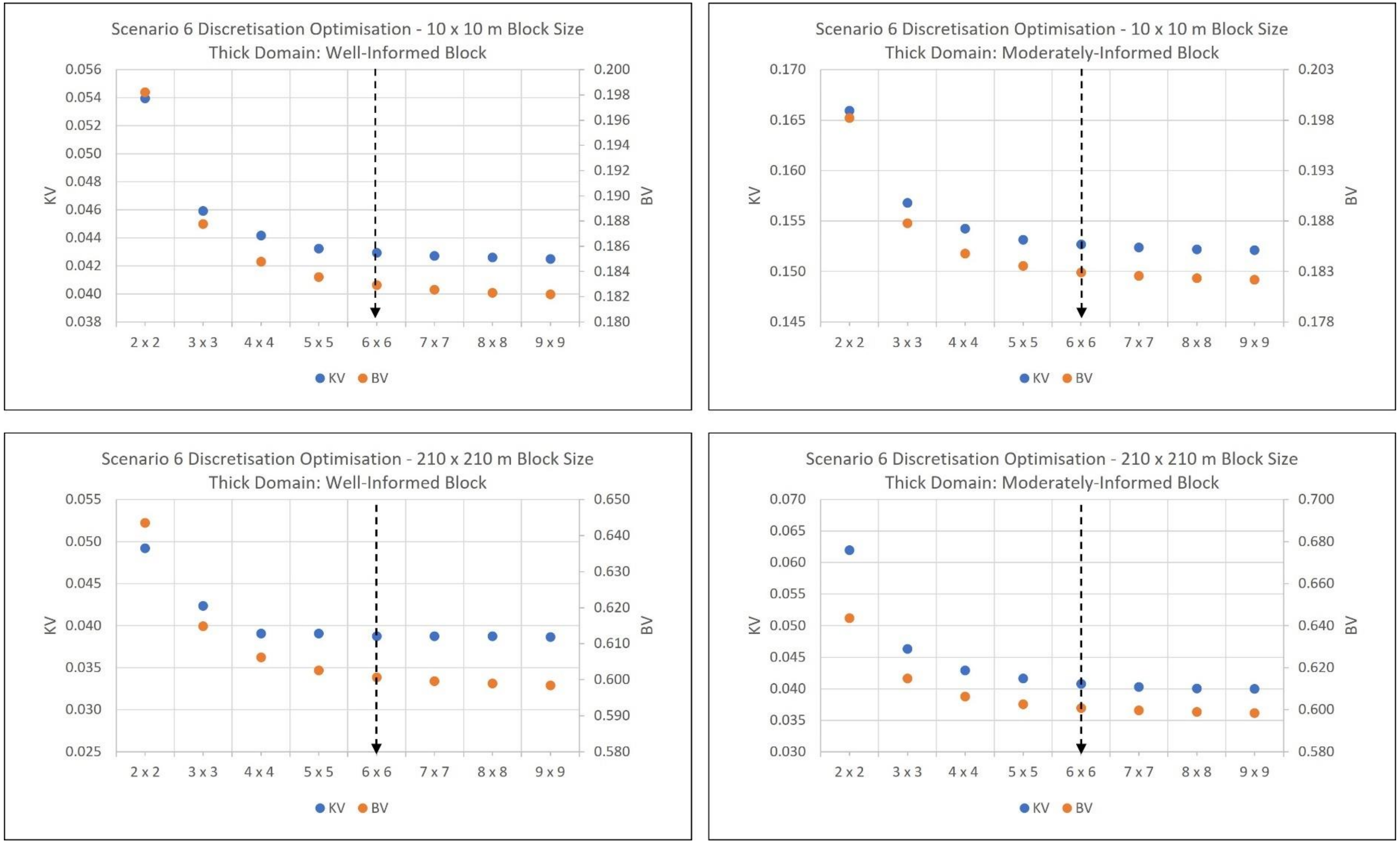

Figure B-3: Scenario Six discretisation exercise